Development of Low Cost Ball End Magnetorheological Finishing Process

A Dissertation Submitted

In Partial Fulfillment of the Requirements

for the Degree of

Master of Engineering

in

CAD/CAM & Robotics

by

Akshay Khurana

to the

MECHANICAL ENGINEERING DEPARTMENT

THAPAR UNIVERSITY, PATIALA

July, 2015

CERTIFICATE

I hereby declare that the thesis entitled "**Development of Low Cost Ball End Magnetorheological Finishing Process**" is an authentic record of my study carried out as requirements for the award of the degree of **Master of Engineering** in **CAD/CAM Engineering** at **Thapar University, Patiala** under the supervision Dr. Anant Kumar Singh, Assistant Professor, Mechanical Engineering Department, Thapar University, Patiala during July, 2013 to July, 2015. The matter embodied in this report has not been submitted in partial or full to any other university or institute for the award of any degree.

Akshay Khurana

Date: 13/07/2015

Akshay Khurana

Roll No: 801381001

It is certified that the above statement made by the student is correct to the best of my/our knowledge and belief.

14/07/2015

Dr. Anant Kumar Singh
Assistant Professor
Mechanical Engineering Department
Thapar University, Patiala - 147004

Countersigned by

Dr. S.K. Mohapatra
Sen. Professor & Head
Mechanical Engineering Department
Thapar University, Patiala – 147004

Dr. S.S. Bhatia
Dean of Academic Affairs
Thapar University, Patiala - 147004

ii

Acknowledgements

I express my sincere gratitude to my guide Dr. Anant Kumar Singh, Assistant Professor, Mechanical Engineering Department, Thapar University, Patiala, for their valuable guidance, proper advice and constant encouragement during the course of my thesis work.

I do not find enough words with which I can express my feeling of thanks to the entire faculty and staff of Mechanical Engineering Department, Thapar University, for their help, inspiration and moral support which went a long way in successful completion of thesis work. I heartily thankful to my entire research team especially Prince Garg, Vishwas Grover, Nitin Chawla and Talwinder Singh Bedi.

(Akshay Khurana)

Abstract

A finishing process for nanofinishing of workpiece surfaces using a low cost ball end MR finishing tool is developed. It is used to finish both ferromagnetic and non-ferromagnetic using 'smart' fluid name as magnetorheological polishing (MRP) fluid. It is mainly constituted of base fluid, carbonyl iron particles and abrasive particles. The existing ball end magnetorheological finishing process is able to finish 3D complex shapes but comparatively as likely to higher initial setup cost. The uniformity in magnetic field produced by the earlier ball end finishing process was less at the tool tip surface due to central hole in rotating core. In the presently developed a low cost ball end MR finishing process produce a more uniformity in the magnetic field at the tool tip surface due to without any central hole in rotating core.

The finite element analysis of the present developed low cost ball end magnetorheological finishing tool was done in MAXWELL ANSOFT V13 (student version) to analysis the magnetic flux density distribution at the tool tip surface. The electromagnet modelling of ball end magnetorheological finishing tool was done for both core with central hole and core without central hole. The magnetostatic finite element analysis with workpiece was done on ferromagnetic to observe the magnetic flux density at the tip of ball end magnetorheological finishing tool. The CAD modelling of C-shape bracket and the present ball end magnetorheological finishing tool have been carried out in CREO elements/PROE. A low cost ball end ball end magnetorheological finishing tool has been made up and attached to the developed set up.

A PLC controlled experimental setup is developed with the aim of study the process description and performance during precise finishing of the workpiece surfaces. The experimentation was carried out on mild steel workpiece in order to find the effect of finishing time on the change in the value of surface roughness. The initial average surface roughness value was measured as 440 nm using surftest. Scanning electronic microscope (SEM) analysis was carried out before/after finishing in order to determine the surface morphology of the workpiece. The results concluded that the average surface roughness value decreases to 20 nm from initial surface roughness value 440 nm in 90 minutes of finishing time in the present developed finishing setup. The presently developed low cost ball end magnetorheological finishing set up was found comparatively more finishing capability in terms of finishing time and more uniformity of magnetic field at the tip surface of the tool.

Contents

List of Figures

List of Tables

Nomenclature

Ra	centre line average roughness value (µm)
Rz	peak roughness value (µm)
Rq	RMS roughness value (µm)
F_f	finishing force
F_n	normal force
F_s	shear force
Z	working gap in mm
I	current in ampere
N	number of turns
Bz	magnetic field in tesla
L	length of the belt
C	centre distance between the two pulleys
P_1	pitch circle diameter of the driving pulley
P_2	pitch circle diameter of the driven pulley
N_1	rpm of the motor shaft
N_2	rpm of the solid core

Abbreviation

AFF	abrasive flow finishing
BEMRF	ball end magnetorheological finishing
MR	magnetorheological
MRF	magnetorheological finishing
MRAFF	magnetorheological abrasive flow finishing
CIP	carbonyl iron particle
SiC	silicon carbide

MRAH	magnetorheological abrasive honing
RMS	root mean square
CAD	computer aided design
PLC	programmable logic controller
HMI	human machine interface
RPM	rotation per minute
ANSYS	analysis of system
FEA	finite element analysis
MRP	magnetorheological polishing
SEM	scanning electronic microscope
RTD	resistance temperature detector

Chapter 1

Introduction

1.1 Introduction

Surface finishing is a broad range of industrialized processes that change the surface of a manufactured product to achieve a precise property. The main benefits of finishing processes are: better sealing capability, reduce surface friction, and remove burs and other surface imperfection. The different types of traditional finishing processes are honing, lapping & grinding etc. The traditional finishing processes are less suited regarding the size and shape of the material for finishing. A large amount of heat is generated during the traditional processes which results in the failure of the material. Milling is usually carried out to finish flat surfaces, whereas honing is usually carried out to finish cylindrical (external and internal) surfaces. The control over the forces during the traditional finishing processes is very less which results in poor surface finish. In the traditional processes, there is direct contact between workpiece and tool which results to sub damage of surface, reduced strength and consistency of the component. The ball end milling tool is used to finish the deeper grooves & 3D intricate shapes which cannot effectively done by traditional methods.

The traditional processes such as grinding, lapping, honing etc. are used for finishing purposes and which uses the cutting tool as multi point in the abrasive form to perform the various types of finishing operations. The deformation of surface such as micro cracks which damage the surface topography due to the normal forces produced during these processes. The different types of traditional finishing processes are explained as below:

Among all abrasive finishing processes, grinding is used most widely for finishing of workpieces is shown in Fig. 1.1. The mechanism on which honing is based that the relative motion between the workpiece surface and abrasives particles which are implanted on circumference of grinding wheel. The absorbent rotating body which is abrasive particles results in material removal when it comes in contact with workpiece.

Lapping works on three body abrasive wear principle. There is lesser constraint between workpiece and active abrasives during surface finishing when normal force was reduced with increase in working gap. With the abrasive action, workpiece was finished with 3-body wear

mechanism. For lower normal force, the percentage change in surface roughness was found less in terms of material removal is shown in Fig. 1.2.

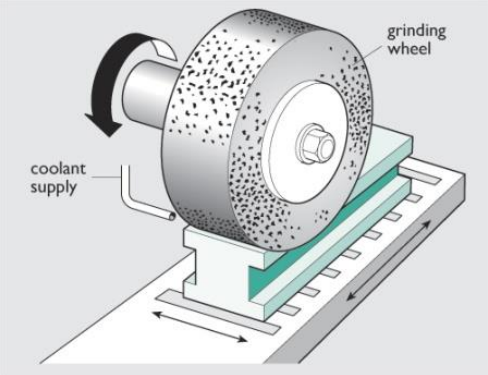

Figure 1.1: Grinding process

(http://core.materials.ac.uk/repository/ou_manufacturing/t173_2_045i.jpg)

By adding abrasive slurry between lap surface and workpiece, and moved in random paths under pressure after hold against lap.

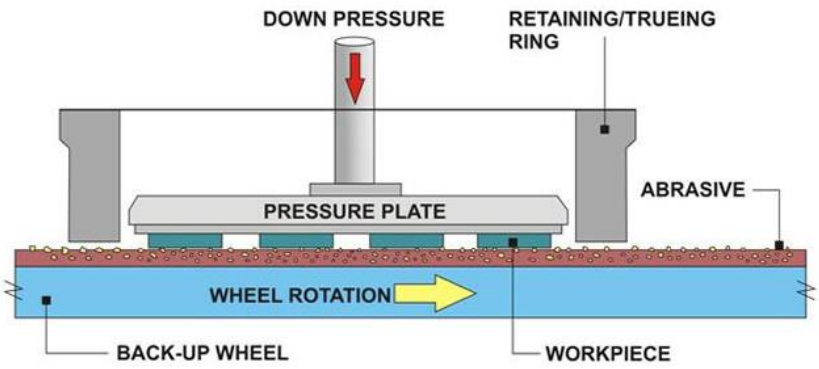

Figure 1.2: Lapping process

(http://www.azom.com/images/Article_Images/ImageForArticle_5657 (1).jpg)

Honing is one of the traditional finishing process in which usually cylindrical (internal & external) surfaces are finished is shown in Fig. 1.3. The honing is comparatively more sticking pressure on workpiece than lapping. Due to oil retain in cross hatched pattern, the surface after finished by honing process has self lubricating property.

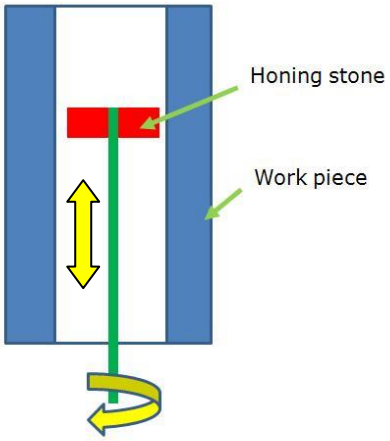

Figure 1.3: Honing process (http://blog.mechguru.com/wp-content/uploads/2011/09/honing.jpg)

1.2 Advanced finishing process

The advanced finishing process is used to finish typical 3D shaped component with a nanometre surface roughness and have great response in industry. For getting a high product quality, the external magnetic field can be used for controlling the forces and also for the polishing of brittle materials. The precise surface accuracy lies in the range of 10-100 nm. Whereas with advanced finishing process, surface micro roughness is less than 10 nm RMS can be achieved. The brief explanation of each advanced finishing process as described below:

1.2.1 Abrasive flow finishing

AFM process is used to renovate the performance of automotive engines by enhancing the surface finish of internal medium of intake ports. The experimental setup consisted of a Hydraulic oil inlet, Hydraulic cylinder, Smooth entry profile, Top cover plate, Dynamometer etc. For obtaining precise finishing, they used polymeric carrier. The marks of abrasive onto the workpiece are due to the radial force, where as the axial force component is responsible for the removal of chip. Due to the complex geometry, it is very complicated to get precise surface finish on the internal way of ports. The AFM process can be used to polish in different mediums like air, liquid, or fuel flows. The main parts used in the AFM are the tool, machining unit, support frame, bottom cover plate and types of carrier.

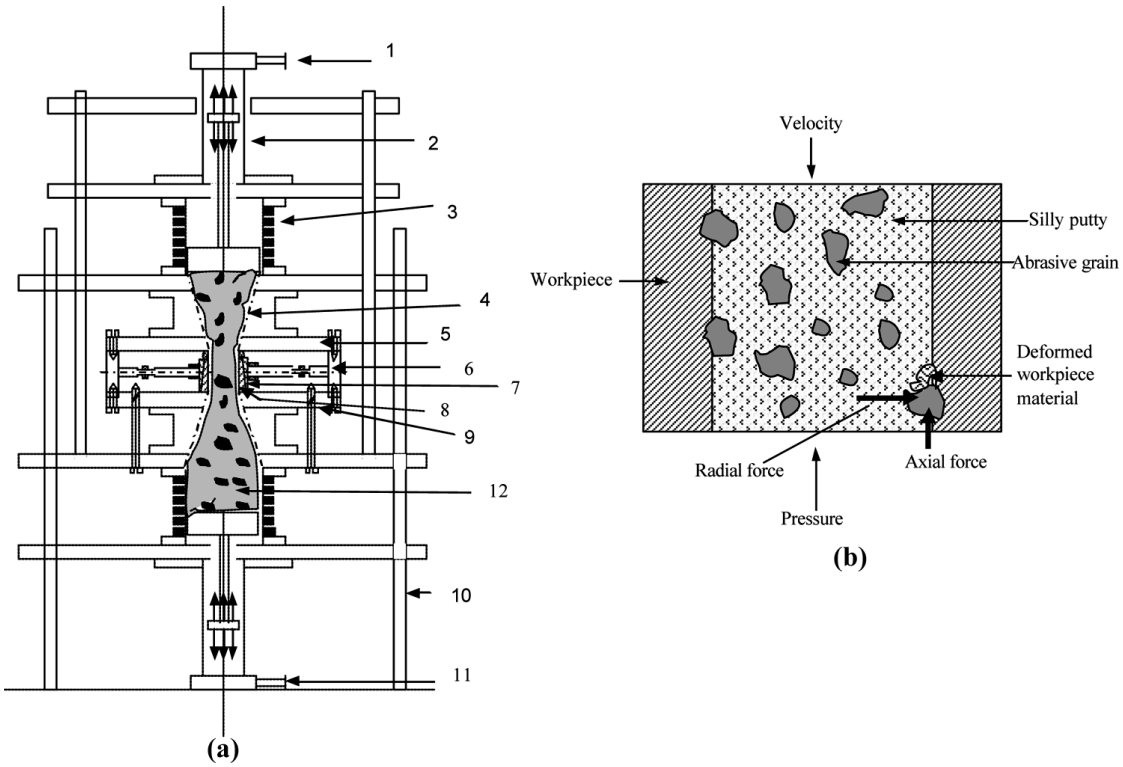

Figure 1.4: (a) Schematic diagram of experimental set-up: 1- oil inlet, 2-Hydraulic cylinder, 3-Smooth entry profile, 4- cover plate, 5-Dynamometer, 6-Split cylindrical fixture with workpiece, 7-Bottom cover plate, 8-Support frame, 9- oil outlet, 10-Medium with abrasive particles; (b) Types of forces performing on a grain. (Jain, 2008)

They compared the performance of surface finish by using R-AFF and AFF on various types of workpiece that is Al alloy/SiC MMC with 10%SiC, Al alloy/SiC MMC with 15% SiC and Al alloy. The value of extrusion pressure and the number of cycles remains constant whereas the workpiece circulating speed varies.

1.2.2 Magnetic abrasive finishing

The parameters which are affecting the surface quality generated during the MAF are identified as: (i) voltage (DC) applied to the electromagnet,

(ii) Working gap,

(iii) Rotational speed, and

(iv) Abrasive size (mesh number).

According to the experimental results a modification in surface roughness, working gap and voltage are the major important parameters followed by grain mesh number and then rotational speed. For finishing of the component, magnetic field is used in magnetic abrasive finishing process. MAF finishing was first presented in the Soviet Union, with additional crucial research in the country like, Japan (Yamaguchi and Shinmura, 2004). MAF process consisted of a North and South Pole of permanent magnet and the workpiece. The abrasive particles which are magnetic in nature were applied in working gap. With the magnetic field, the abrasive particles aligned in a line and form a brush like arrangement for accurate finishing of the work material. The brush which was formed works as a multi point cutting tool for removing the material. The force which was induced normally due to magnetic abrasive particles is accountable for the incursion of magnetic abrasive particles onto the workpiece.

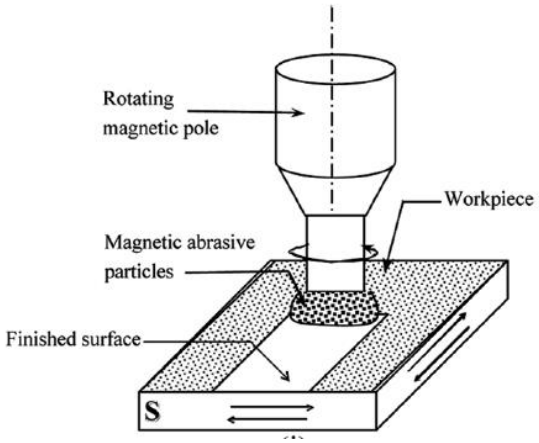

Figure 1.5: Experimental setup of magnetic abrasive finishing (Jain, 2008)

They evaluated the effect of rotational speed on the surface roughness by using MAF with double dipole tip set for finishing of stainless steel tube. The parameters for example rotational speed and finishing time were varied.

1.2.3 Magnetic abrasive jet finishing

The Magnetic abrasive jet finishing has been introduced for finishing of components with a flat or cylindrical inner surfaces as well as intricate shaped surface. This type of finishing process is a modification of MAF process in which compressed air which is working fluid mixed with magnetic abrasive. And it is passed into the tube and the magnetic field is given on the outer surface of the tube. The magnetic abrasives finish the internal surface of the tube

more accurately, where the magnetic abrasive in the jet diverse with the air is moved to the internal surface with the help of magnetic forces due to magnetic poles.

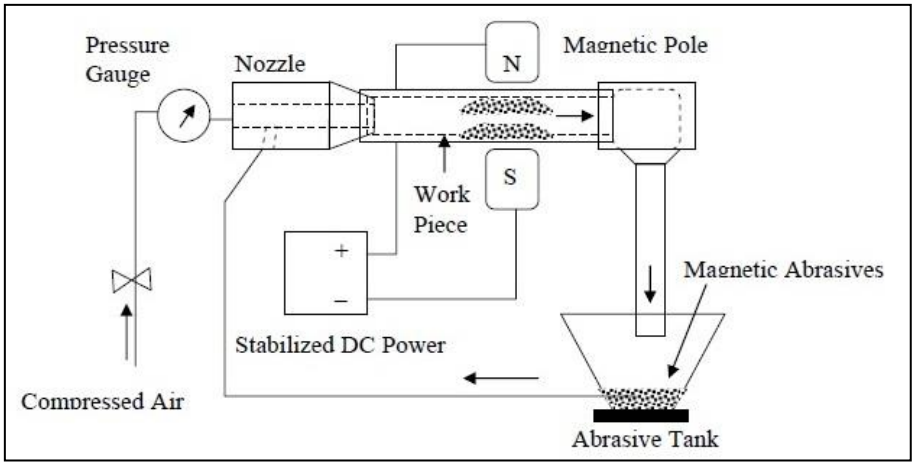

Figure 1.6: Experimental setup of magnetic abrasive jet finishing (Kim *et al*., 1997)

Kim *et al*., (1997) performed their experiment for finishing of SUS304 cylindrical tube by using iron and Al_2O_3 particles. The experimentation was carried out with the help of jet velocity 20-40 m/sec, magnetic flux 0.4T, jet pressure 1-4 atm, magnetic abrasive 50, 80 and 100 mesh size,. The results concluded that surface roughness can only give better results when there is increase in the mesh size and jet velocity.

1.2.4 Magnetic float polishing

The finishing processes studied in the prior sections have been developed for flat, cylindrical surfaces and their combinations resulting to complex 3dimensinal surfaces. Magnetic float polishing process is used for the accurate finishing of the ceramics balls and bearing rollers with the help of fine abrasive particles. The experimental setup and mechanism of magnetic float polishing process is shown in Fig. 1.7. Spindle, drive shaft, aluminium base, steel yoke, mixture of magnetic and abrasives particle etc are the various components in magnetic float finishing process. Magnetic float polishing process is based upon the hydrodynamic actions of magnetic fluid and due to the use of magnetic field that rise abrasives and a non-magnetic float suspended in it. The shaft is moved downhill to contact the ceramic balls and push them downward to gather the desired force level. Due to the influence of force and relative motion between the balls and abrasives, the balls are highly polished.

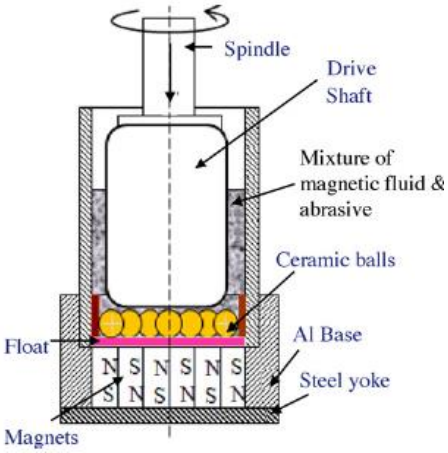

Figure 1.7: Mechanism of magnetic float polishing process (Jain, 2009)

1.2.5 Magnetorheological finishing

The high accuracy lenses are mainly ready of brittle material such as glass. And which results to crack while finishing. A technology has been developed to amend the lens finishing process known as Magnetorheological Finishing to conquer the difficulties being faced in finishing the lenses. This process gives birth to "smart fluid", known as Magnetorheological (MR) fluid which is made up of magnetic and abrasive particles such as carbonyl iron particles (CIPs) and silicon carbide particles mix in a medium like paraffin wax, mineral oil, or water which is known as carrier medium. In the absence of magnetic field, an ideal MR-fluid shows Newtonian behaviour (in which stress is directly proportional to strain). When they apply external magnetic field only then they can see the magnetorheological effect. It behaves as non-Newtonian fluid in the existence of external magnetic field. When the magnetic field is given then all the carbonyl iron particles align themselves in the direction of magnetic field. It is called as Bingham plastic model in the presence of magnetic field.

MR fluid is consists of 20 percentile of carbonyl iron particles, 20 percentile of silicon carbide and 60 percentile of base fluid. The magnetorheological finishing has vast application in finishing of brittle material such as high precision lens. The MR fluid composition is helpful for finishing optical glasses, glass, ceramic, etc. (Jain, 2009). MRF is used for high accurate finishing of concave, convex, flat or spherical shapes etc. (Jain, 2009).

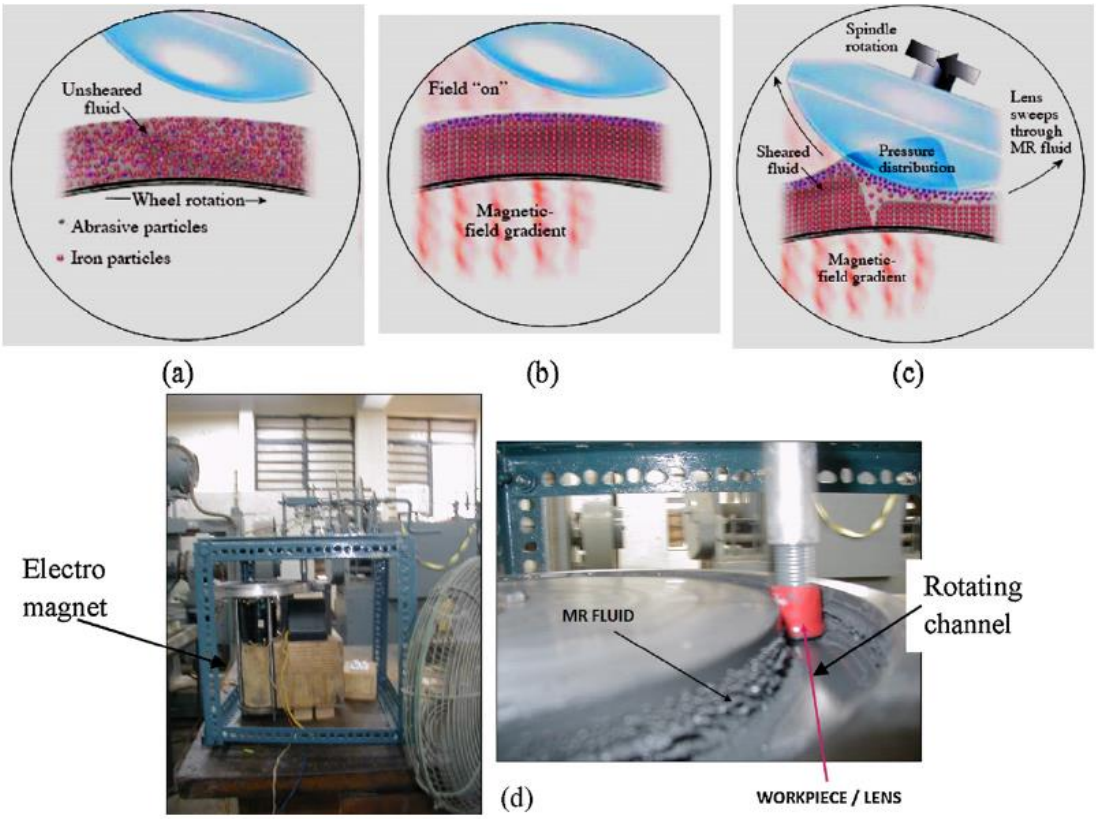

Figure 1.8: (a–c) Material removal mechanism in magnetorheological finishing and (d) MRF experimental setup (Mathur et al., 2003)

1.2.6 Magnetorheological abrasive flow finishing

Magnetorheological abrasive flow finishing process is the recently invented finishing process. The finishing medium acts as agreeable stage and overcomes shape restraint essential in almost all the traditional processes in Abrasive flow finishing process. In order to overcome the limitation of an abrading forces produced during the abrasive flow finishing processes process alongside with the combination of magnetorheological finishing for controlling the rheological properties, a newer finishing process was introduced known as magnetorheological abrasive flow finishing process (Seok *et al*., 2007) as shown in Fig. 1.9. MRAFF process consisted of CIPs particles, abrasive particles along with the base media. The finishing action on a single profile due to external magnetic field is as shown in Fig. 1.10. Due to the increase in magnetic field, the CIPs particles formed a chain over the abrasive particle for the precise finishing. The amount of material removed from the peaks of the workpiece surface by an fine abrasive grains depends on the bonding strength given by the magnetic field induced structure of MR-polishing fluid and the extrusion pressure applied

by a piston. The level to which the magnetic particles stiffened is strongly dependent on the external magnetic field for controlling the viscosity of the fluid (Seok *et al*., 2009; Kordonski *et al*., 1999).

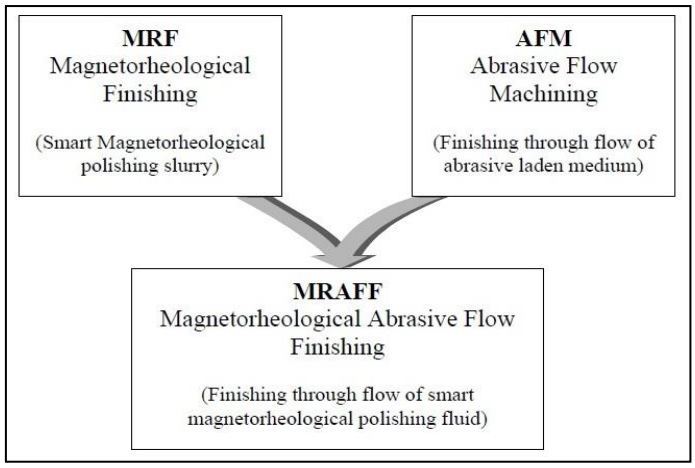

Figure 1.9: Improvement of magnetorheological abrasive flow finishing process (Jha and Jain, 2004)

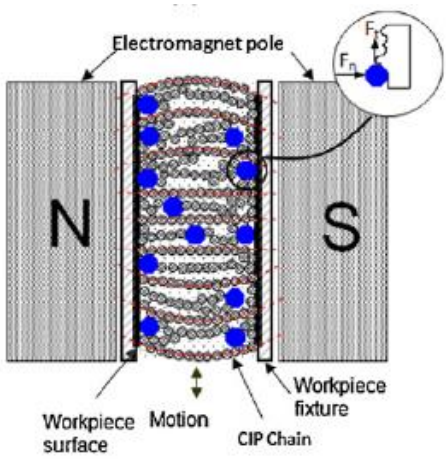

Figure 1.10: Method of magnetorheological abrasive flow finishing process (Jain, 2009)

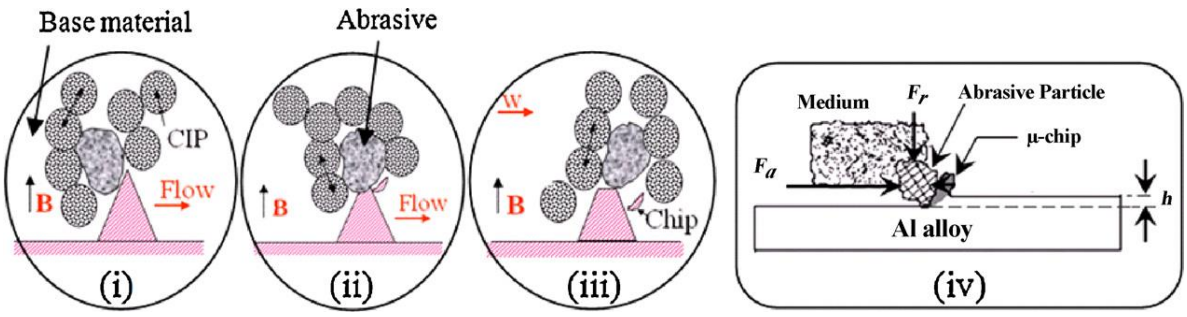

Figure 1.11: (i–iii) Stages of removal of material in case of MRAFF process, and (iv) micro-chip formation in abrasive flow machining process. (Jain, 2009)

Jha and Jain, (2004) revealed the effect of diverse magnetic field strength on the surface finish by using magnetorheological abrasive flow finishing process for finishing of stainless steel. The finishing was carried out by MR fluid (usually a mixture of 20% CIPs, 20% SiC abrasive powder and 60% visco plastic base medium).

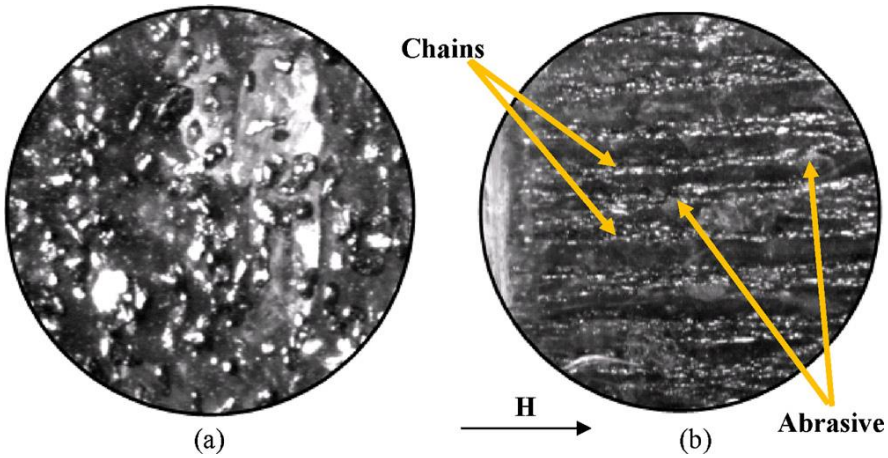

Figure 1.12: Arrangement of CIPs chain structure (a) in nonattendance of magnetic field and (b) on the attendance of magnetic field (Jain, 2009)

1.2.7 Magnetorheological jet finishing

The Magnetorheological jet finishing have been newly developed for finishing of parts with a freeform optics, steep concave, cavities etc. The experimental setup of magnetorheological jet finishing is as shown in Fig. 1.13. This type of finishing process is a modification of MRF process in which MR fluid diverse with magnetic abrasive is forced into the internal surface of the work material and is magnetized by an axial magnetic field when it comes out of the nozzle. The magnetic abrasive particles finish the internal surface of the work material more precisely. The jet snapshot image of magnetic abrasive jet finishing is as shown in Fig. The jet of water loses its coherence when passes through the nozzle. When the magnet is off, the jet of MR fluid passes through nozzle losses its coherence due to its high viscosity. When the magnetic is on, the stable jet of MR fluid passes through the nozzle with low viscosity and high velocity jet.

Kordonski *et al*., (2006) performed their experiment for finishing of fused glass silica. The finishing was done by MR fluid (usually mixed with magnetic abrasive particles). The experimentation was performed both on flat and concave shaped work material. The result concluded that the surface roughness of flat and concave shaped work material reduces to 0.013 µm and 0.040 µm.

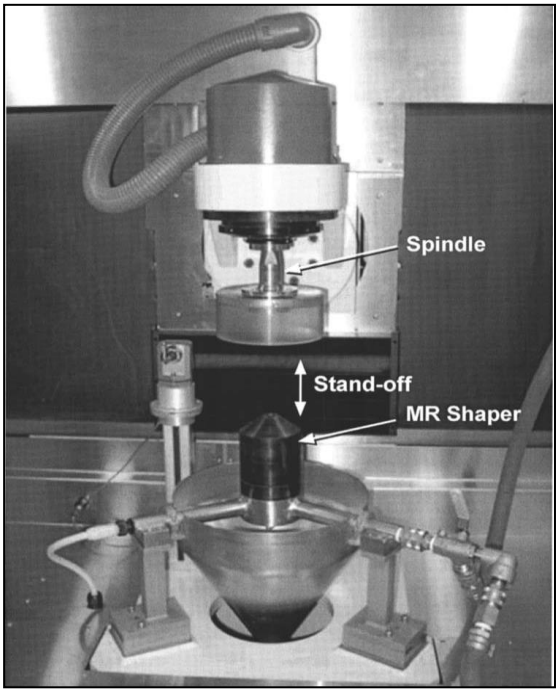

Figure 1.13: Experimental setup of magnetorheological jet finishing (Kordonski *et al*., 2006)

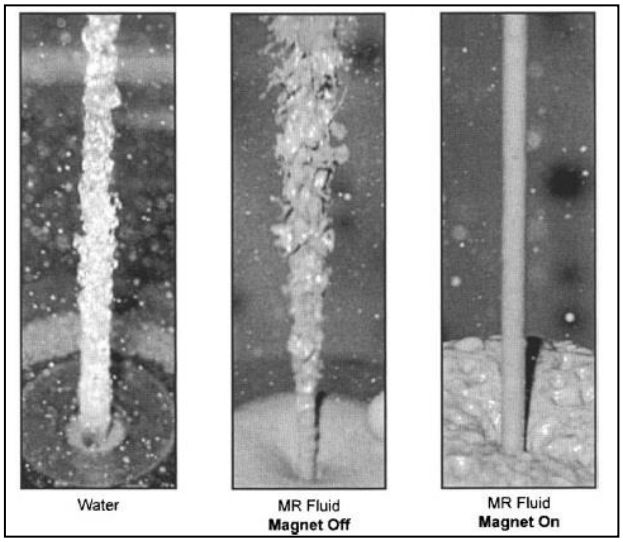

Figure 1.14: Jet print image (Kordonski *et al*., 2006)

1.2.8 Ball end type magnetorheological finishing

The main advantage of using ball end type of finishing process is to have a better control over the forces and produces a precise surface finish of a 3D work surface (Singh *et al*., 2012). Figure 1.15 shows the experimental setup of ball-end type magnetorheological finishing process. Magnetorheological fluid consists of carbonyl iron powder, abrasive particles, water

and additives (Sidpara *et al*., 2009) form a chain like structure for precise finishing of the work material. An additive includes stabilizers and surfactant for controlling the corrosion and wear rate (Genc and Phule, 2002). The MR polishing fluids restrict the steadiness against sedimentation and low viscosity in the lack of magnetic field (Bica, 2002). A magnetic field assisted finishing process was formed for producing extremely accurate finished surfaces with the help of magnetic abrasive (Ruben, 1987). The CIPs acquire the magnetic field strength and further combined into a chain like structure for finishing (Furst and Gast, 2000). Due to the shearing stress, material removal has taken place (Brecker *et al*., 1969).

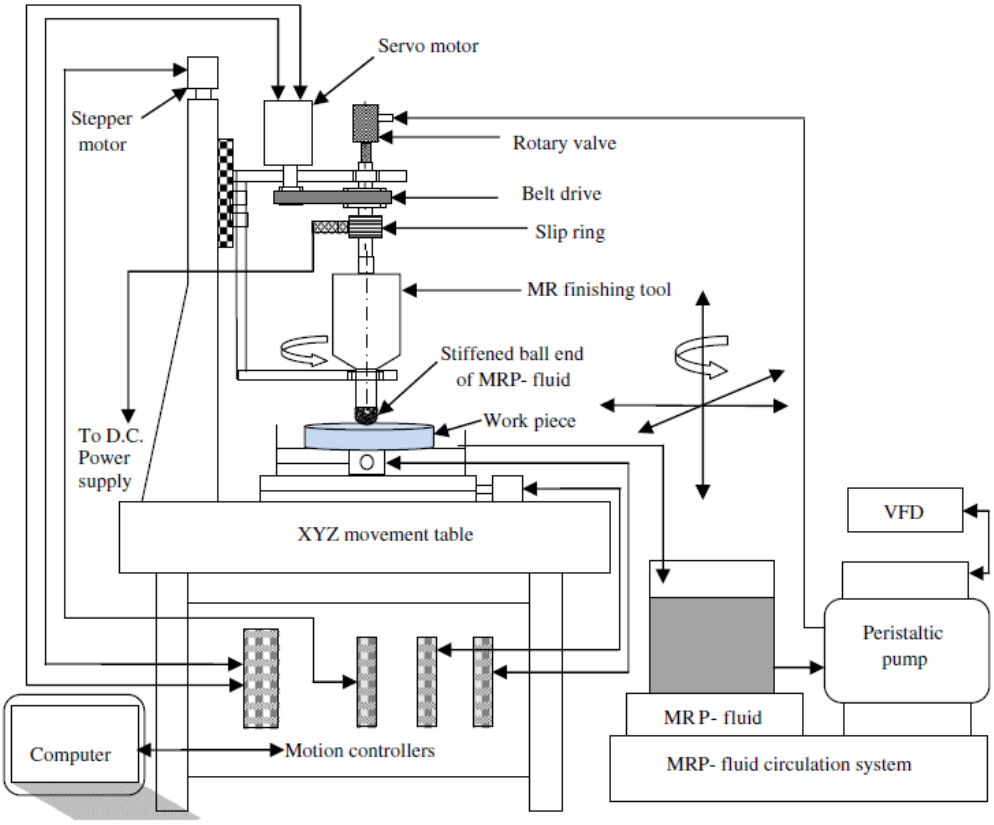

Figure 1.15: Investigational setup of ball-end type of magnetorheological finishing process (Singh *et al*., 2011)

The material removal mechanism during the ball end MRF process is as shown in Fig. 1.16. Due to the higher shear strength, the carbonyl iron particles chains will be capable to grasp abrasive particles more tightly and strongly like a single body for more period of time. The abrasive particles will penetrate more firmly on the roughness peaks due to higher magnetic field as shown in Fig. 1.16 (a). The elevated yield strength of finishing mark of MRP fluid circulates on the workpiece surface, than the high shear strength of engaged abrasives

particles will be capable to remove the peaks in the form of μ chips as shown in Fig. 1.16 (b). When nonstop feed rate is given to the workpiece then the final surface finish can be getting after wear of unevenness peaks due to abrasion as shown in Fig. 1.16 (c).

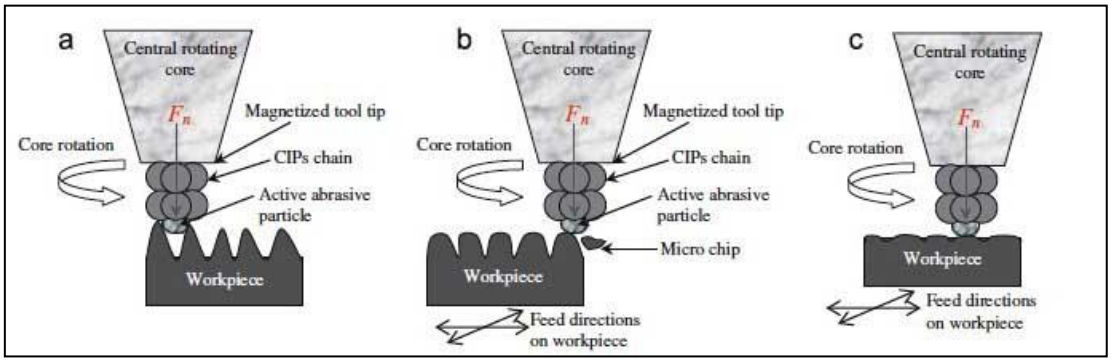

Figure 1.16: Mechanism of ball-end type of magnetorheological finishing process (Singh *et al*., 2013)

Singh *et al*., (2012) performed their experiment in ball-end based MR finishing tool for finishing of ferromagnetic material (EN31). The finishing was carried out by MR polishing fluid. With the process parameters (speed- 500 RPM, current- 4 Amp, time- 30 min and working gap- 0.66 mm), the results concluded that the surface roughness reduces to 19.7 nm with 120 min of a time interval as illustrated in Fig. 1.17 and Fig. 1.18.

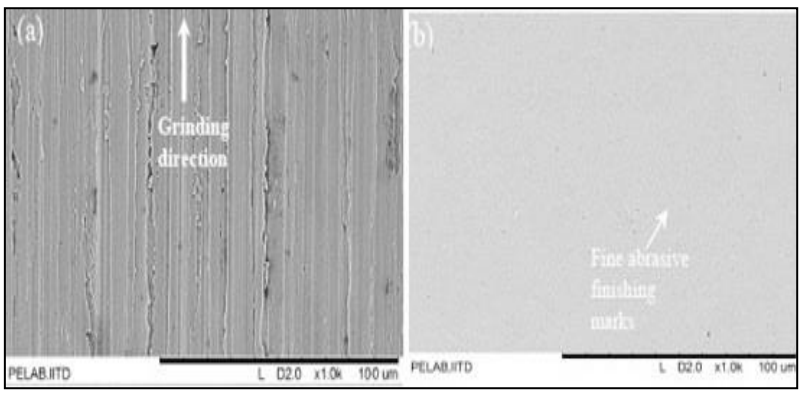

Figure 1.17: SEM analysis at 1000x (a) Initial surface without ball end MR finishing (b) Finished surface with 120 min of finishing time (Singh *et al*., 2012)

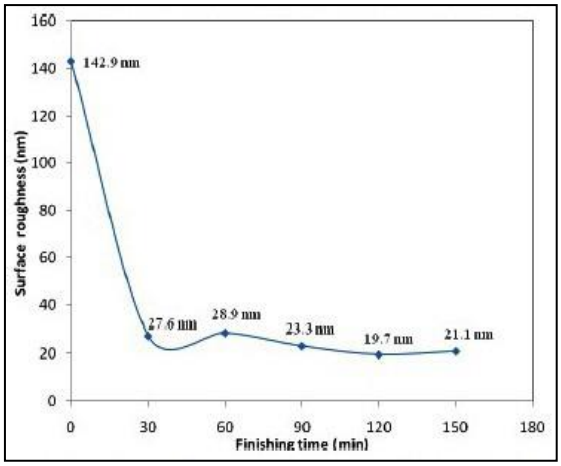

Figure 1.18: Effect of finishing time on surface roughness value of ferromagnetic workpiece (Singh *et al*., 2012)

1.3 Advantage of advanced finishing processes

- Closer tolerances can be achieved
- Increase the life of the work material
- Better sealing capabilities
- Decreasing the wear and friction losses
- Used for finishing of internal and external surfaces
- Reduces the surface defects (such micro cracks, cavity etc.)

1.4 Application of advanced finishing processes

The advanced finishing processes have its wide applications in finishing of automotive parts (such as bore of an IC engine, fuel injector component, cam shaft lobes, bearing race, connecting rod etc.) finishing of dies, electronic component, medical instrument, turbine component etc.

Chapter-2

Literature Review

2.1 Literature review

In this chapter, the literature survey of different authors in the field of advanced finishing processes (with/without the help of magnetic properties) have been discussed and their brief observations are drawn from the authors work and are represented for better understanding.

Cheng *et al.*, (2008) worked on wheel shaped polishing tool for finishing of K9 glass mirror by the use of MR fluid (usually a mixture of 33.84% carbonyl iron powder, 57.34% silicon oil, 2.82% stabilizing agent and 6% cerium agent). The experimental studies were conducted in two sets (with/without abrasive particles). The results declared that the surface roughness reducesto 0.47 nm (with viscosity- 8.9 Pa, voltage- 2V, time- 20 min).

Jain, (2008) studied the performance of different abrasive flow finishing processes for making a precise finishing in the level of nanometer without producing any damage to the work material. The author reviewed that the different advanced finishing processes can be used for finishing different shapes of work material such as complex shape, spherical, flat surface and cylindrical depending upon the type of finishing required.

Jain, (2009) reviewed the different types of finishing processes such as abrasive based advances micro finishing processes and nano finishing processes with external forces. The author summarizes the work done by the various authors with the help of various finishing processes. The different types of finishing processes can be selected depending upon the type of work material and finishing condition.

Jha and Jain, (2006) evaluated the effect of different grades of CIPs particles (CS and HS) on the surface finish by using MAFF for finishing of stainless steel material. MR polishing fluid (usually a mixture of 20% CIPs, 20% SiC abrasive powder and 60% visco plastic base medium) with which the finishing was done. The results concluded that higher improvement in surface roughness between 0.32-0.09 μm was made by using CIPs (CS) with SiC-800 mesh size as illustrated in Table 2.1.

Table 2.1: Surface roughness results (Jha and Jain, 2006)

Expt. No.	CIP dia. (D_{CIP}) (µm)	SiC dia. (D_{SiC}) (µm)	D_{CIP}/ D_{SiC}	Initial Ra (µm)	Final Ra (µm)	ΔRa^a (µm)	%ΔRa
1.	18.0 (CS)	19.00	0.95	0.32	0.09	-0.23	-17.87
2.	18.0 (CS)	12.67	1.42	0.28	0.17	-0.11	-39.28
3.	18.0 (CS)	7.50	2.40	0.31	0.23	-0.08	-25.80
4.	3.5 (HS)	19.00	0.18	0.26	0.23	-0.03	-11.54
5.	3.5 (HS)	12.67	0.28	0.28	0.24	-0.04	-14.28
6.	3.5 (HS)	7.50	0.47	0.25	0.24	-0.01	-4.00

Niranjan and Jha, (2014) worked on ball-end magnetorheological finishing process for finishing of mild steel. The experimentation was carried out by the use of bidisperse MR polishing fluid. The results concluded that the surface roughness value decreases to Ra-0.1406 µm as illustrated in Fig. 2.1.

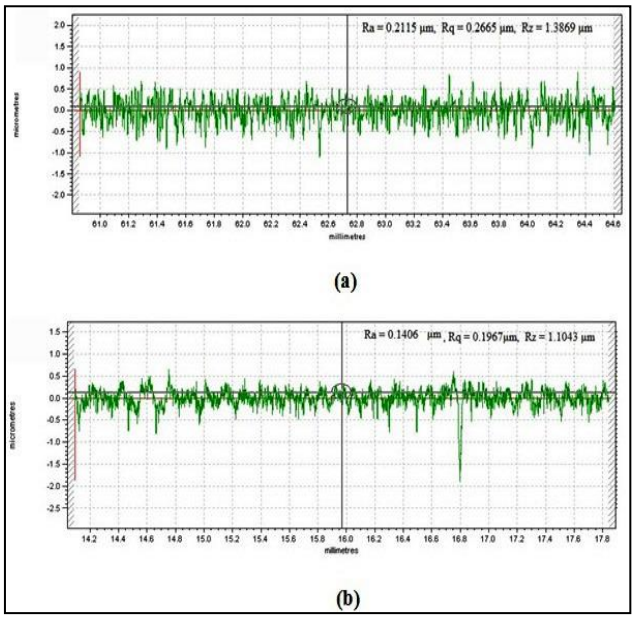

Figure 2.1: Surface roughness profile (a) before finish (b) after finish using bidisperse MR fluid (Niranjan and Jha, 2014)

Shankar *et al*., (2010) performed theoretical and experiment investigation on R-AFF process for comparing the performance of ΔRa and MR at different rotational on different types of work material specifically Al alloy, Al alloy/SiC MMC with 10% SiC and Al alloy/SiC MMC with 15% SiC. The results concluded that the R-AFF yields enhanced hardness and superior MRR as compared to the AFF in case of Al alloy/SiC (10%) MMC as illustrated in Fig. 2.2 below.

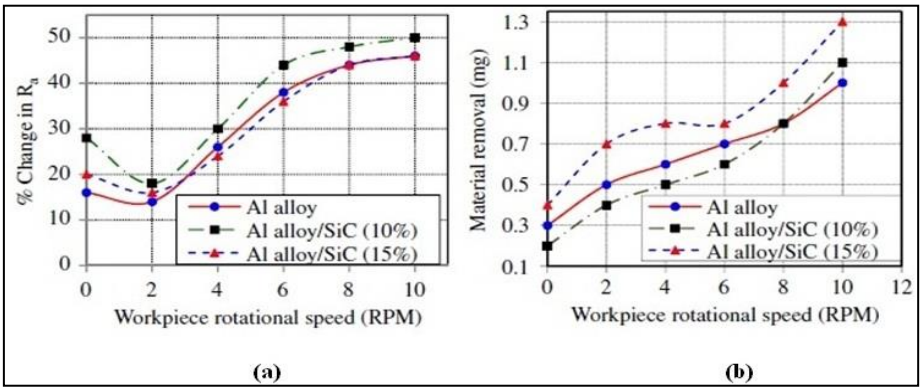

Figure 2.2: Consequence of workpiece on rotational speed on (a) Ra (b) MR for the three workspaces in AFF (RPM- 0) and in R-AFF (Shankar *et al*., 2010)

Sidpara and Jain, (2011) compare the performance of forces between the working gap and CIPs concentration by means of magnetorheological fluid based finishing method for finishing of the single crystal silicon. The authors use MR fluid (a mixture of CIPs and abrasive particle (SIC)). From the results, it was concluded that the normal and tangential forces reduces with increase in working gap but enhance with increase in CIPs concentration.

Sidpara and Jain, (2013) reported the outcome of normal and tangential forces with the angle of curvature of the surface and rpm of the tool by using magnetorheological finishing process on the freeform surface (stainless steel). The finishing was done by MR fluid (usually a mixture of CIPs, abrasive particles and glycerol). From the results it was concluded that both normal and tangential forces decreases with increases in the angle of curvature ($\theta = 5^o$, 15^o and 25^o) and increases with the increase in rotations.

Singh *et al*., (2004) worked on magnetic abrasive process in order to determine the outcome of process Parameters on the surface finish by using a mixture of 75% iron and 25% SiC with different parameters. It is found that the value of surface roughness ΔRa was improved within the selected parameters of voltage-11.5 V, working gap-1.25 mm, speed-180 RPM improving the surface roughness values as shown in Fig. 2.3 below.

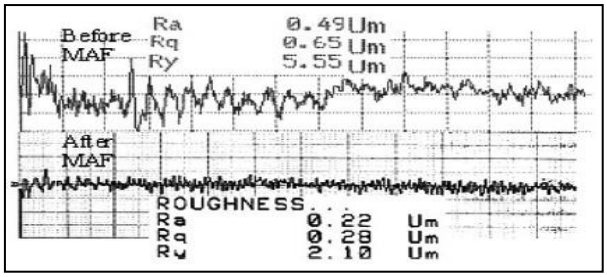

Figure 2.3: Surface roughness values before and after finishing (Singh *et al*., 2004)

Sidpara and Jain, (2012) evaluated the theoretical and experimental analysis of normal and tangential forces by using magnetorheological finishing process for finishing of single crystal silicon. The finishing was done by MR fluid (usually a mixture of CIPs, abrasive particles and glycerol).

Wang and Lee, (2009) worked on magnetic finishing process for precise finishing of cylindrical type (SKD-110 mould steel. The finishing medium includes silicone gel, steel grid (SG) and silicon carbide. The results concluded that the surface roughness with magnetic field shows better results. With the increase in the quantity of SiC particles, the surface roughness decreases, whereas MRR increases.

Singh *et al*., (2012) performed their experiments on ball end MRF tool for finishing of ferromagnetic magnetic material with different projections (such as flat, 30^{o}, 45^{o} and 50^{o} curve surface) as shown in Fig. 2.4. According to the results it was found that the surface roughness of flat, 30^{o}, 45^{o} and 50^{o} curve surface reduces to 18.7 nm, 30.4 nm, 71.0 nm and 123.7 nm. The finite element analysis is shown in Fig. 2.5 and Fig. 2.6.

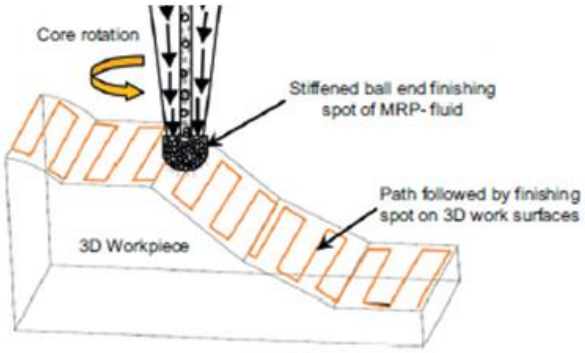

Figure 2.4: Schematic of a (BEMRF) process of the complex 3D workpiece surfaces (Singh *et al*., 2012)

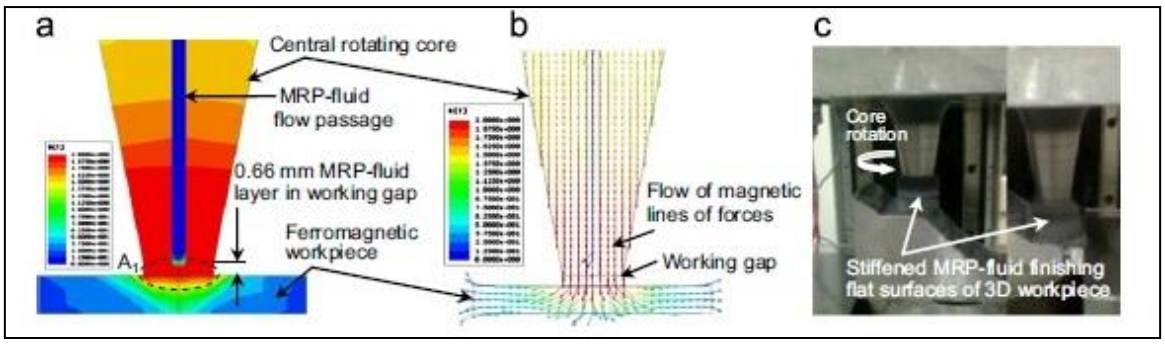

Figure 2.5: FEA for (a) magnetic flux density distribution (b) flow of magnetic lines of forces (c) finishing of the flat surfaces of a complex 3D workpiece (Singh *et al*., 2012)

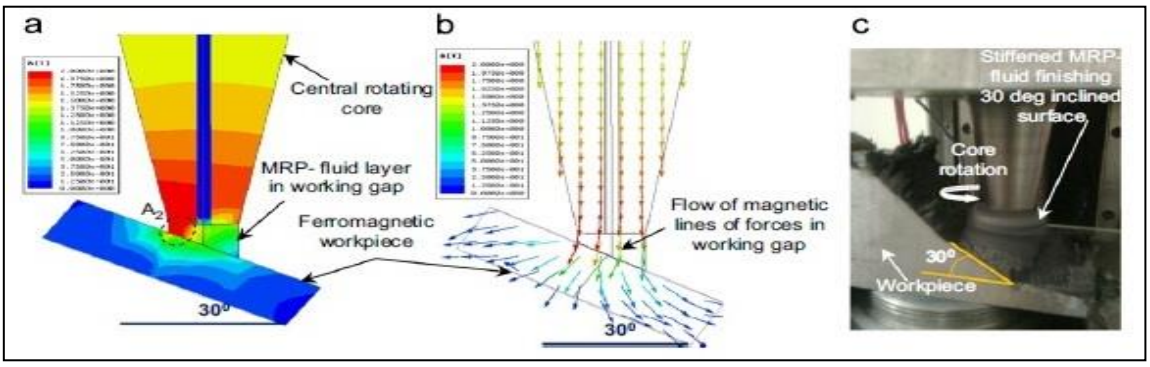

Figure 2.6: FEA for (a) magnetic flux density distribution (b) flow of magnetic lines of forces at 30^{o} inclined surface (c) snapshot of finishing the 30^{o} inclined surfaces of a complex 3D workpiece (Singh *et al*., 2012)

Wang and Hu, (2005) compared the value of MRR and surface roughness with finishing time with the help of magnetic assisted finishing process for finishing. The experimentation was carried away with 4 different types of abrasive particle were Al_2O_3/Fe (20% Al_2O_3), TiC/Fe (20% TiC), TiC/Fe (35% TiC), TiC/Fe (7% TiC) along with a finishing fluid (stearinic acid and transformer oil). The results concluded that the value of MRR increases whereas the value of surface roughness decreased with the increased in finishing time.

Singh *et al*., (2013) compare the theoretical and experimental investigation on MRR with different working gaps by using ball end type MR finishing tool for finishing ferromagnetic material. The theoretical observation was carried out by using the mathematical formulas for calculating the normal forces at different working gap. The finishing was carried out with MR fluid (usually a mixture of 20% CIPs, 20% SiC abrasive powder and 60% visco plastic base medium. The results concluded that the surface roughness decrease to 0.028 µm with 0.66 mm working gap as illustrated in Fig. 2.7 below.

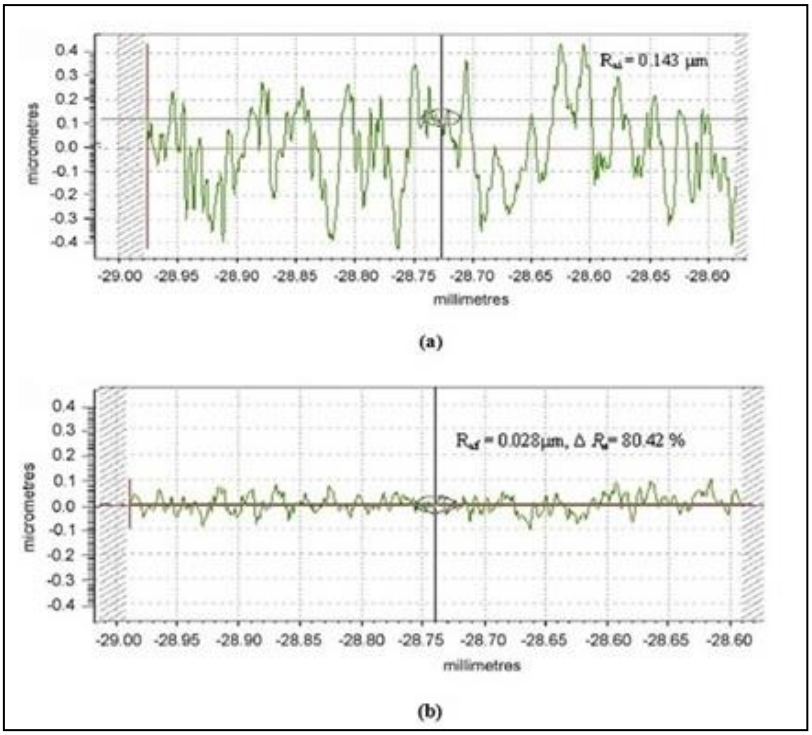

Figure 2.7 Surface roughness profiles (a) Initial (b) After BEMRF at 0.66 mm working gap with Fn- 16.35 N (Singh *et al*., 2013)

Yamaguchi and Shinmura, (2004) performed their experiment on the magnetic assisted finishing process. The experimentation was performed by using different iron particle (150, 330 and 510 µm), diamond abrasive (0-1, 2-4, 4-8 and 8-12 µm) and lubricant (0.1, 0.2, 0.25, 0.3 and 0.35 ml) for precise finishing of alumina ceramic tube. The results concluded that with the use of iron particle (330 µm), diamond abrasive (0-1 µm) and lubricant (30 ml), the surface roughness reduces to 0.02 µm.

Yin and Shinmura, (2004) compare the performance of surface roughness and deburring on three different substrates by using vibration-assisted magnetic finishing process. The finishing was carried out with process iron particles, WA magnetic alumina and straight oil type grinding fluid on magnesium alloy (AZ31B), stainless steel (SU304) and brass (C2680). The results concluded that the surface roughness and deburring was found to better in magnesium alloy (AZ31B) as compared to other 2 materials.

Das et al. (2012) compare the performance of R-MRAFF with MRAFF in order to study the effect of number of cycles and extrusion pressure on the change in surface finish ΔRa. The finishing was carried out with the help of CIPs, SiC abrasive particles along with visco plastic medium. The preliminary experiment was carried on, brass, stainless steel and EN-8 work

materials. The result concluded that the highest improvement in surface finish was observed in case of brass whereas least in case of EN-8. The experimental analysis was carried with the help of R-MRAFF for finishing of stainless steel and brass work material by the use of ANOVA method. The process parameters such as, rotational speed, extrusion pressure, number of finishing cycles, and vol. Ratio of CIP/SiC were varied. The result concluded that surface roughness of brass reduces to 0.05 µm whereas for stainless steel reduces to 0.11 µm.

Jha et al. (2007) performed their experiment on magnetorheological abrasive flow finishing process to facilitate the study the outcome of extrusion pressure and number of cycles at the time finishing stainless steel work material. The finishing was carried out with the help of (20% CIPs, 20% SiC abrasive particles and 60% visco plastic base medium. The result concluded that with the increase in extrusion pressure up to 3.75 MPa, and number of finishing cycle, the average surface roughness value decreases.

Das et al. (2010) worked on revolving MAFF process for finishing of stainless steel work material. The finishing was carried out with the help of MR polishing (usually contains 26.6% Fe powder, 13.4% SiC abrasive along with base medium). The preliminary experimentation along with design of experiment and response surface regression analysis were also carried out in order to determine the outcome of abrasive particle size, rpm of magnet and finishing time on the surface roughness. The results concluded that with the increase in RPM (up to 150) and finishing time (1600 sec) the surface roughness founds to be better, whereas with the decrease in abrasive particle size (150), the surface roughness founds to be better.

Judal et al. (2013) developed a new vibration assisted magnetic abrasive finishing process for finishing of aluminium workpiece. The finishing was carried out with the help of steel grit and Al_2O_3 abrasive. The outcome of various process parameters such as rpm, frequency, magnetic flux density and dimension of abrasive particles on MRR was investigated. The result concluded that with the enhance in rpm and magnetic flux density and frequency of vibration, the value of MRR increases. The surface roughness value Ra reduces to 0.18 µm.

Hong et al. (2012) performed their experiment on MR polishing for finishing of alumina reinforced zircon ceramics (3YTZP/Al_2O_3-20%). The finishing was carried out with MR fluid (50% CIPs, abrasive diamond particles and DI water). The main process parameters (speed- 200 and 300 RPM, magnetic field- 3.8, 4.7, 5.5 and 6.1KA/m, Time- 10, 20, 40 and 60 min). The results concluded that with 300 RPM, magnetic field- 3.8 KA/m and electric current- 0.5 Amp the surface roughness decreases from 0.272 µm to 1.960 nm.

Cheng et al. (2010) developed a dual axis MRF tool with internal magnet for finishing of BK7 mirror. The finishing was carried out with the help of MR fluid (includes 10% CeO_2 abrasive particles). The mathematical modelling was carried out in order to calculate material removal. The process parameters were (magnetic field strength- 860KA/m and polishing time- 1 min). The results concluded that the surface roughness value decreases from 328.42 nm to 42.93 nm.

Kang et al. (2012) designed and developed a newly built magnetic abrasive finishing (with double dipole tip set) for finishing of austenite 304 stainless steel tubes. The mixed type magnetic abrasive consists of (80% iron particles and 20% magnetic abrasive) along with a soluble type barrel finishing compound. The process parameters were (magnetic flux- 1.26-1.29T, speed- 500-30000 rpm, processing time- 10 to 20 min and workpeice pole tip clearance- 0.3 mm). The initial surface roughness of 304 stainless steel was 2-3 µm. The results concluded that at 10000 rpm the surface roughness decrease to 0.1 µm (for 10 min) whereas, the surface roughness at 10000 rpm decrease to 0.11 µm (20 min).

Schmitt et al. (2013) performed their experiment on a commercially available honing machine for finishing of 16MnCr5 hardened steel. The honing machine uses a single stone tool equipped with a honing stone containing CBN with abrasive in a metallic sintered bond and a two guide stone with a diamond grains. The experimental parameters were speed- 1600 rpm, stroke velocity- 0.26 m/sec and material removal- 3 mm respectively. The experimentation was carried by the use of 3 closed loop controller (P1, P2 and P3) for controlling the process. The result concluded that the straightness was slightly better for P3 controller, whereas parallelity was better for P2 controller. The (P2 and P3) controller provides the better results as compared to P1 controller.

Kordonski et al. (2004) performed their experiments on newly planned and developed magnetorheological jet finishing process for finishing of merged glass silica (optics). MR jet polishing system was mounted on 5-axis computer numeric control platform equipped with polishing control software. The MR fluid was prepared with the help of water and abrasives mixture. The initial surface roughness's of fused glass silica were 0.47 µm p-v, 0.14 µm rms. The experimentation was also conducted on small concave fused glass silica with initial surface roughness were 210 nm p-v and 50 nm rms. The roughness profile was measured with the help of (New View 500 white light) interferometer. The theoretical and experimental MRR and rate of the work profile was also evaluated. According to the results, it is concluded that the surface values of fused glass silica reduces to 13 nm p-v and 2 nm rms whereas, for

concave fused glass silica reduces to 44 nm p-v and 6 nm rms. The theoretical and experimental observation

Gheisari et al. (2014) developed a magnetorheological finishing process for even more accurate finishing of Aluminium work material (cylindrical type). The MR fluid consists of water based suspension of micron sized diamond particles. The process parameters were (current- 9A and working gap- 5 mm). The initial surface roughness of the work material was 170 nm. The experimentation was conducted in three sets. In first set, the work material speed varies from 250-1000 rpm. In second set, the process time varies from 20-100 min. In third case, the effect of a fast RAM on the surface roughness was considered. The results concluded that with the increase in rotational speed (1000 rpm), the surface roughness value improves by 40 nm. With the increase in finishing time of 90 min, the surface roughness value reduces to 42 nm whereas, when the fast RAM (with 0.5 m/sec) was applied, the surface roughness value improves by 78 nm.

Das *et al*., (2008) reported the effect of number of cycles on the surface finish by using magnetorheological abrasive flow finishing process for finishing of stainless steel workpiece. The finishing was done by MR fluid (usually a mixture of 20% CIPs, 20% SiC abrasive powder with 60% visco plastic base medium. The results concluded that with the increase in the number of cycles, the value of surface finish increases for both experimental and theoretical cases.

2.2 Research Gap

From the literature review, it has been found that the developed ball end milling process with the centrally hole in the core is used for nano finishing. The main likely limitations of this developed process are –

- Due to central hole in core for MR polishing fluid, comparatively very less or almost negligible finishing occurs at centre point when finishing has done without giving feed.
- Non uniform magnetic flux density at the tool tip surface due to central hole in core.
- Comparatively more costly because of feeding the MR polishing fluid centrally, they have used variable frequency drive (VFD), peristaltic pump, rotary valve and slip ring etc.

To overcome these limitations, the process is developed without central hole in the core. The main advantages of using this process are as given below-

- Due to without central hole in core, almost uniform finishing occurs when finishing is done without giving feed.
- Almost Uniform magnetic flux density on the tool tip surface due to without central hole in core which results in uniform finishing.
- Comparatively less costly because of MR polishing fluid is directly feed externally at the tool tip surface during the finishing operation.

2.3 Objectives of the present work

To achieve the main objective such as development of low cost ball end MRF process, the following sub-objectives are:-

- To carry out the finite element analysis for analyzing the distribution of magnetic flux density at the tool tip surface for both the cases such as with hole and without hole in the tool rotating core.
- To fabricate the low cost ball end magnetorheological finishing tool.
- To fabricate the fixture to hold the work piece during the finishing operation.
- To demonstrate the performance of present developed finishing process in terms of uniformity in magnetic field at the tool tip surface and uniformity in surface roughness values on the finished surface without giving any feed during the finishing operation and comparatively less time for nanofinishing.

2.4 Methodology

The current work is to development of low cost ball end Magnetorheological Finishing Process. In this chapter, step by step methodology is defined for the selection of various components.

- Proper selection of z slide and motor
- Proper selection of x-y slide
- CAD model of MRF tool
- Finite element analysis of MRF tool
- Fixture for holding MRF tool
- Selection of bearing
- Selection of timing belt and pulley

The Finite element analysis is done in MAXWELL ANSOFT V13 (student version) and then CAD modeling is done of MRF tool in CREO elements/PROE. The flow diagram narrated in the Fig. 2.8 displays the design steps of followed in fabrication of the MRF tool.

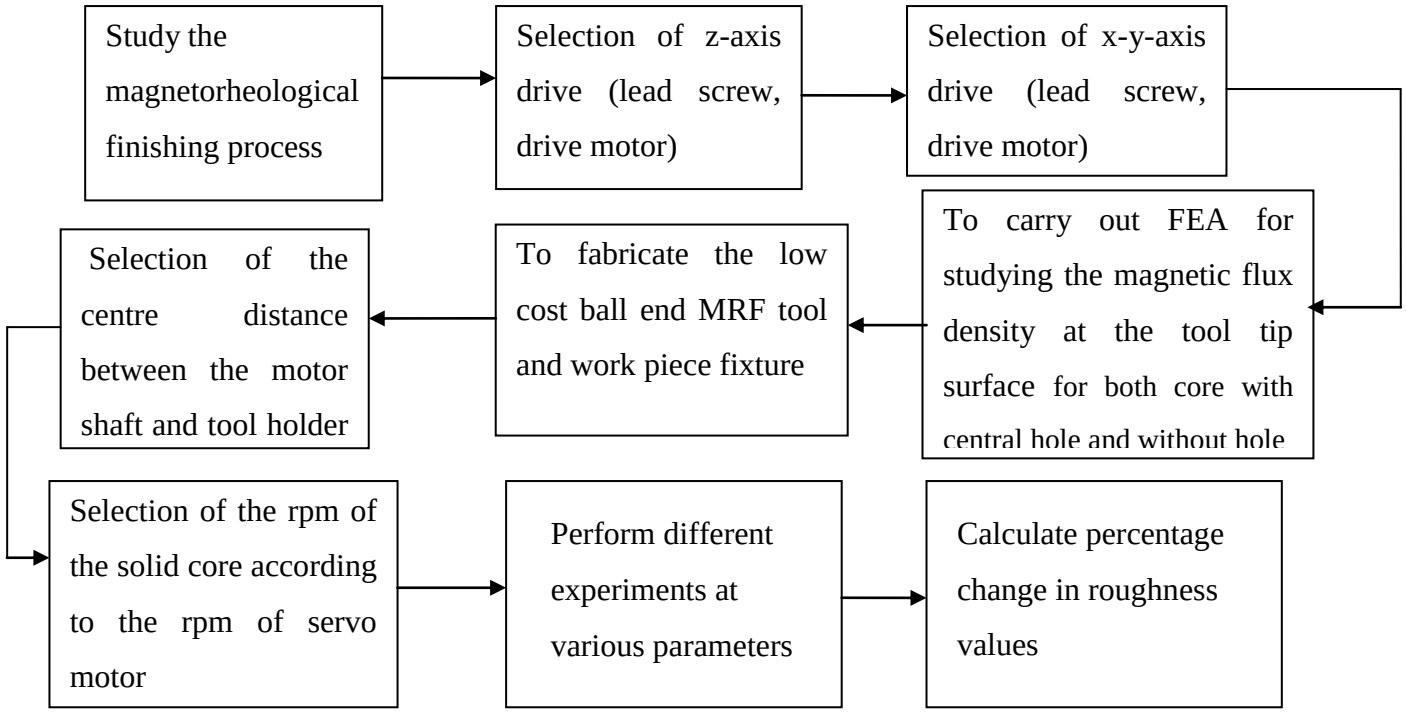

Figure 2.8: Flow chart for the development of ball end MRF tool

Chapter-3

Development of Low Cost Ball End Magnetorheological Finishing Process

From literature review, it has been found that ball end MRF process is used for milling type of finishing operations usually on flat and 3dimensional surfaces. The ball end MRF process has advantages over finishing the surfaces such as deeper locations in workpiece. In the present developed low cost ball end MR finishing process, cost and uniformity in magnetic field are taken as bigger issues. It can finish surface of workpiece in the same way as in earlier ball end MR finishing process but difference is in the supply of MR polishing fluid externally at the tool tip surface. A PLC controlled experimental setup with human machine interface (HMI) is developed to examine the process performance. The magnetostatic simulations were done on ferromagnetic materials to observe the magnetic flux density at the tip of MR finishing tool. The experiments were conducted on the flat mild steel strip to study the effect of finishing time on the change in surface roughness values.

3.1 Development of low cost ball end magnetorheological finishing process

In this chapter, the procedure for development of low cost ball end magnetorheological finishing process has been explained. The schematic diagram of a low cost ball end MR finishing machine setup is shown in Fig. 3.1. Removal of material and finishing of surfaces in low cost ball end magnetorheological finishing process is based on abrasive action. When electromagnet is switched on, the MRP fluid becomes stiff. The carbonyl iron particles (CIP's) chain holds the abrasive particle, as the flux density is maximum at the tool tip so the CIP's chain attract towards the tool tip. The material removal mechanism in low cost ball end magnetorheological finishing process is shown in Fig.3.3. The MRP fluid is comprises of CIP's, abrasive particles i.e. silicon carbide and base fluid. The material removal process takes place due to shearing between solid core and workpiece. As it is super finishing process, removal of material is very less in microns.

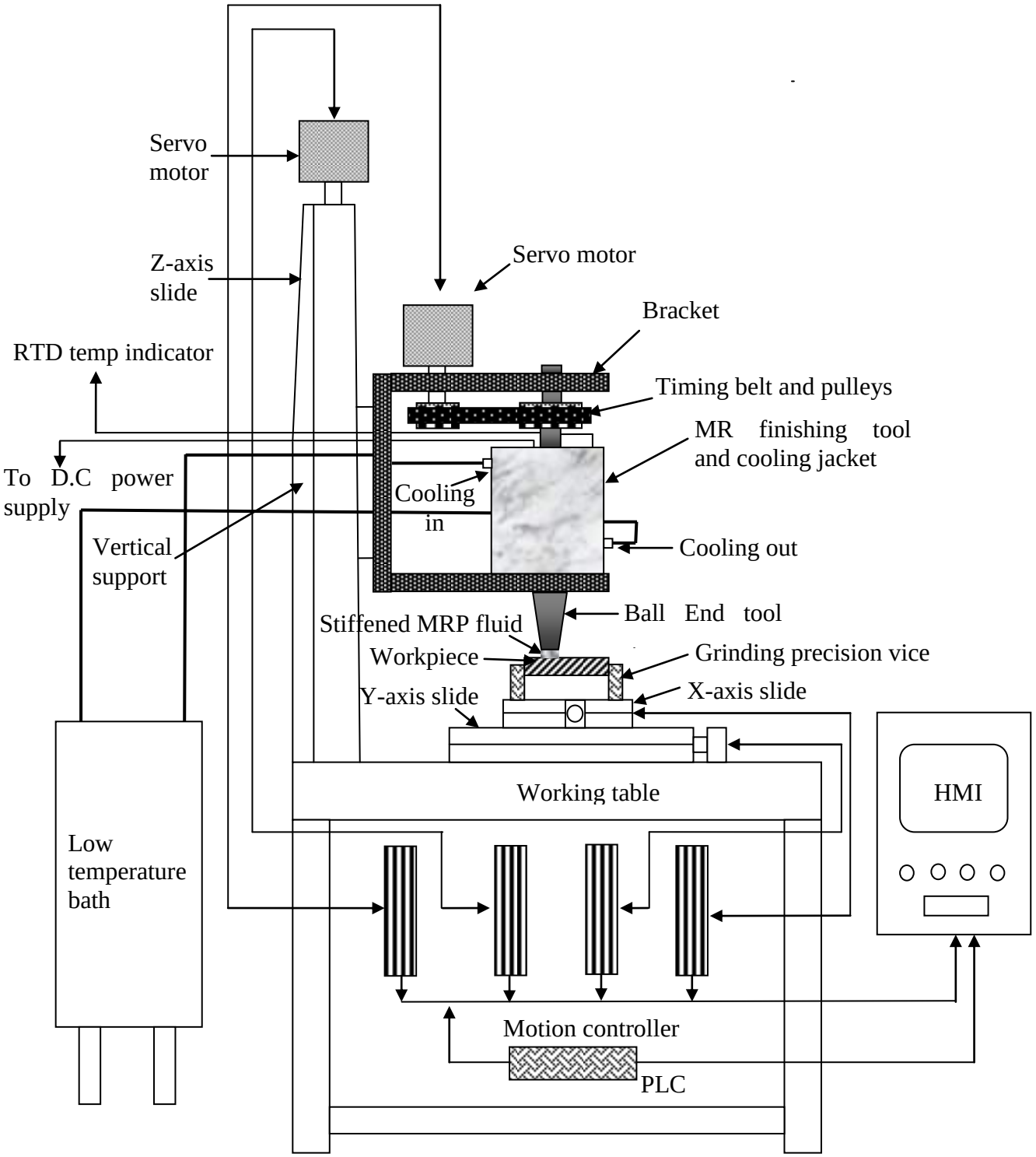

Figure 3.1: Schematic diagram of the low cost ball end MR finishing process

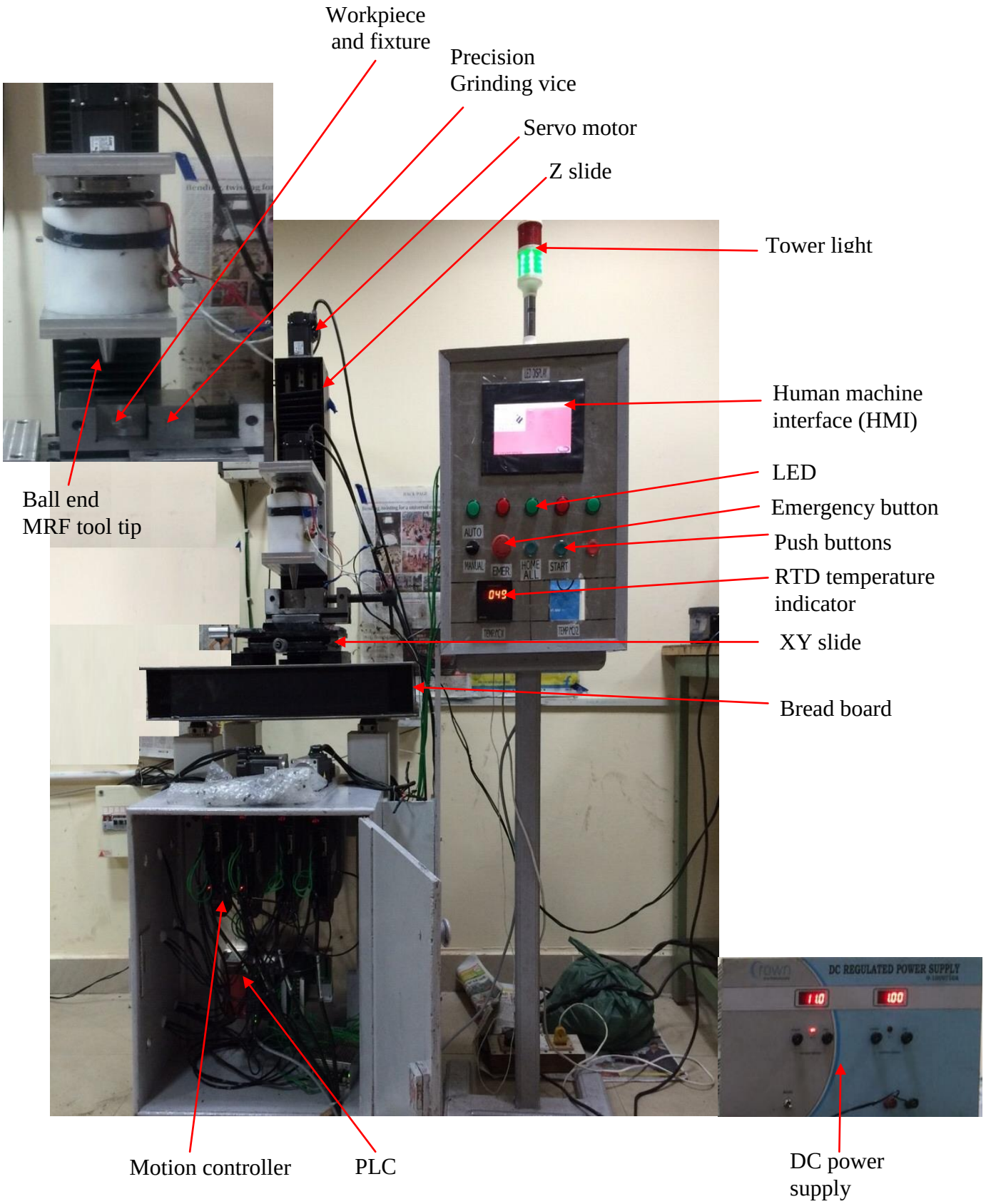

Figure 3.2: Photograph of the low cost MR finishing machine setup

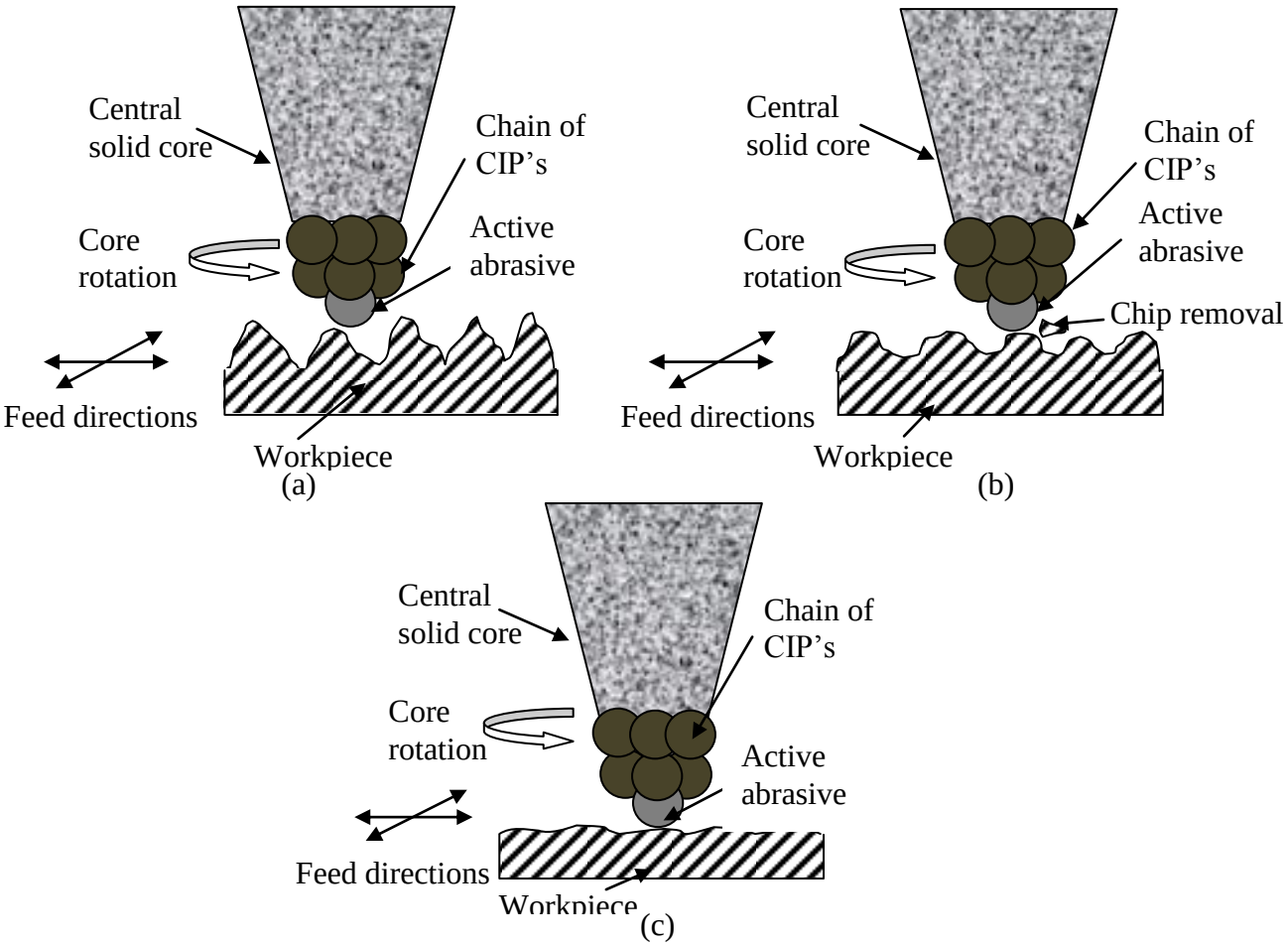

Figure 3.3: Schematic diagram of mechanism of material removal (a) initial roughness peaks of workpiece surface and gripped abrasives particle with CIP's chain (b) micro chip removal (c) final roughness peak

3.2 Finite element analysis of MRF tool

The finite element analysis of MRF tool is done in MAXWELL ANSOFT V13 (student version). The previous work is done with central hole in core but in present work without central hole in core is used which enhances surfaces finish. It will improve homogeneity in surface finish and good magnetic field variation around tip and workpiece. There are different phases in MAXWELL ANSOFT V13 for finite element analysis of MRF tool. The phases which are used in analysis of this MRF tool are given below-

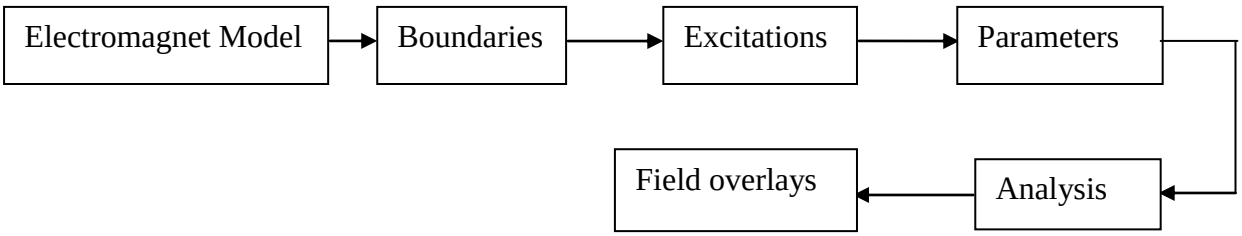

Figure 3.4: Flow diagram of different phases in MAXWELL ANSOFT V13 (student version)

Initially in finite element analysis, start with draw model in MAXWELL ANSOFT V13. It is the part of ANYS which is used for magnetic field analysis. In modelling, draw the electromagnet with appropriate dimensions. There is one option add material in which the value of relative permeability has given for adding material. In this case, for adding MR fluid relative permeability 5 is given. Secondly, in FE analysis boundaries has selected. There are different boundaries like insulating, master, slave etc. But for MRF tool, insulating boundary is selected for coil. After selecting insulating it appears with insulating hatching.

Thirdly, in MAXWELL ANSOFT V13 excitations have selected. In excitations, there are different assigning parameters like current, current density, voltage, voltage density etc. In this case, current which is NI i.e. number of turns into current in ampere is given at both the end of copper coil. After that in analysis, parameters have selected. In this software there are different parameters like force, torque and matrix. For MRF tool, parameter force is selected for calculating normal force at workpiece in Newton.

After selecting boundary, proceed for analysis. In this step, for analysis firstly add solution setup and give it any name then analyse it. After completing this further proceed for last but not least named field overlays. In this step fields i.e. both B and H fields is drawn with proper selection of lists and planes from software. In field overlays, there are several other options like modify plots, animate etc.

For finite element analysis, process parameters are gap, current and number of turns. The numbers of turns are taken 2000 and current is 5 amps for this analysis.

3.2.1 Electromagnet modelling of MRF tool

The electromagnetic modelling of MRF tool is the first phase in the MAXWELL ANSOFT V13. For comparison between core with central hole and without central hole, both electromagnet models have made. The electromagnet model of MRF tool is shown in Fig.

3.5. There are some parameters which are assigned to electromagnet model are shown in Table 3.1 below. These parameters are included with relative permeability and material. The current and number of turns which are constants also given in table below. According to the table, it is very clear about the relative permeability values which were used while modelling.

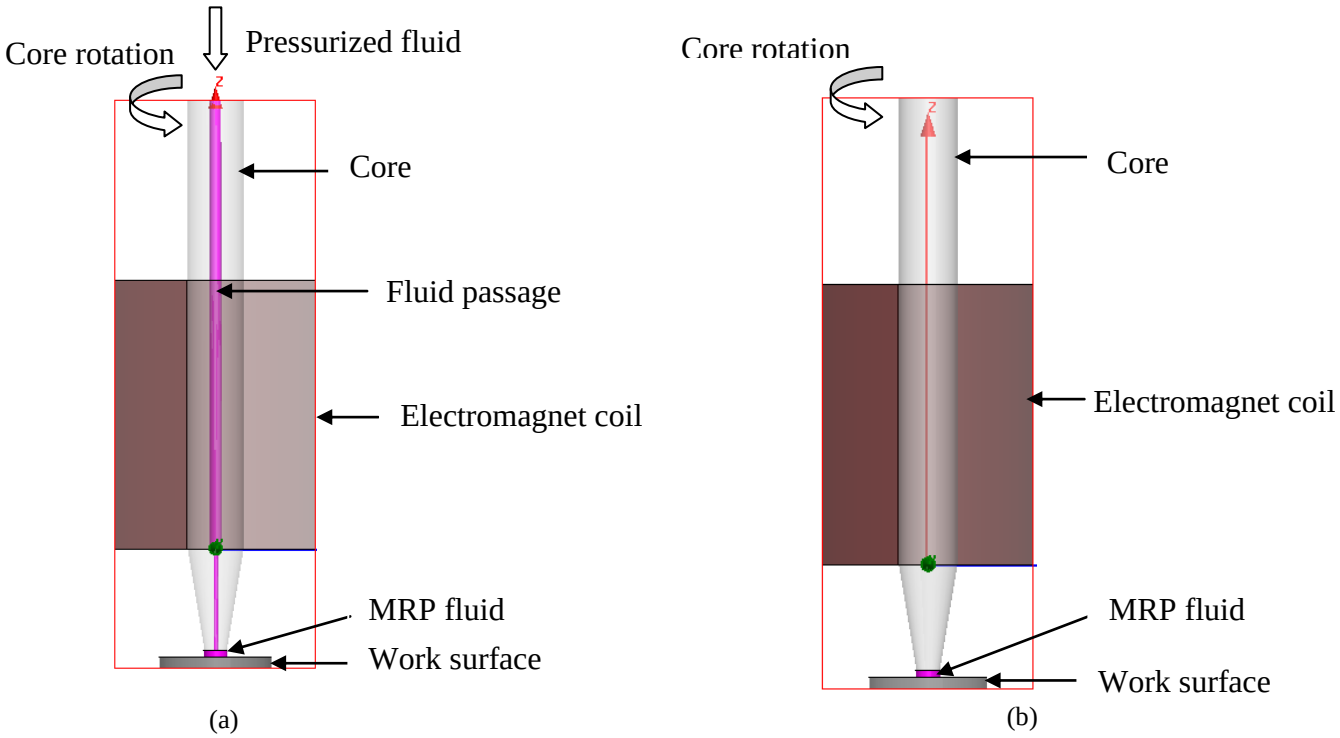

Figure 3.5: Electromagnet model of core (a) with central hole (b) without central hole

Table 3.1: Parameters assigned to electromagnet model

Parameter	**Material**	**Relative Permeability**	**Current**	**No. of turns**
Electromagnet coil	Copper	1	5A	2000
Inner core	Iron	4000		
MR Polishing fluid	MRP fluid	5		
Ferromagnetic	Iron	4000		
Non ferromagnetic	Copper	1		

3.2.2 Magnetostatic FEA with workpiece

After making electromagnet model of both core with central hole and without central hole, start with magnetostatic simulations along with workpiece. There are various cases which are studied for both ferromagnetic and non ferromagnetic workpiece by changing gap between

workpiece and MRF tool. So, therefore some of the simulations with field overlays are as follows below-

With gap=0.5 mm for ferromagnetic workpiece

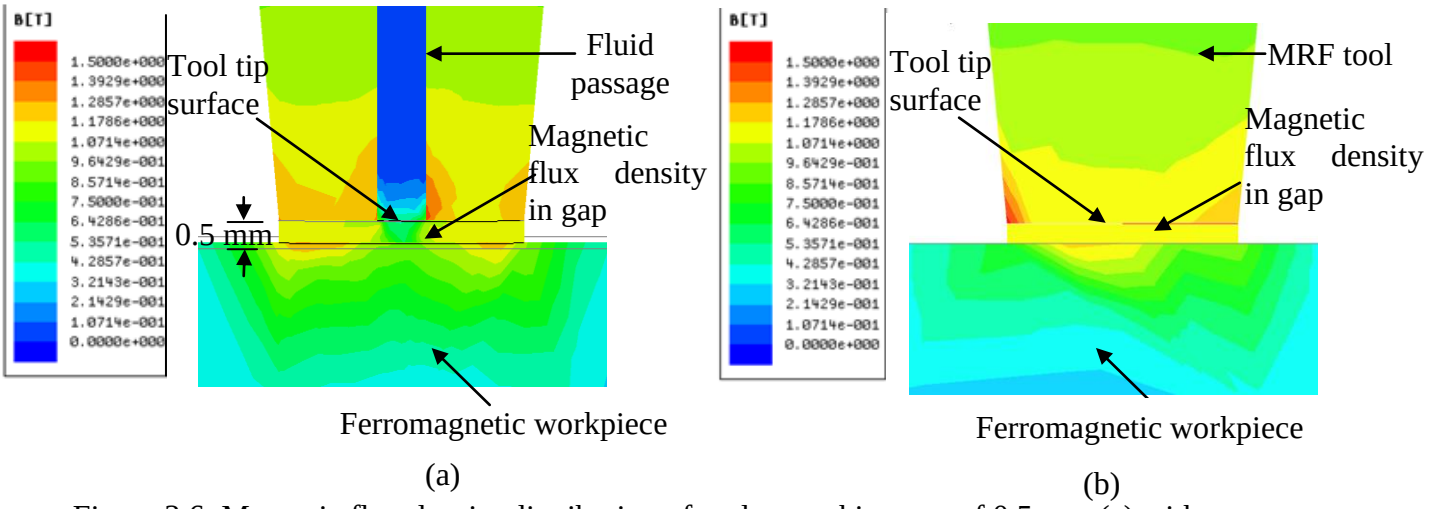

Figure 3.6: Magnetic flux density distribution of tool at working gap of 0.5 mm (a) with central hole and (b) without central hole

According to the results of simulation in MAXWELL ANSOFT V13, the magnetic field at working gap is less in case of core with central hole as compare to without hole as shown in Fig. 3.6 above. The uniformity of magnetic field in solid core i.e. Fig. 3.6 (b) is more than in core with hole i.e. Fig. 3.6 (a) at 0.5 mm gap.

With gap=1 mm for ferromagnetic workpiece

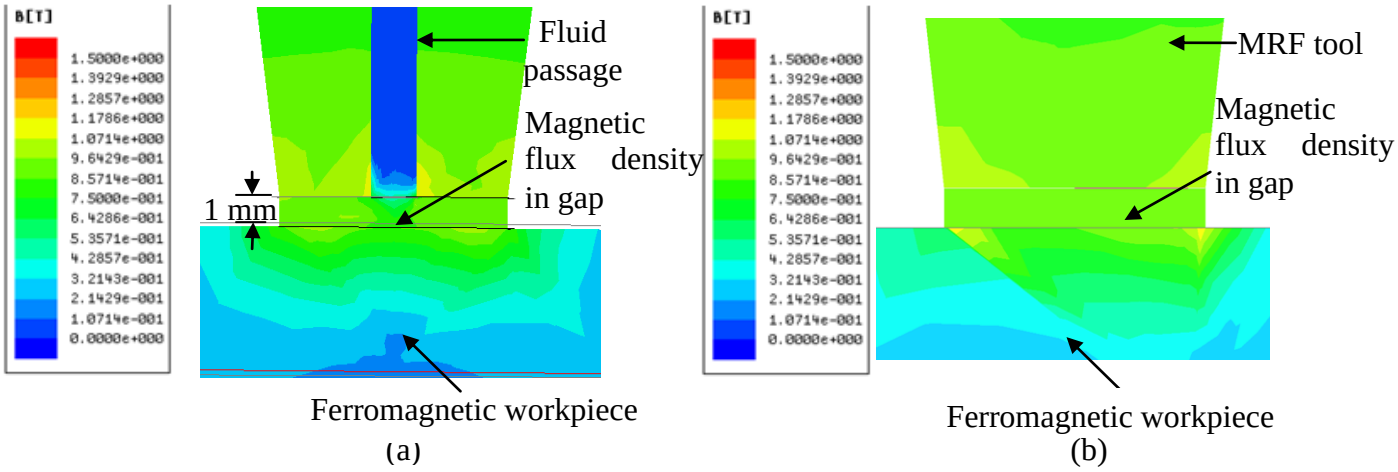

Figure 3.7: Magnetic flux density distribution of tool at working gap of 1 mm (a) with central hole and (b) without central hole

According to the results of simulation in MAXWELL ANSOFT V13, the magnetic field at working gap is less in case of core with central hole as compare to without hole as shown in Fig. 3.7 above. The uniformity of magnetic field in Fig. 3.7 (b) is more than Fig. 3.7 (a) i.e. uniformity in without hole is more than with hole at 1 mm working gap.

With gap=1.5 mm for ferromagnetic workpiece

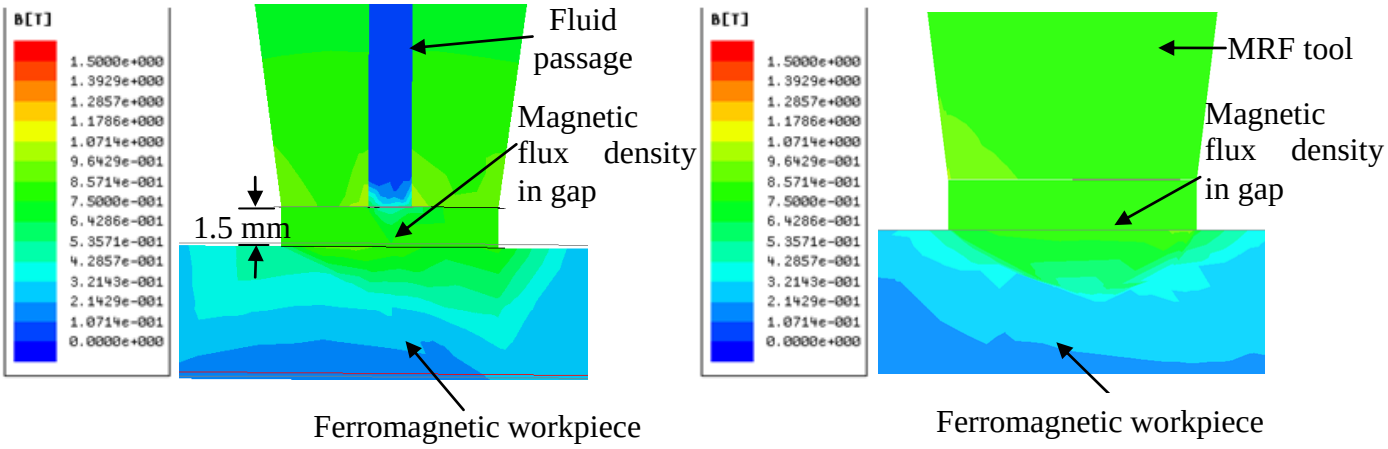

Figure 3.8: Magnetic flux density distribution of tool at working gap of 1.5 mm (a) with central hole and (b) without central hole

According to the results of simulation in MAXWELL ANSOFT V13, the magnetic field at working gap is less in case of core with central hole as compare to without hole as shown in Fig. 3.8 above. The uniformity of magnetic field in Fig. 3.8 (b) is more than Fig. 3.8 (a) i.e. uniformity in without hole is more than with hole at 1.5 mm working gap.

With gap=2 mm for ferromagnetic workpiece

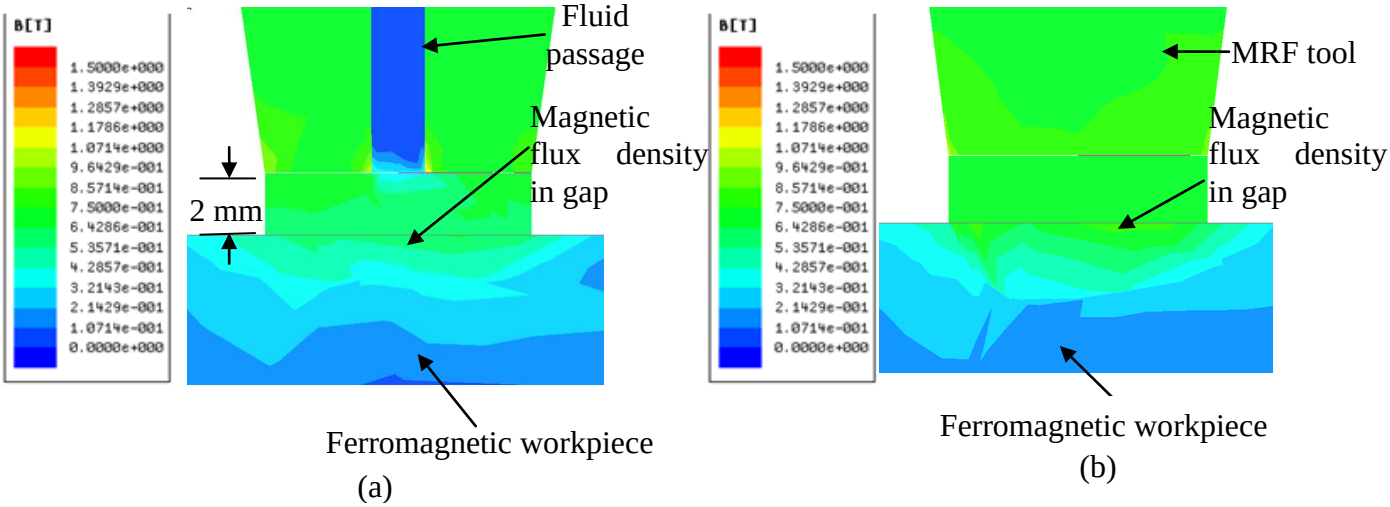

Figure 3.9: Magnetic flux density distribution of tool at working gap of 2 mm (a) with central hole and (b) without central hole

According to the results of simulation in MAXWELL ANSOFT V13, the magnetic field at working gap is less in case of core with central hole as compare to without hole as shown in Fig. 3.9 above. The uniformity of magnetic field in Fig. 3.9 (b) is more than Fig. 3.9 (a) i.e. uniformity in without hole is more than with hole at 2 mm working gap.

With gap=2.5 mm for ferromagnetic workpiece

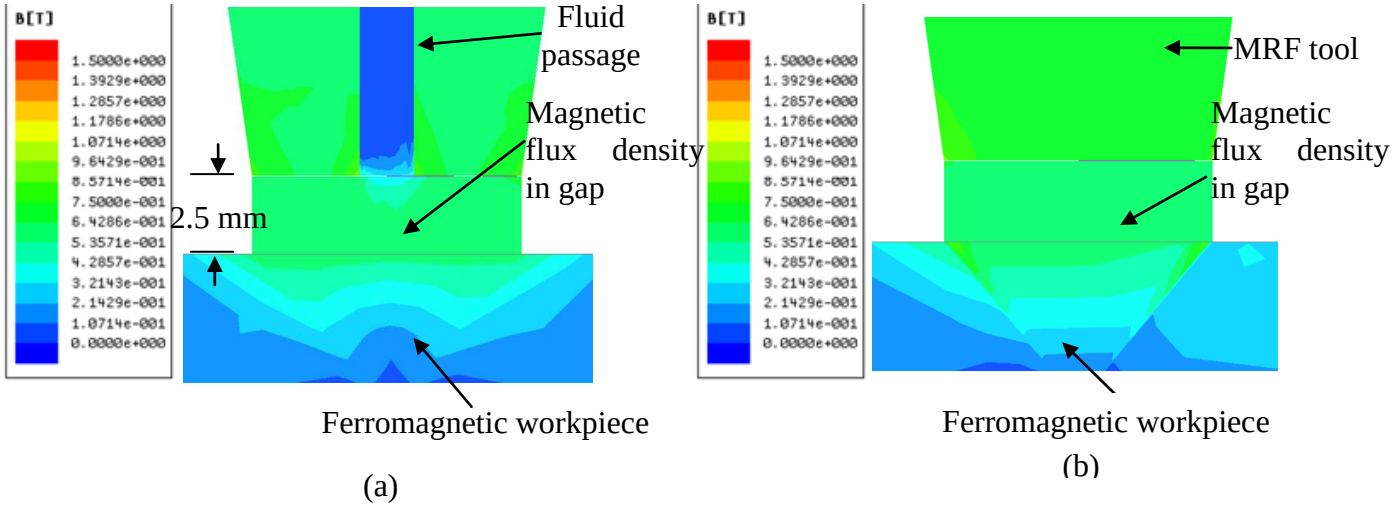

Figure 3.10: Magnetic flux density distribution of tool at working gap of 2.5 mm (a) with central hole and (b) without central hole

According to the results of simulation in MAXWELL ANSOFT V13, the magnetic field at working gap is less in case of core with central hole as compare to without hole as shown in Fig. 3.10 above. The uniformity of magnetic field in Fig. 3.10 (b) is more than Fig. 3.10 (a) i.e. uniformity in without hole is more than with hole at 2.5 mm working gap.

With gap=3 mm for ferromagnetic workpiece

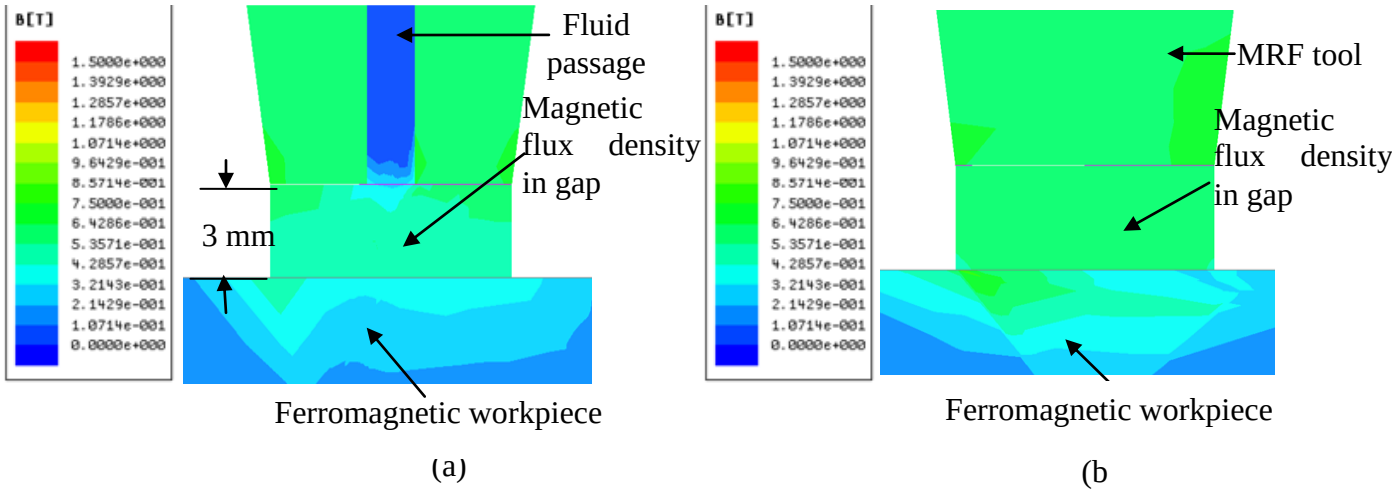

Figure 3.11: Magnetic flux density distribution of tool at working gap of 3 mm (a) with central hole and (b) without central hole

According to the results of simulation in MAXWELL ANSOFT V13, the magnetic field at working gap is less in case of core with central hole as compare to without hole as shown in Fig. 3.11 above. The uniformity of magnetic field in Fig. 3.11 (b) is more than Fig. 3.11 (a) i.e. uniformity in without hole is more than with hole at 3 mm working gap.

The tables for values of simulation results for core with central hole and core without central hole for ferromagnetic workpiece are as given below respectively-

Table 3.2: Simulations results of core with central hole and core without central hole

Sr.No.	**Process Parameters**			**Simulation results of magnetic flux density at the tool tip surface in case of core with central hole**	**Simulation results of magnetic flux density at the tool tip surface in case of core without central hole**
	Z(mm)	I(A)	N	Bz(T)	Bz(T)
1	0.5	5	2000	1.0714	1.1786
2	1			0.9642	1.0714
3	1.5			0.8571	0.9642
4	2			0.7500	0.8571
5	2.5			0.6428	0.7500
6	3			0.5357	0.6428

Where Z= working gap in mm, I= current in ampere in tesla

N= number of turns, B_z= magnetic field

According to the Table 3.2, it is clearly visible the values of magnetic field in tesla for both core with hole and core without hole. Therefore, the graph between working gap and magnetic field is shown in Fig. 3.12 below.

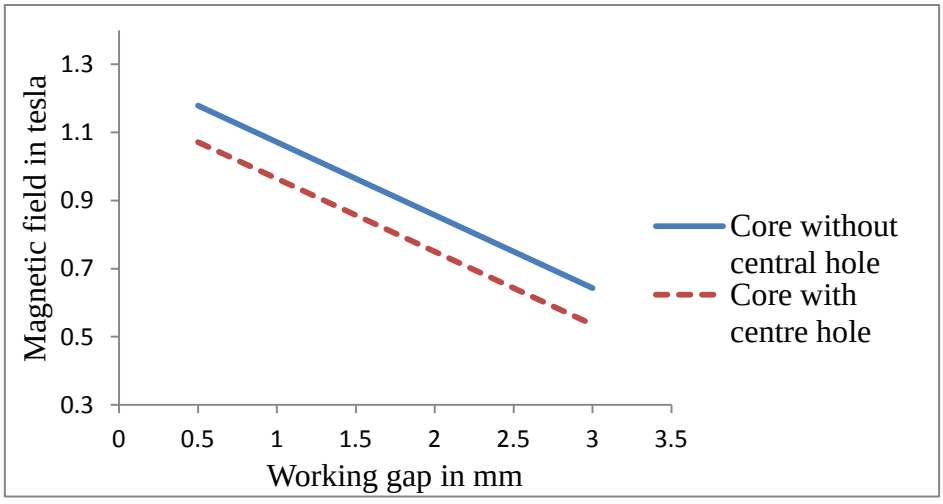

Figure 3.12: Graph between magnetic field and working

In Figure 3.12, it is very clear that magnetic field is more in solid core than core with hole. Secondly, as working gap increases magnetic field decreases continuously. At working gap 0.5mm, magnetic field is max in solid core i.e. 1.1786 tesla and magnetic field in core with centre hole is 1.0714 tesla.

According to the finite element analysis of MRF tool, it is concluded that magnetic flux density distribution in working gap is almost uniform in core without central hole rather than core with central hole. With the help of uniform magnetic field in working gap, almost uniform finishing will occur at workpiece. So, therefore without giving feed in any direction workpiece surface can be finished. But in case of core with central hole, small unfinished surface at centre point has left due to non uniform magnetic field.

3.3 CAD modelling and drawings of the present ball end MRF tool

The selection of all the components with CAD models and appropriate drawings are as given below-

3.3.1 Selection of z slide and motor

The selection of z slide is very important step because the entire load of MRF tool which include servo motor, brackets etc are on carriage of z slide. z –slide consist of a lead screw which converts the rotary motion into the linear motion. The parameters selected for the z-axis slide is shown in Table 3.3. The drawing of the z- axis slide is shown in Fig. 3.14. The pitch of the lead screw is 1mm which means on one complete rotation of screw, carriage will move 1 mm. The selection of travel length of z slide is 400 mm so that any change in workpiece height can be easily accepted.

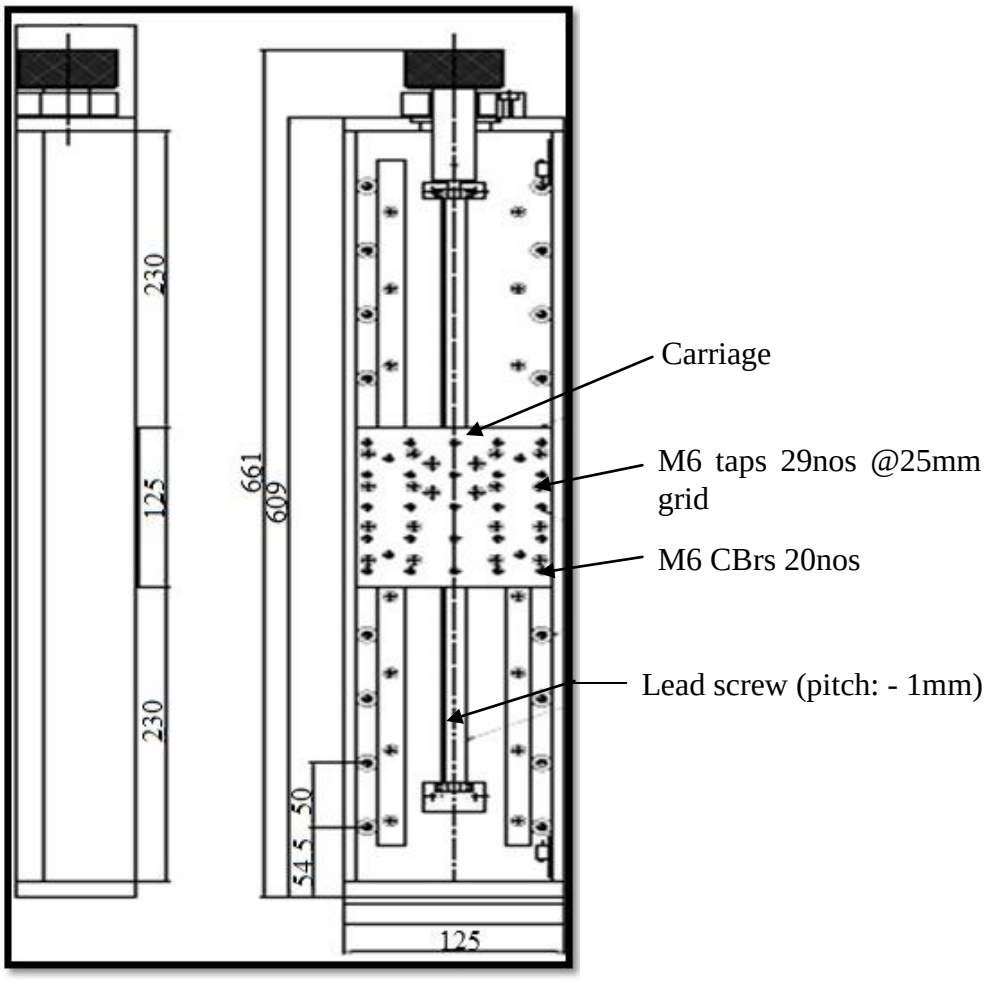

Figure 3.13: Drawing of z slide

Table 3.3: Parameters of selected z-slide

Pitch of the lead screw	1 mm
Diameter of the lead screw	14 mm
Length of the z slide	609 mm
Breadth of the z slide	125 mm
Total moving length	400 mm

The servo motor is selected for the rotation of core and lead screw with rpm 3000. The other parameters and drawing of drive motor are also given below with Table 2.4 and Fig. 2.15.

Table 3.4: Parameters of selected drive motor

Weight of motor	1.4 kg
RPM of motor	3000
Power of motor	400 W
Rated torque, Max. torque	1.3 Nm, 4.5 Nm

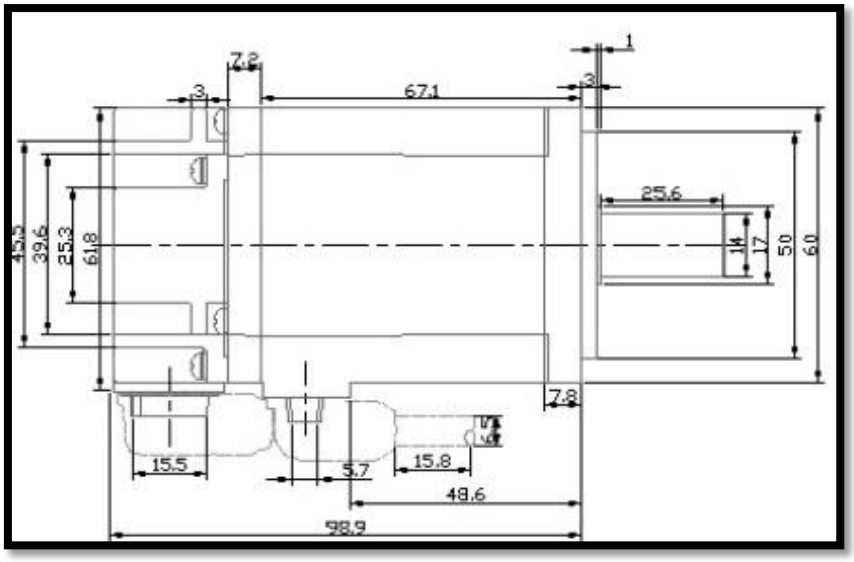

Figure 3.14: Drawing of servo motor

3.3.2 Selection of x-y slide

The selection of x-y slide is also very important step because the workpiece holder which is precision grinding vice mounted on this slide and further workpiece fixture with workpiece attach on it. x-y slide consist of a lead screw which converts the rotary motion into the linear motion. The parameters selected for the x-y axis slide is shown in Table 3.5. The drawing of

the x-y axis slide is shown in Fig. 3.16. The pitch of the lead screw is 1mm which means the same as in z slide. All the parameters are designed to suitable range for work in any other workpiece in future also.

Table 3.5: Parameters of selected x-y slide

Pitch of the lead screw	1 mm
Diameter of the lead screw	10 mm
Total length of the lead screw	250 mm
Length of the x-y slide	250 mm
Breadth of the x-y slide	200 mm
Total moving length	200 mm
Material of the x-y slide	Aluminium

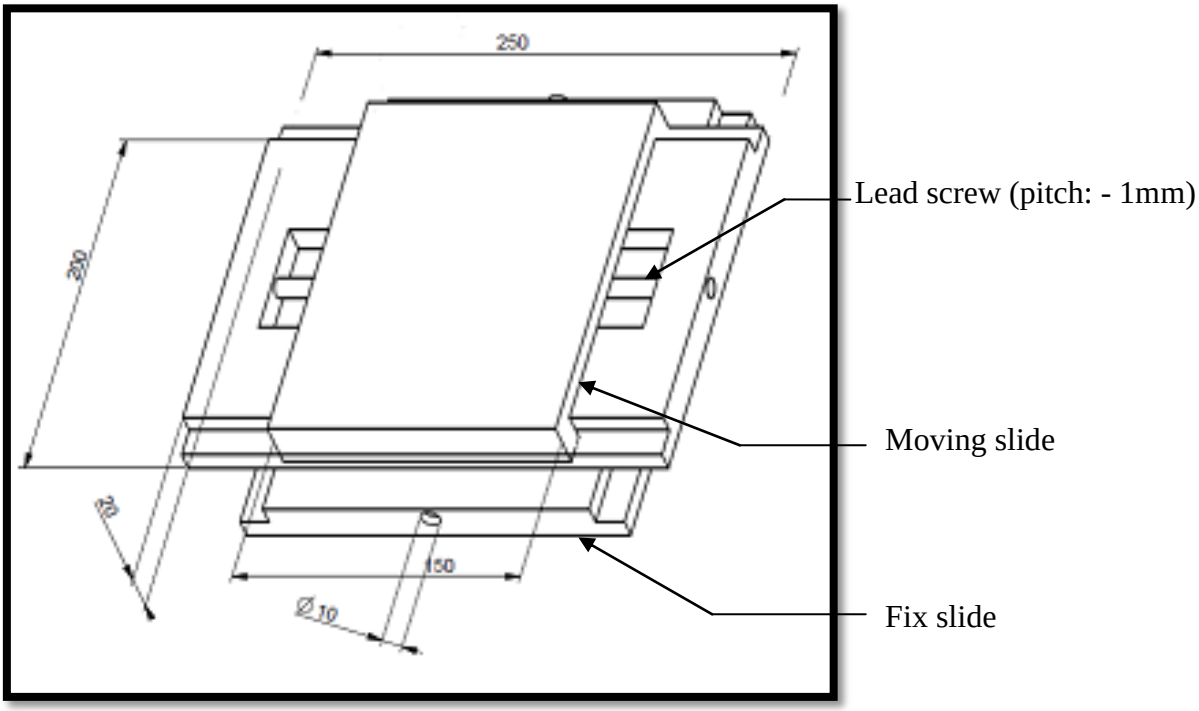

Figure 3.15: Drawing of x-y slide

3.3.3 CAD model of ball end MRF tool

The whole magnetorheological finishing tool comprises of sub parts which are follows as below-

- Solid core
- Aluminium bobbin

- Electromagnet coil
- Cooling jacket

The solid core is made up of mild steel because it is magnetic in nature. The magnetic property of solid core helps in nanofinishing. The core is centrally placed and rotated with the help of drive motor, timing belt and timing pulley. A small step is made in core to move bearing upside. The aluminium bobbin is placed around solid core for winding copper wire and it is used to place the whole winding stationary as core is rotating. The bobbin is made up of aluminium because it is nonmagnetic in nature. The total numbers of coiling turns are 2100 and finally it is covered with insulation tape. 20 gauge (0.84 mm) copper wire is used for coiling and two 2 wire PT100 thermocouples are used for temperature sensor. The cooling jacket is made up of nylon which is used to cool the whole winding of cooper wire. So to reduce the coiling temperature, transformer oil is used in cooling jacket. A separate apparatus name as low temperature bath is used to cool the transformer oil. The cad model of MRF tool and drawings of each parts are as given below-

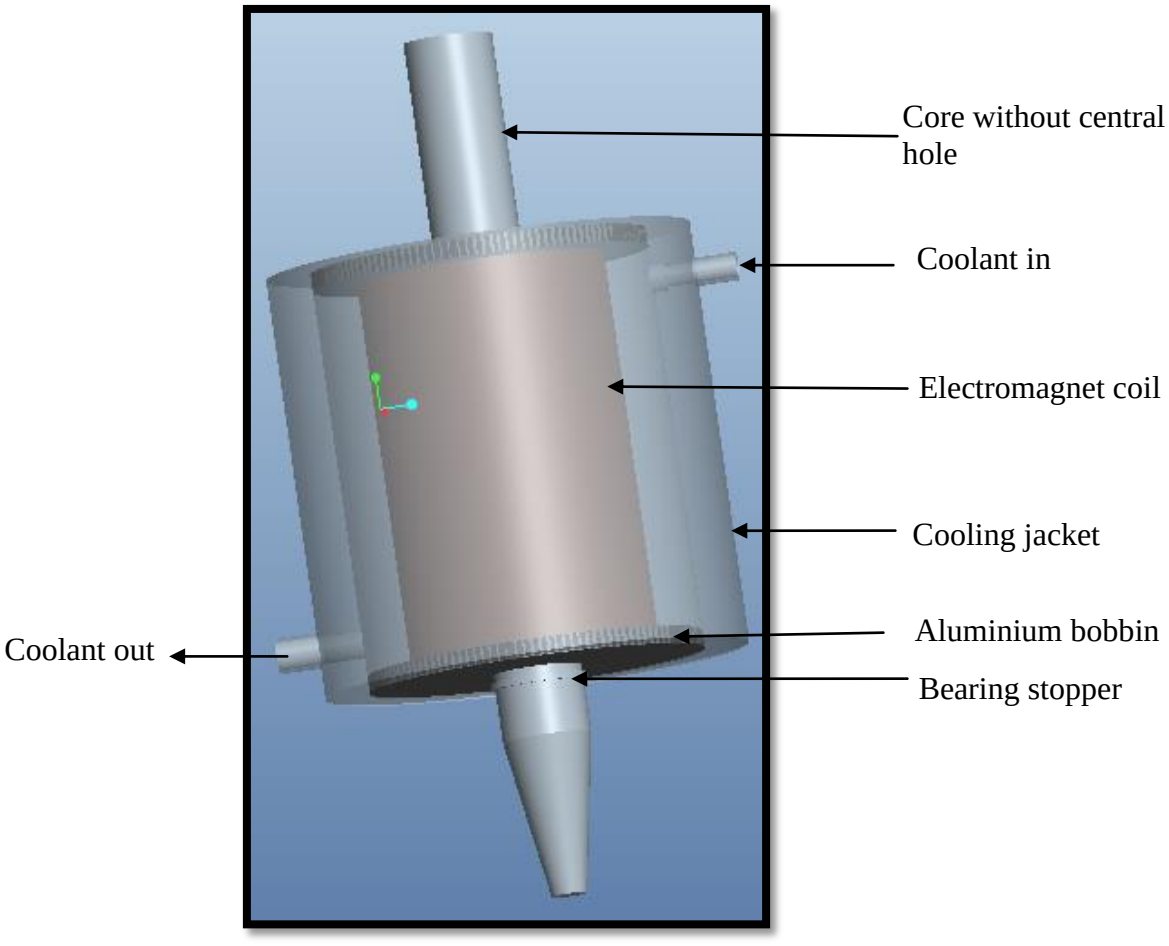

Figure 3.16: CAD model of ball end MRF tool

There is no contact between aluminium bobbin and bearing stopper because core is rotating and bobbin is stationary. Therefore, the bobbin is placed on bottom bracket so that gap is maintained between bobbin and step. The step is in contact with ball bearing as inner portion of bearing is rotated with solid core. There is also small gap between diameter of solid core and aluminium bobbin.

The drawings of the entire components i.e. solid core, aluminium bobbin, cooling jacket and electromagnet coil etc are shown below in Fig. 3.18 and done in CREO elements/PROE.

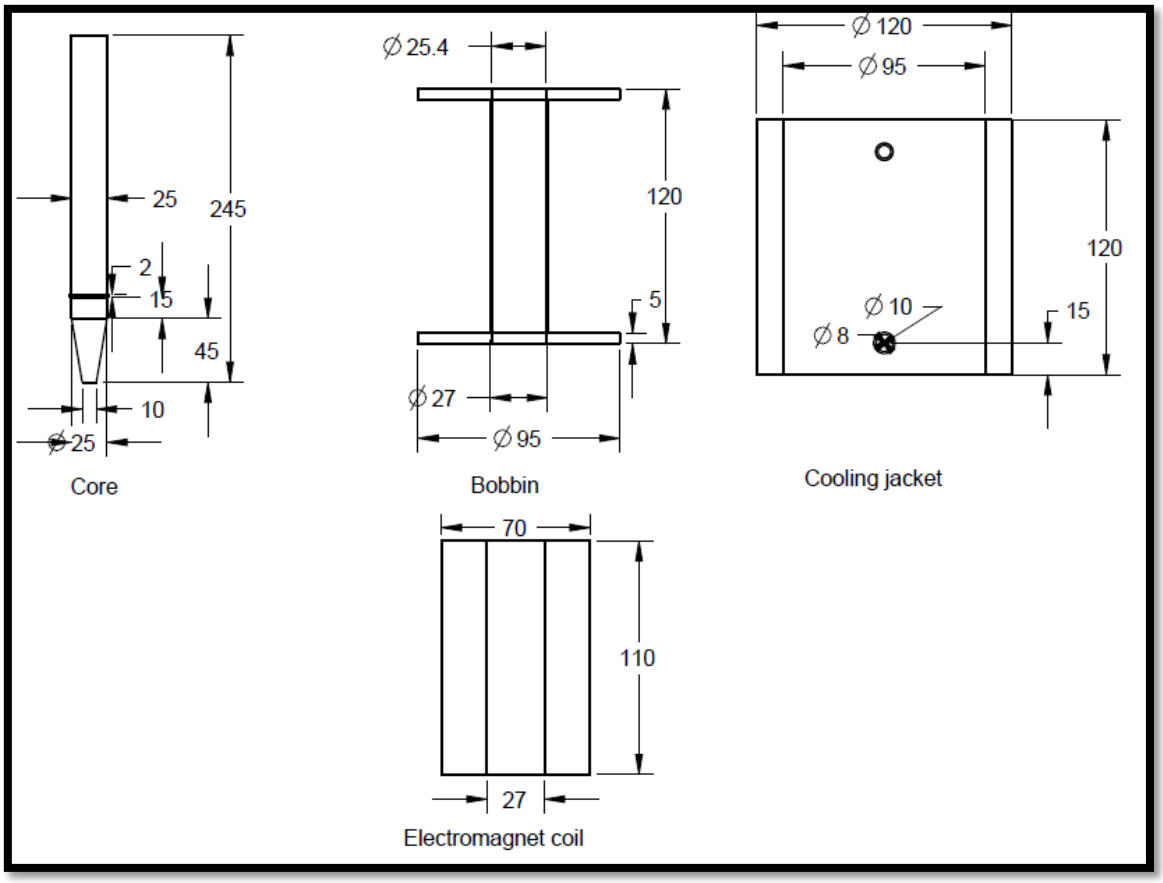

Figure 3.17: Drawings of ball end MRF tool part

3.3.4 Fixture for holding the present ball end MRF tool

The purpose of fixture is to hold the servo motor and ball end MRF tool. The fixture of ball end MRF tool made up of aluminium brackets i.e. top, bottom and side bracket which is shown in Fig. 3.19. The material for the brackets are aluminium because it is non magnetic in nature and it will not affect on magnetic field. The mechanical property of aluminium is shown in table 3.6 below. The main consideration points for modelling of fixture are as follows-

- Centre distance between servo motor axis and ball end MRF tool axis
- Thickness and width of bracket
- Distance between top and bottom bracket

Table 3.6: The mechanical properties of the aluminium 60610 for bracket (http://asm.matweb.com/search/SpecificMaterial.asp?bassnum=MA6061T4)

Density	2700 kg/m^3
Young's modulus	68.9 GPa
Ultimate tensile strength	124 MPa
Ultimate yield strength	55.2 MPa
Ultimate bearing strength	228 MPa
Poisson's ratio	0.33

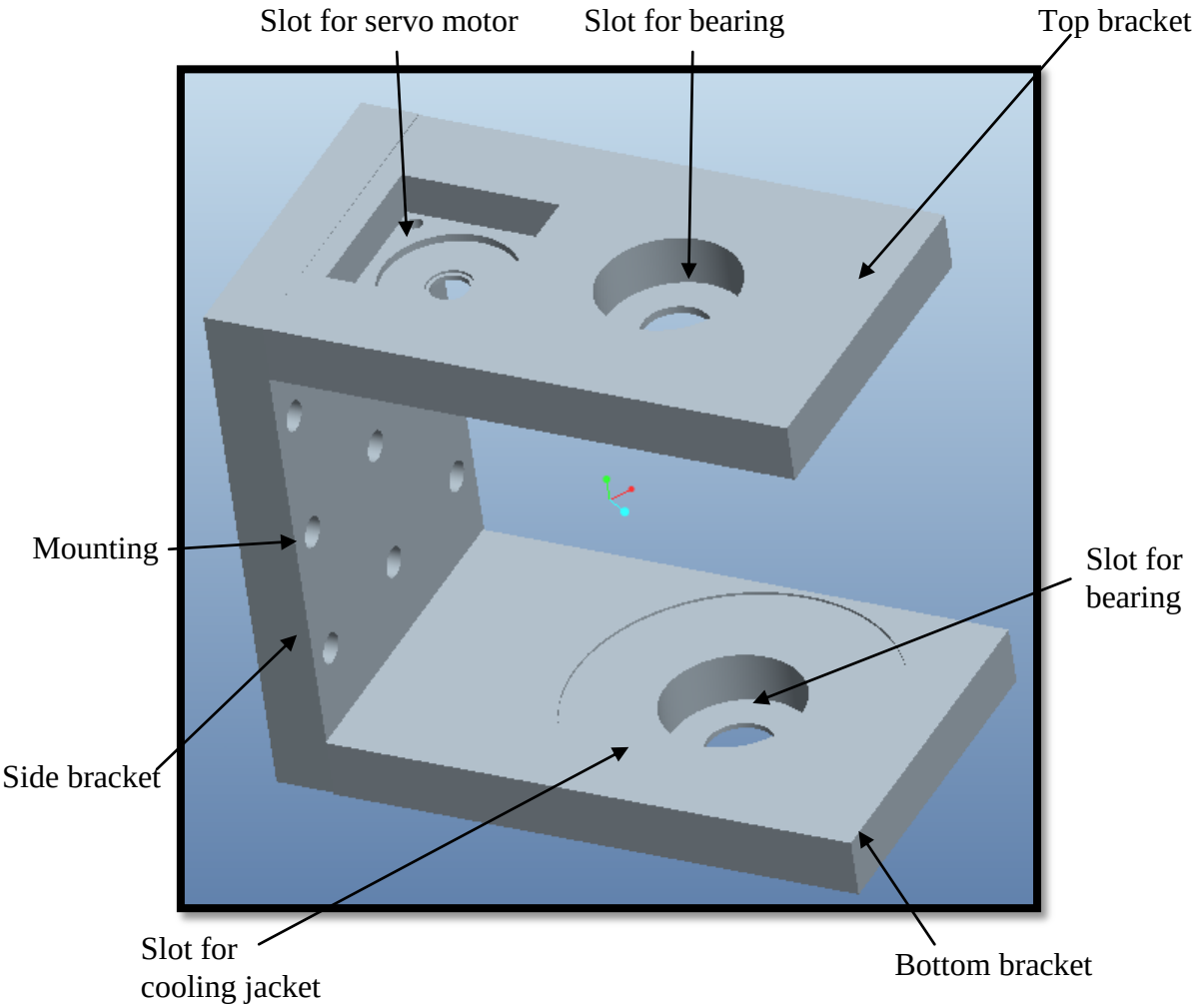

Figure 3.18: CAD model of ball end MRF tool fixture

This fixture helps in holding drive motor, bearings, timing pulley, timing belt and MRF tool. The height of bearing is 15mm but in the bottom bracket, the depth of bearing slot is 19mm. Because there is 2 mm space left for bearing stopper and further 2 mm gap for stopper and aluminium bobbin. The distance between top and bottom bracket is 156mm. And the width of all three brackets is 125mm because diameter of cooling jacket is 120mm. The length of the top and bottom bracket is 200mm. More importantly the distance between servo motor centre axis and solid core centre axis is 86mm because after calculation it should reach to exact length of timing belt. Further CAD model of whole arrangement including servo motor, timing belt and timing pulley is shown in Fig. 3.20.

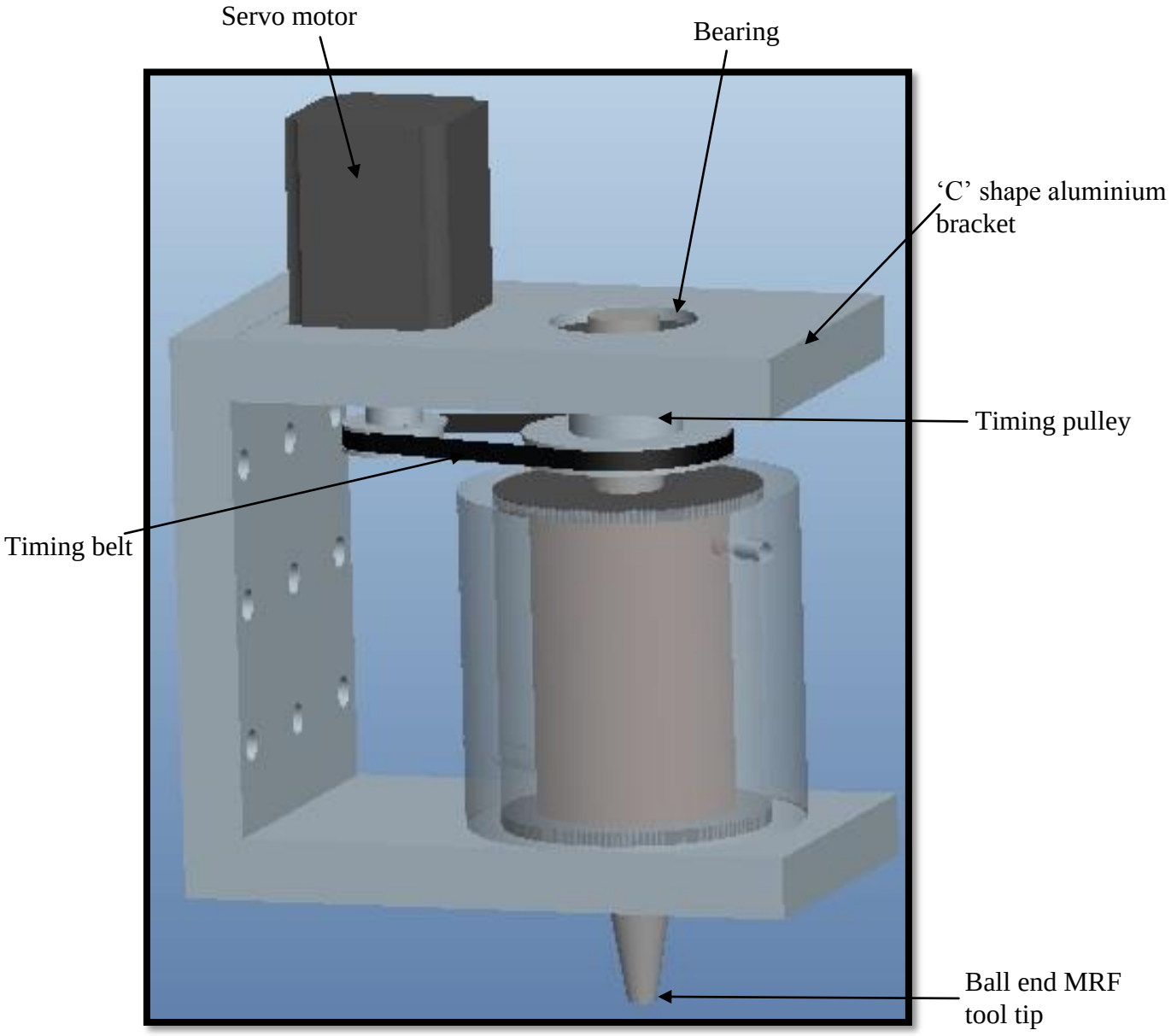

Figure 3.19: CAD model of ball end MRF tool with fixture

After fabricated all these components i.e. brackets, solid core, aluminium bobbin, cooling jacket, timing belt and timing pulleys etc placed at their positions as shown in figure above. Then attach this whole apparatus with z slide carriage. The weight carrying capacity of z slide carriage is about 25kg. The drawings of all three brackets are shown below with proper labelling. There should be gap between bigger timing pulley and aluminium bobbin because wires of thermocouple and copper coil have taken some space. And there should also be some distance between both pulleys and top bracket so that while rotating it cannot touch the bracket. The solid core is centrally aligned between two bearing because it can minimise the vibrations while rotation of core. The detailed drawings of all three brackets are shown in Fig. 3.21, Fig. 3.22 and Fig. 3.23.

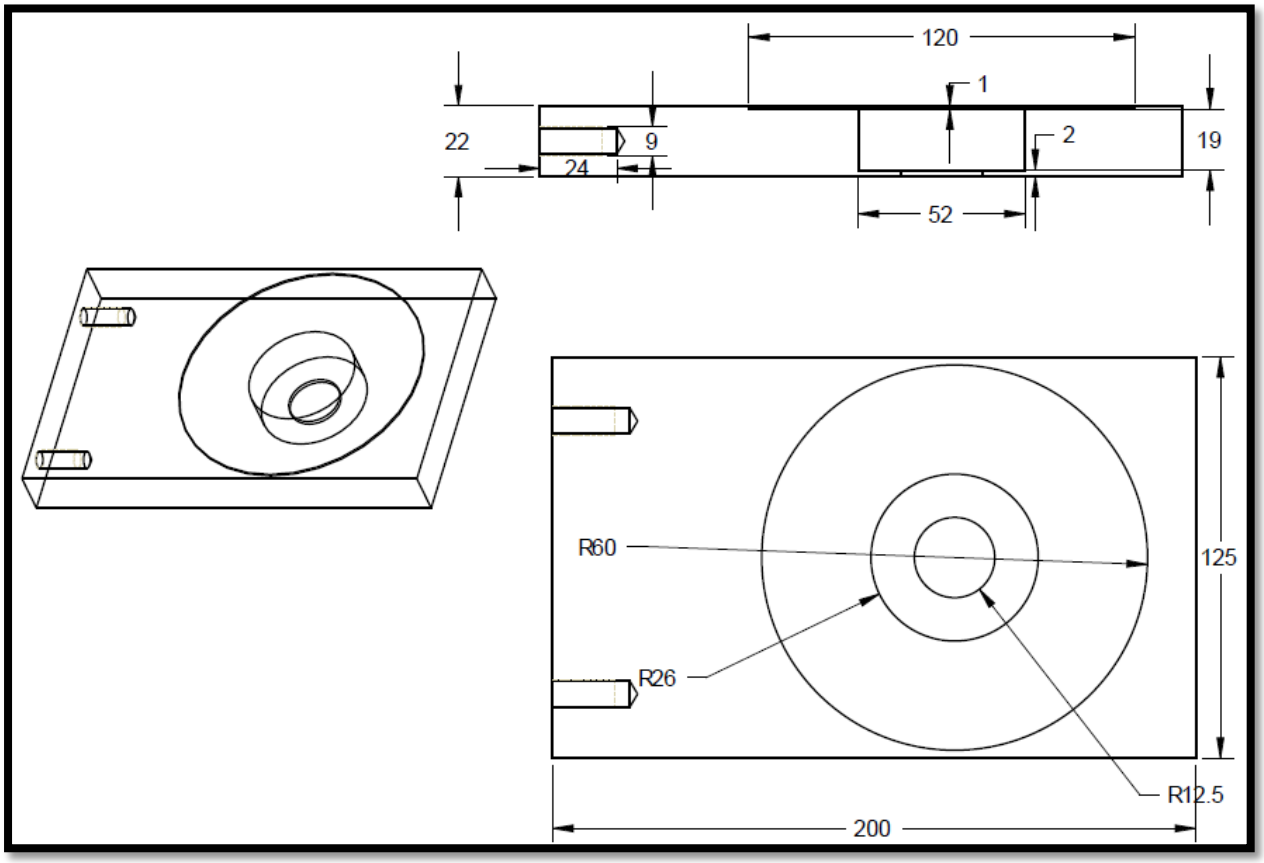

Figure 3.20: Drawing of bottom bracket

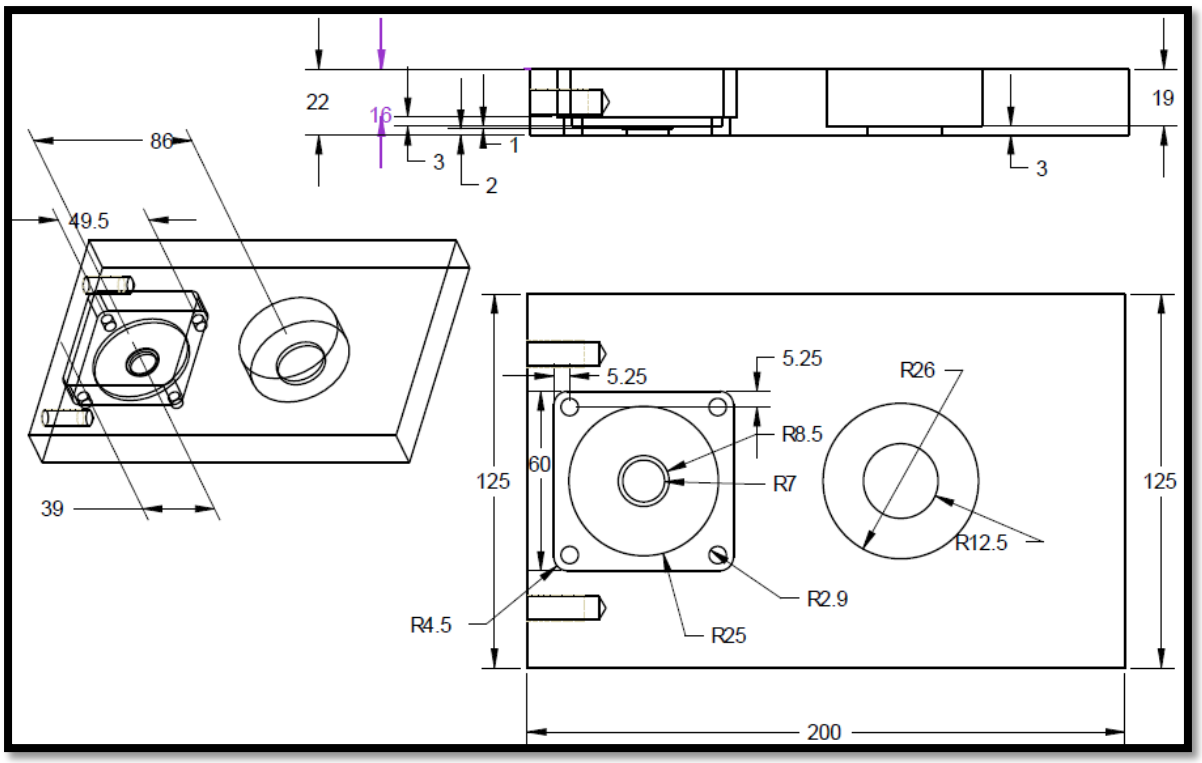

Figure 3.21: Drawing of top bracket

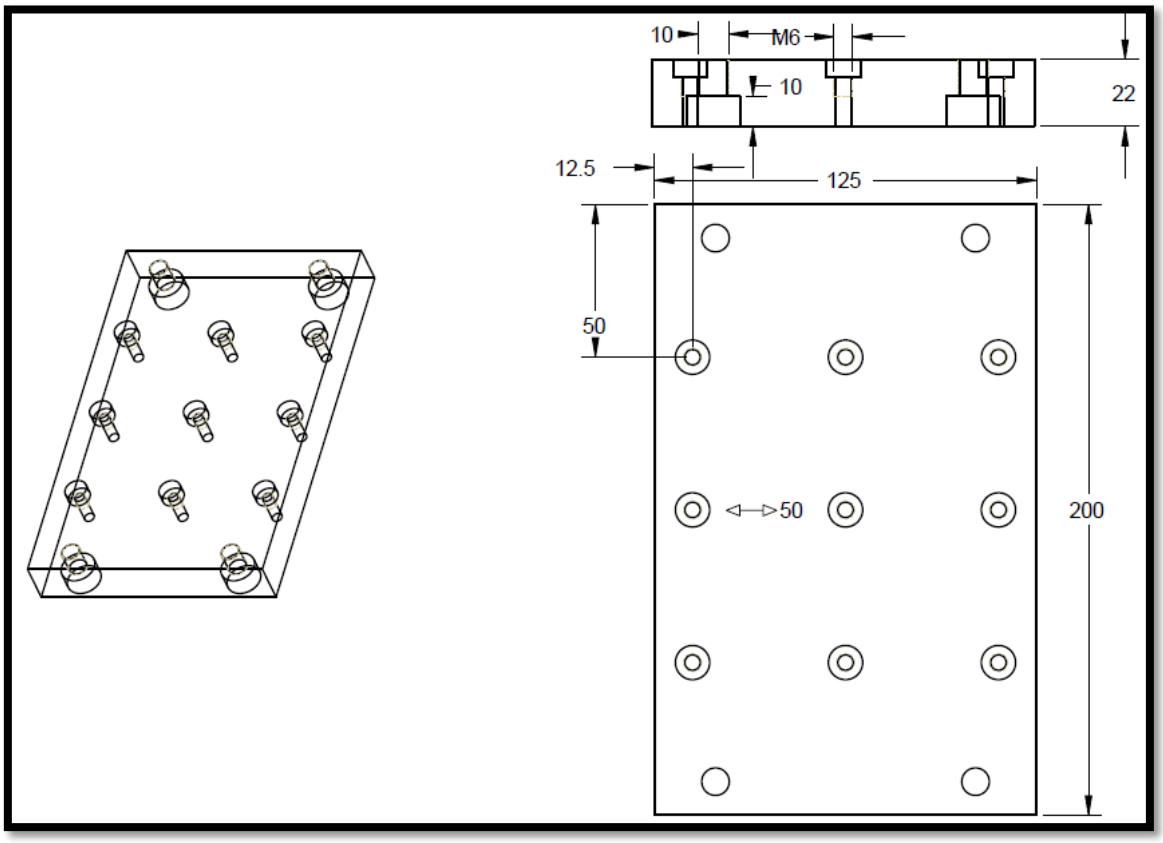

Figure 3.22: Drawing of side bracket

3.3.5 Selection of bearing

The bearing is used to control the vibrations of large rotating shafts. In this process, two self lubricating SKF ball bearings are used to control the vibrations. In self lubricating bearing, there is no need of lubrication. According to diameter of solid core which is 25mm, there are two models in SKF self lubricating bearing which are as follows-

1. 25*47*12 (inner diameter* outer diameter* height)
2. 25*52*15 (inner diameter* outer diameter* height)

From the above two models, the bearing with height 15 is more effective in this process because more is the surface contact with bearing, lesser is the vibrations.

Figure 3.23: Self lubricating ball bearing

(http://file.seekpart.com/productsimage/2013/7/19/201371914301215877.jpg)

3.3.6 Selection of timing pulleys and belt

The timing pulley and belt is used for transmission of power effectively. In the current process, there are two timing pulleys one is driver and other is driven. The driver pulley is mounted on servo motor which is of 24 teeth from where the power transmitted. The driven pulley is mounted on MRF tool (core) which is of 48 teeth. Both pulleys are made up of aluminium and of XL shape. There are some advantages of timing pulley and belt over simple pulley and belt are as given below-

-No slippage

-Less vibration

-Higher speed and power capacities

-Easy synchronization

-Effective at shorter and moderate distance

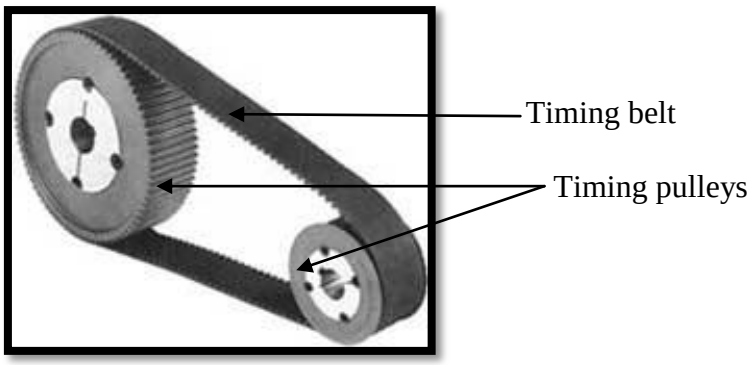

Figure 3.24: Timing pulleys and belt (http://www.cross-morse.co.uk/images/tb1.jpg)

3.3.6.1 Calculation of the length of belt

Length of belt is calculated by the formulae as given in Eq. 3.1

$L=2C+\pi (D_1 +D_2)/2+ (D_1 +D_2)^2/4C$ (3.1)

L= Length of the belt

C= Centre distance between the two pulleys

P_1= Pitch circle diameter of the driving pulley

P_2= Pitch circle diameter of the driven pulley

C=86 mm

P_1=39 mm

P_2=78 mm

By putting the values of C, P_1, P_2 equation 3.1, got the length of belt which is 359.2 mm

Therefore the timing belt selected for the belt pulley mechanism is 142 XL which is having length 360 mm.

3.3.6.2 Calculation of the rpm of solid core according to motor shaft

The rpm of the solid core according to the motor shaft is calculated by the formulae:

$N_1/N_2=D_1/D_2$ (3.2)

N_1= rpm of the motor shaft

N_2= rpm of the solid core

P_1= Diameter of the driving pulley

P_2= Diameter of the driven pulley

N_1= 3000 (maximum rpm of the motor)

P_1=39 mm

P_2=78 mm

Therefore, by putting these values in equation 3.2, got the maximum rpm of the core without central hole i.e. 1500 rpm.

3.3.7 CAD model of workpiece and workpiece fixture

The workpiece and fixture both are made up of mild steel and it is magnetic in nature. The cad model and drawing of both workpiece and fixture are shown in figure below. The bar which is used as workpiece made of mild steel instead of glass but it shows the same application like in medical field. They use these glass bars for testing of blood samples and it should be of super finish. So, try to get same level of finishing in MS bar instead of glass for performing experiment. For holding this bar in grinding precision vice some support from base need to give which is fulfilled by mild steel fixture. The CAD model of grinding precision vice with workpiece and fixture is shown in Fig. 3.26.

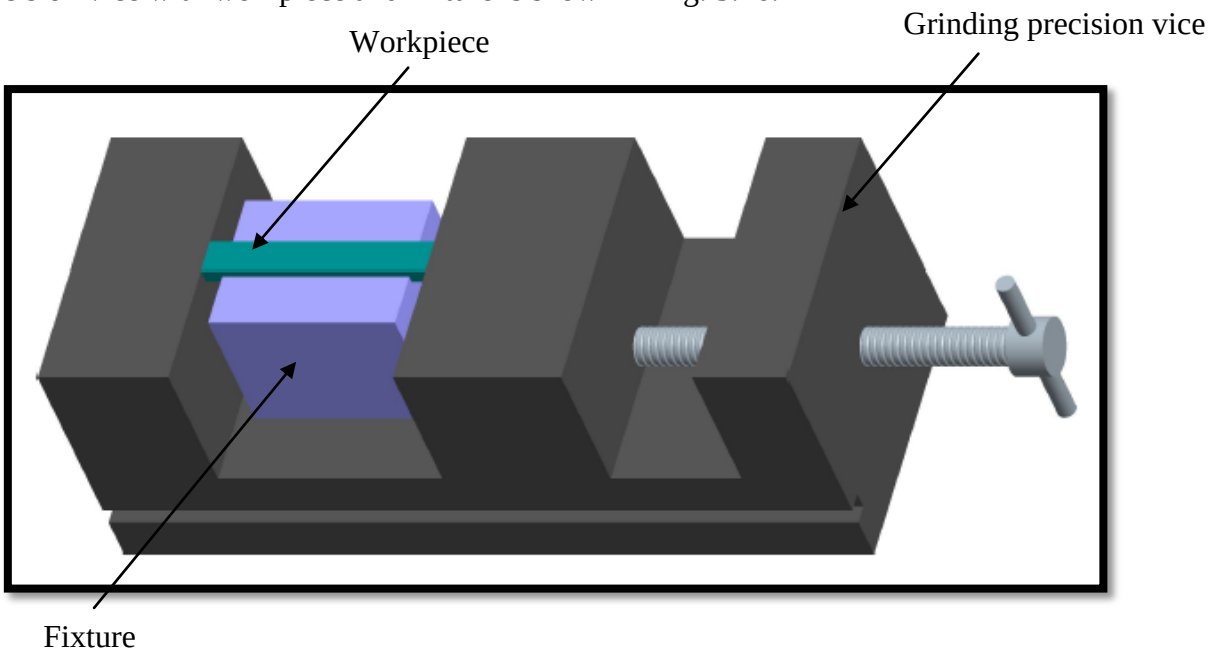

Figure 3.25: Assembled CAD model of workpiece and fixture

The detailed drawing of workpiece and fixture are shown in Fig. 3.27 and Fig. 3.28 below.

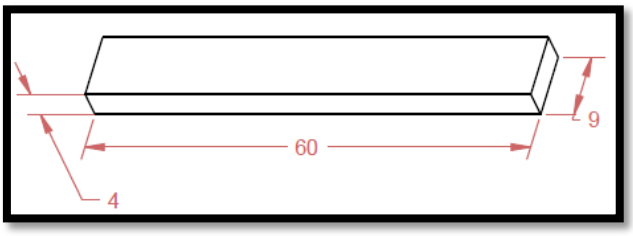

Figure 3.26: Drawing of workpiece

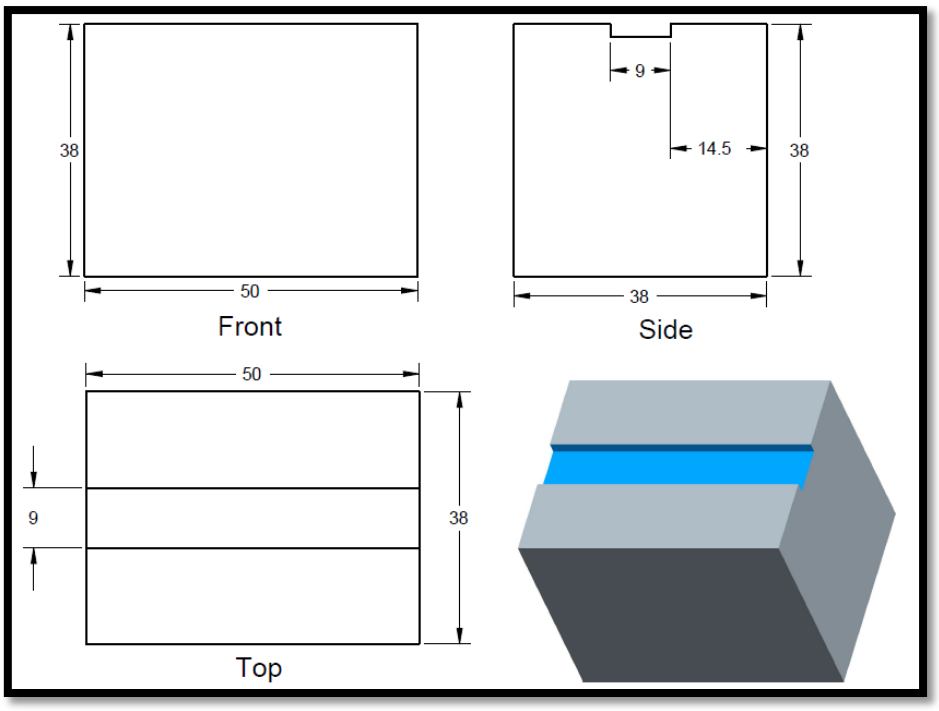

Figure 3.27: CAD model and drawing of workpiece fixture

Therefore, it is concluded from the chapter that core without central hole have some major advantages than core with central hole. From the finite element analysis, uniform magnetic flux density in working gap in core without central hole has found which results in uniform surface finishing. In case of core with central hole, magnetic flux density distribution in working gap is not consistent due to central hole in core and small unfinished spot has left over at centre at the end. Other than FEA, from the CAD modelling of all the components it is very cleared about the development of ball end MR finishing process.

Chapter-4

Synthesis of MR Polishing Fluid and Experimentation

To study the performance of newly developed low cost MRF tool, some preliminary experiments were performed on ferromagnetic work piece for studying the surface roughness.

4.1 Preparation of MRP fluid

MRP fluid is prepared with 20 vol% of abrasive particles i.e. silicon carbide powder, 20 vol% of carbonyl iron particles and 60 vol% of base fluid i.e. 80 wt% of heavy paraffin oil and 20 wt% of AP3 grease. Initially start with mixing of heavy paraffin oil with AP3 grease in a mixing funnel which is made up of stainless steel and multiple blade stirrers with rpm controller on DC motor. Then complete mixing of abrasives and carbonyl iron particles and put it into the base fluid. Pouring of already mixed abrasives and carbonyl iron particles is done step by step with small spoon otherwise it wills sediment in the base of funnel.

4.1.1 Preparation of base fluid

Total amount of base fluid was taken as 1 kg (1000 grams)

In total quantity of base fluid, heavy paraffin oil is 80% by weight= 800 gram

And AP3 grease is 20% by weight= 200 gram

To start with stirring of heavy paraffin oil then adds AP3 grease slowly into it. Keep stirring for sometime till both paraffin oil and grease mixed properly in each other. For measuring density of base fluid, take a small sample of base fluid for 20cm^3 and weight it. Then density = mass per unit volume.

Therefore, the density of base fluid=0.76 gm/cm^3

4.1.2 MR polishing fluid

Total amount of MRP-fluid was prepared as 0.4 l=400 cm3.

In which, the CIP is 20% by volume =80 cm3 and by weight= 80 cm3×7.8 gm/cm3 (density of CIP) =624 gm=0.624 kg. The silicon carbide abrasive powder is 20% by volume=80 cm3 and by weight=80 cm3×3.22 gm/cm3 (density of silicon carbide abrasive powder) =257.6 gm. The base fluid is 60% by volume=400 cm3×60%=240 cm3 and by weight=240 cm3×0.76 gm/cm3 (density of base fluid) = 182.4 gm.

These three components of MRP-fluid in above said percentage was mixed and stimulated in funnel. Thus necessary MRP-fluid has been prepared for conducting the experiments.

Table 4.1: MR polishing fluid compositions (Singh et al. 2011)

Constituent	% volume concentration
Base fluid medium	60
Carbonyl iron powder of CS grade	20
Silicon carbide of mesh size 800	20

4.1.3 Rheological characterization of synthesized MR polishing fluid

Using a parallel plate type rheometer [Anton Paar modular], rheological characterization of the synthesized MR polishing (MRP) fluid was brought out in a shear mode. The shear rate was wide-ranging from 0 to 1000 s−1 and the magnetizing current in the range from 0 to 4 A. The gap was kept 1 mm between the parallel plates. During the experiments, the cooling temperature on the parallel plates was maintained at 25◦C. It is cleared from rheological characterization that when the magnetizing current increases from 0 to 4 A, viscosity increases and as the viscosity increases, the shear strength of the synthesized MR polishing fluid also increases.

Figure 4.1 shows that when the magnetic flux density increases due to the increase in magnetizing current, the shear stress and the viscosity of the prepared MRP fluid increase. This increase in viscosity helps in stiffness of MRP fluid on the tip of this present low cost ball end MR finishing process.

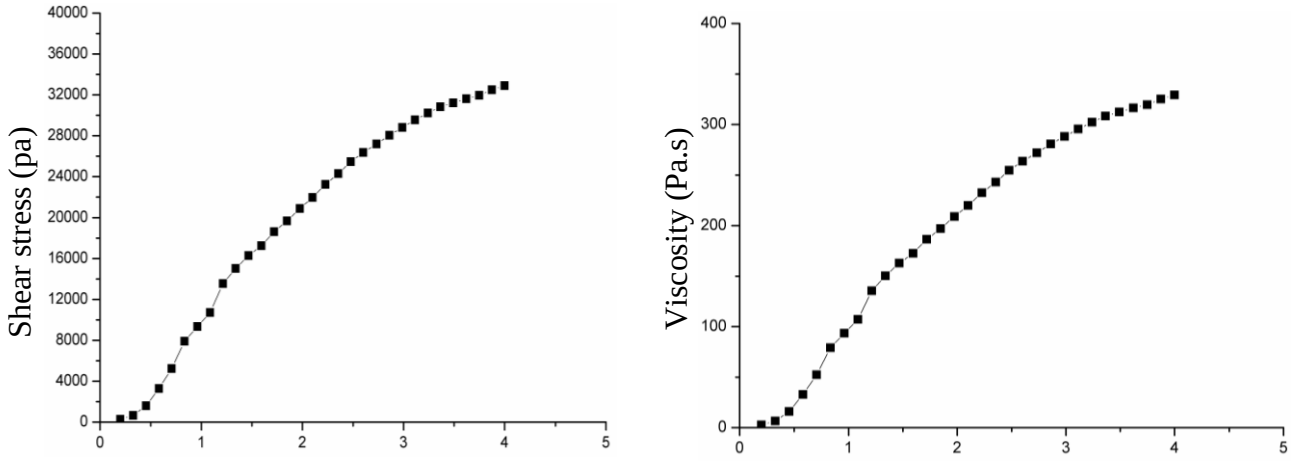

(a) (b)

Figure 4.1: Graph between (a) shear stress and current (b) viscosity and current

4.2 Experimental study of magnetic field at the tip surface of the present ball end MRF tool without central hole in core

To experimentally calculate the magnetic field at tip of core without central hole, various equipments were used which are given below-

- DC power supply
- Gauss meter
- RTD temperature indicator
- MRF tool

For experimentation, start with circuit in which positive and negative terminal of DC power supply attached with the terminals of electromagnet coil in MRF tool. In this DC power supply, 0-10 ampere current can be varying with the change in voltage from 0-100. PT-100 thermocouple is used for measuring temperature inside core. While coiling in the solid core, two thermocouples are used i.e. one is placed after one layer and other is places after 1000 layers. RTD indicator is used for identifying temperature of thermocouple. Gauss meter is used for measuring magnetic field in gauss where 1 gauss = 0.0001 tesla. In the gauss meter, there is probe for measuring magnetic field in which both North and South Pole has written on it.

4.2.1 Experimental study of magnetic field at the tip surface of the present ball end MRF tool without workpiece

Figure 4.1 shows that the experimental study of magnetic field of ball end MRF tool without workpiece. The magnetic field is comparatively less than magnetic field with workpiece due to non proper flow of magnetic field lines. Table 4.2 shows the value of magnetic field by varying distances at core tip at different currents. After getting different values of magnetic field at different current, plot a graph between magnetic field and distance which is shown in Fig. 4.3.

In this graph, it is much cleared that magnetic field is almost uniform at all current and attains its maximum value at centre point. So, therefore in case of core without central hole almost uniform magnetic field has gotten and with the help of uniform magnetic field, almost uniform finishing has taken place. The maximum magnetic field is at centre, so instead of getting spot at centre as in core with central hole ball end MRF tool maximum finishing will be attained at centre.

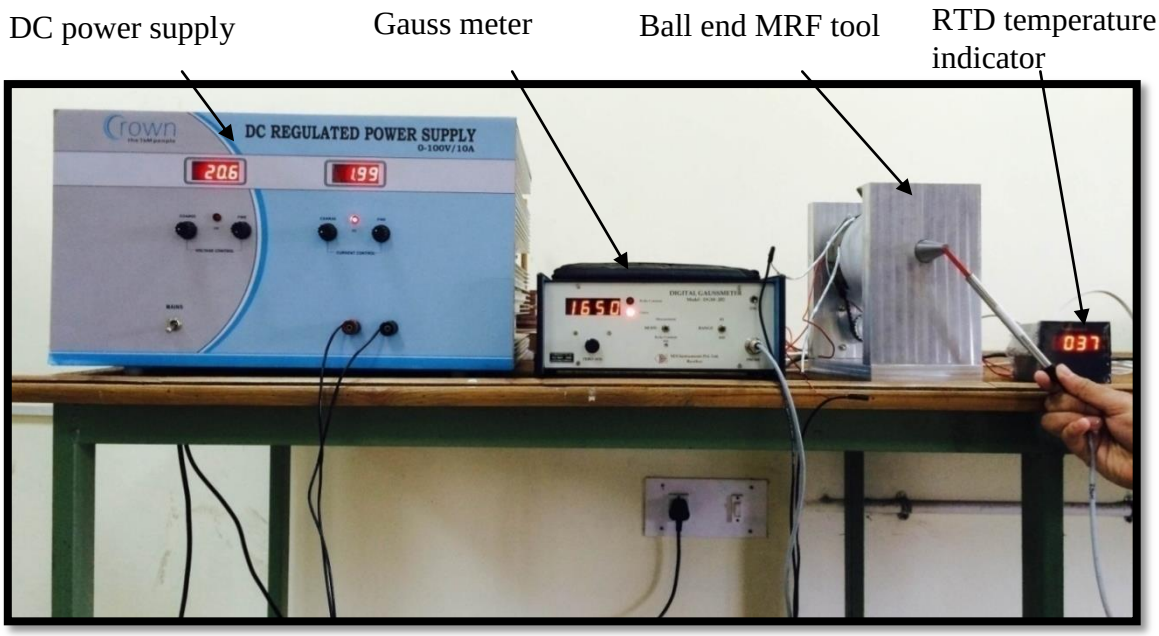

Figure 4.2: Experimental setup for measuring magnetic field without workpiece

Table 4.2: Experimental study of magnetic field with varying distance at different current without workpiece

Distance in mm	Magnetic field in tesla			
	At 1 amp	At 2 amp	At 3 amp	At 4 amp
1	0.1027	0.1743	0.209	0.219
2	0.0973	0.1685	0.2	0.217
3	0.097	0.1668	0.199	0.217
4	0.0937	0.1711	0.202	0.222
5	0.1021	0.1755	0.207	0.23
6	0.118	0.199	0.226	0.25
7	0.105	0.168	0.202	0.216
8	0.093	0.167	0.199	0.218
9	0.0923	0.168	0.199	0.217
10	0.097	0.1727	0.204	0.225

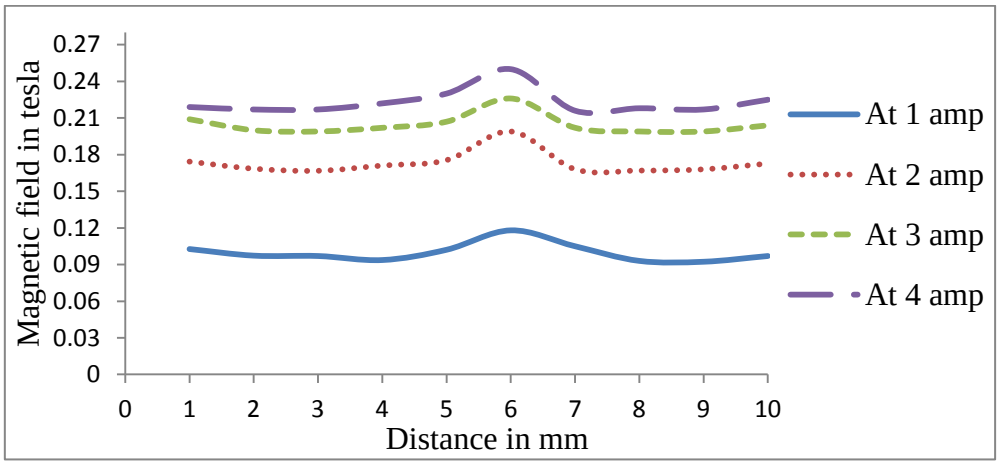

Figure 4.3: Graph between magnetic field and distance along core tip at different currents

4.2.2 Experimental study of magnetic field at the tip surface of the present ball end MRF tool with workpiece

Figure 4.4 shows that the experimental study of magnetic field of ball end MRF tool with workpiece. The magnetic field is comparatively very high than the magnetic field without workpiece due to proper flow of magnetic field lines. Table 4.3, 4.4, 4.5 and 4.6 shows the value of magnetic field by varying distances at core tip at different working gap and magnetizing current. After getting different values of magnetic field at different working gap and magnetizing current, plot a graph between magnetic field and distance which is shown in Fig. 4.5.

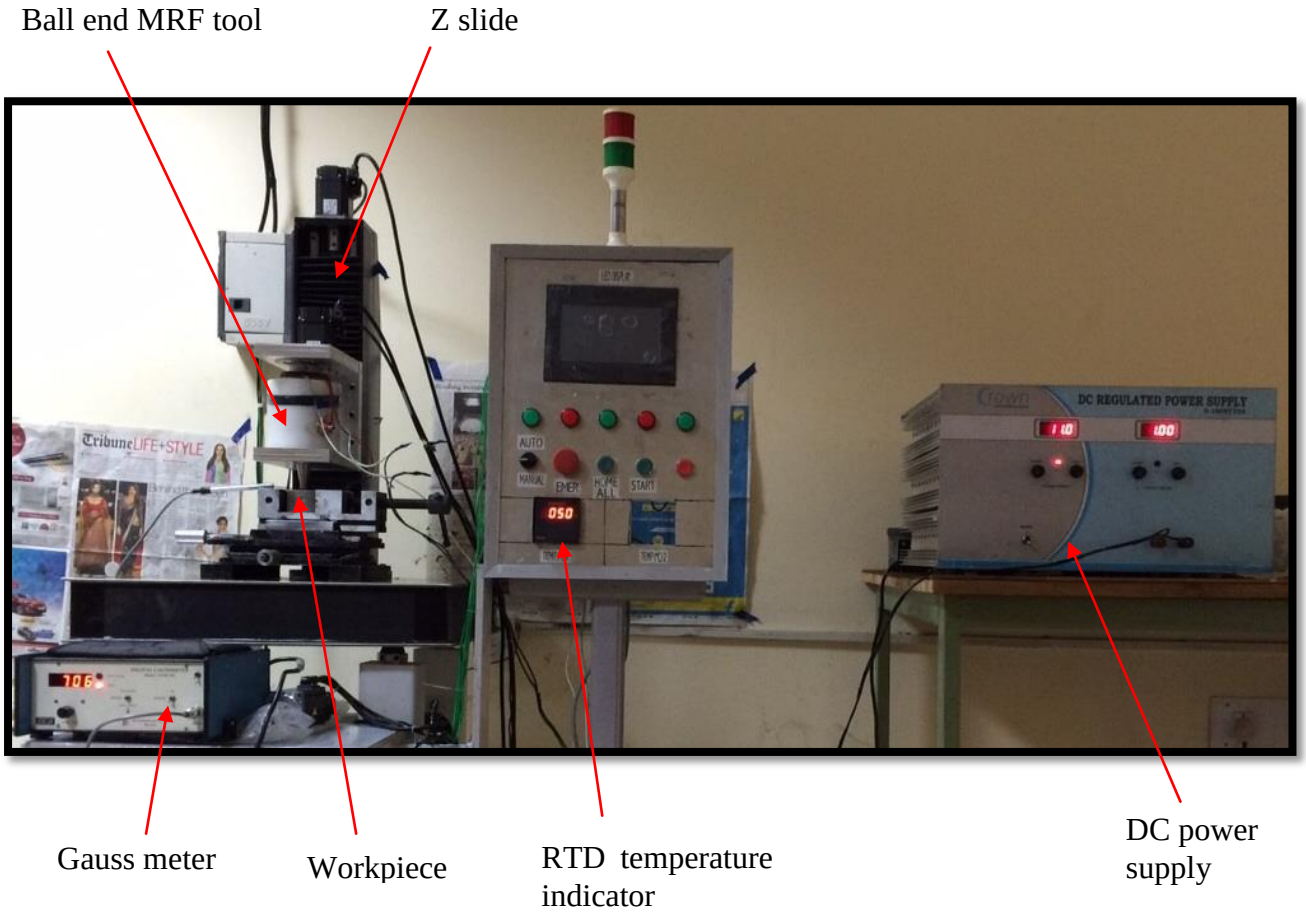

Figure 4.4: Experimental setup for measuring magnetic field with workpiece

The values of magnetic field with changing distance along tool tip with varying working gap at different magnetizing current is shown in figure below. The tables and graphs for the different magnetizing currents and different working gaps are drawn for the measurement of variation in magnetic field along tool tip.

For core without central hole at current 1 amp

Table 4.3: Experimental study of magnetic field with workpiece with varying distance at different working gap at current 1 amp

Distance in mm	Magnetic field in tesla				
	Gap = 0.5 mm	Gap = 1 mm	Gap = 1.5 mm	Gap = 2 mm	Gap = 2.5 mm
1	0.560	0.530	0.505	0.425	0.385
2	0.580	0.550	0.530	0.440	0.405
3	0.600	0.570	0.550	0.460	0.425
4	0.625	0.595	0.575	0.485	0.450
5	0.645	0.610	0.593	0.501	0.470
6	0.635	0.605	0.585	0.490	0.465
7	0.620	0.590	0.570	0.480	0.455
8	0.595	0.575	0.555	0.465	0.430
9	0.581	0.555	0.535	0.445	0.410
10	0.555	0.535	0.510	0.430	0.395

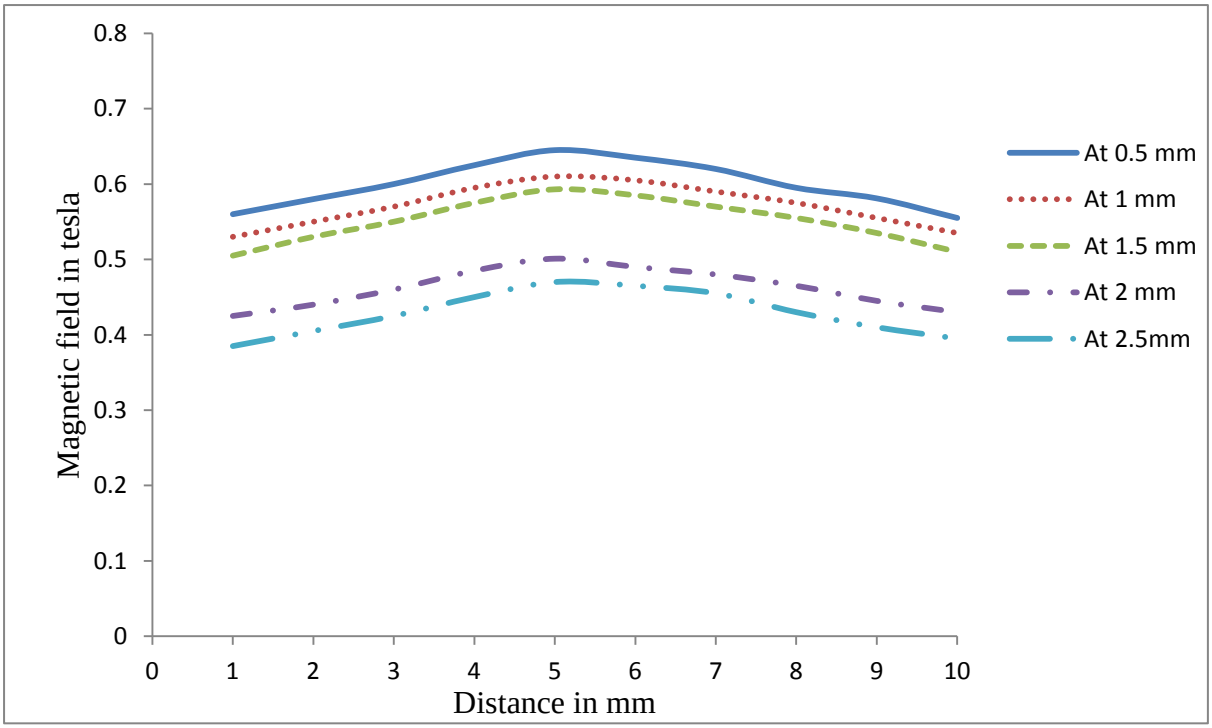

Figure 4.5: Graph between magnetic field and distance along core tip at different working gap at current 1 amp

Figure 4.5 shows the variation of magnetic field with change in distance along tool tip at different working gap. It is cleared that magnetic field is almost uniform and which results to almost uniform finishing.

For core without central hole at current 2 amps

Table 4.4: Experimental study of magnetic field with workpiece with varying distance at different working gap at current 2 amps

Distance in mm	Magnetic field in tesla				
	Gap = 0.5 mm	Gap = 1 mm	Gap = 1.5 mm	Gap = 2 mm	Gap = 2.5 mm
1	0.650	0.610	0.590	0.560	0.530
2	0.670	0.635	0.605	0.585	0.550
3	0.705	0.670	0.630	0.610	0.585
4	0.735	0.710	0.670	0.640	0.615
5	0.755	0.730	0.690	0.665	0.640
6	0.750	0.720	0.680	0.660	0.635
7	0.730	0.705	0.665	0.635	0.620
8	0.710	0.685	0.625	0.605	0.590
9	0.675	0.650	0.610	0.590	0.555
10	0.652	0.605	0.595	0.565	0.535

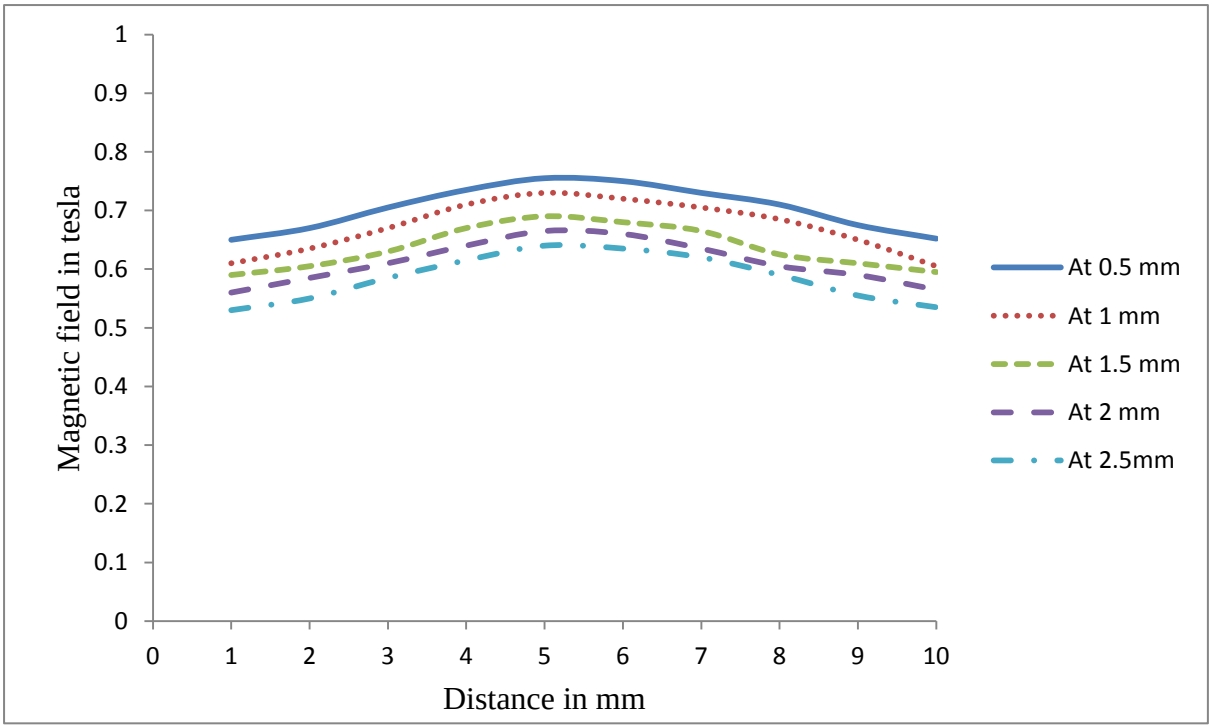

Figure 4.6: Graph between magnetic field and distance along core tip at different working gap at current 2 amps

Figure 4.6 shows the variation of magnetic field with change in distance along tool tip at different working gap. It is cleared that magnetic field is almost uniform and which results to almost uniform finishing.

For core without central hole at current 3 amps

Table 4.5: Experimental study of magnetic field with workpiece with varying distance at different working gap at current 3 amps

Distance in mm	Magnetic field in tesla				
	Gap = 0.5 mm	Gap = 1 mm	Gap = 1.5 mm	Gap = 2 mm	Gap = 2.5 mm
1	0.895	0.835	0.810	0.705	0.655
2	0.915	0.855	0.830	0.725	0.670
3	0.940	0.870	0.855	0.750	0.690
4	0.965	0.890	0.875	0.775	0.715
5	0.985	0.905	0.889	0.798	0.746
6	0.980	0.900	0.880	0.790	0.740
7	0.970	0.885	0.870	0.780	0.720
8	0.945	0.860	0.855	0.755	0.695
9	0.920	0.850	0.835	0.730	0.675
10	0.905	0.840	0.815	0.710	0.660

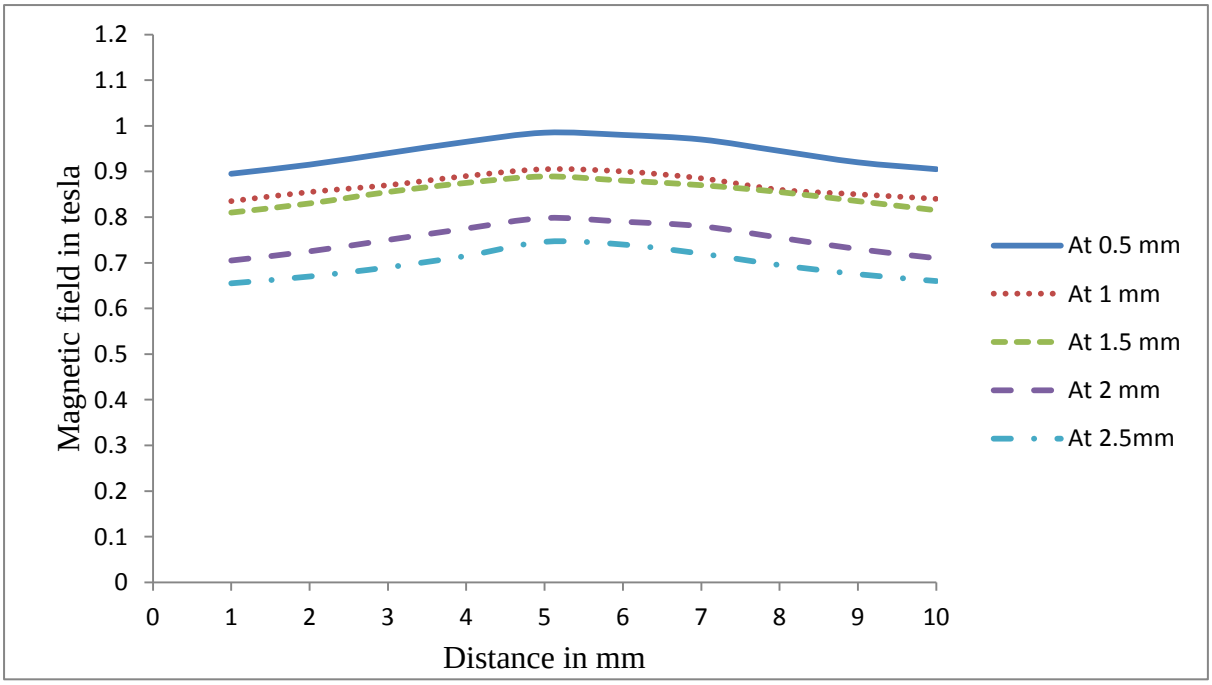

Figure 4.7: Graph between magnetic field and distance along core tip at different working gap at current 3 amps

Figure 4.6 shows the variation of magnetic field with change in distance along tool tip at different working gap. It is cleared that magnetic field is almost uniform and which results to almost uniform finishing.

4.3 Experimentations

The beginning experiment is conducted on one point on ferromagnetic workpiece without giving feed in any direction. DC power of 2A and 22 V is abounding to the electromagnet coil for excitation. The magnetic flux density is produced at the tip of the MRF tool is around 0.7 T. The different finishing times are used for finishing cycle. The variation in surface roughness is measured at workpiece material at every 30 minutes. The MRF tool is rotated at 100 rpm. The working gap is set at 0.6 mm between the tool tip and workpiece surface. The MRP-fluid with 800 grain size silicon carbide abrasive particle is used for ferromagnetic work material. Table 4.6 shows the experimental conditions for ferromagnetic workpiece.

Table 4.6: Experimental conditions for ferromagnetic workpiece

Parameter	Conditions for mild steel workpiece
Total finishing time (min)	90
Total rotation speed (rpm)	100
Working gap distance (mm)	0.6
SiC abrasive (20 vol %) (mesh)	800
DC power supply	22.6 V, 2 A
Magnetic field at tool tip	0.7

The finishing experiment was performed on flat mild steel workpiece of size 60×9×4 mm. The workpiece was hold between grinding precision vice and supported from base with the help of mild steel fixture. The grinding precision vice was further mounted on X-Y slide for linear movements in both directions. The initial surface roughness value was 440 nm produced by grinding the workpiece on grinder and measured in MITUTOYO surftest SJ400. The SEM analysis at 1000× and initial surface roughness profile is shown in Fig.4.8.

(a)

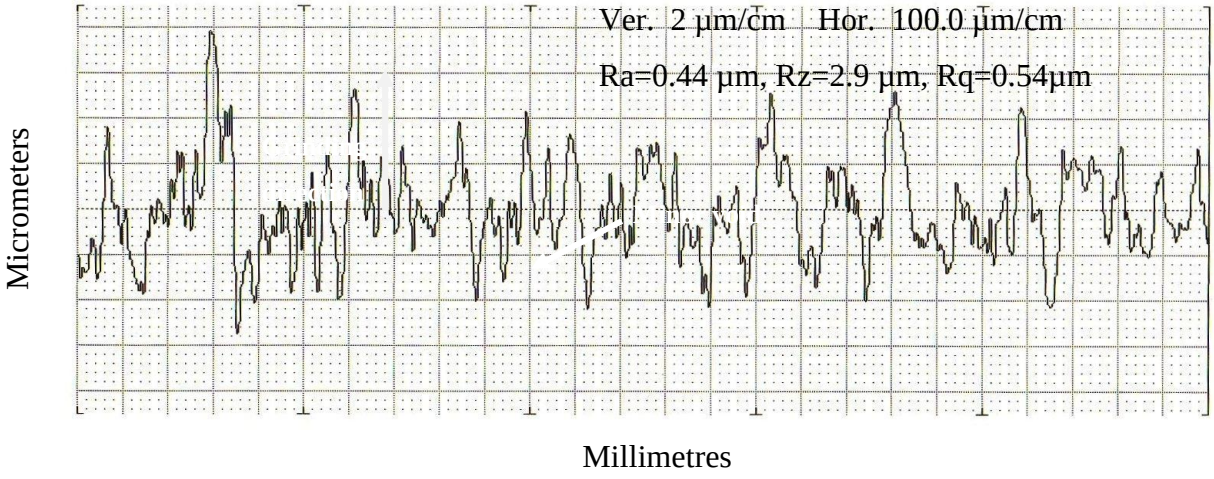

(b)

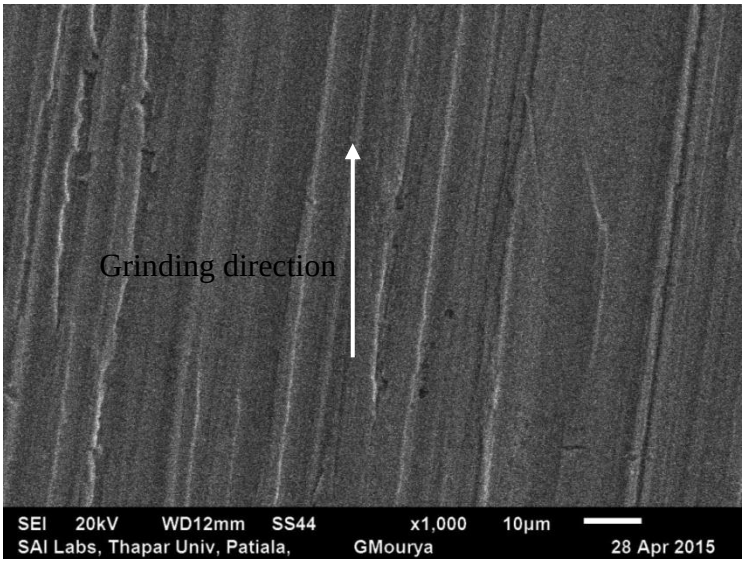

Figure 4.8: Initial surface of mild steel workpiece (a) surface roughness profile (b) SEM analysis at 1000×

4.4 Results and discussion

The experiments are performed on ferromagnetic work material for measuring the outcome of finishing time on final surface roughness value. The experimental result of consequence of finishing time on surface roughness for ferromagnetic work material is shown in Fig. 4.9. The experiments are performed on current 2 A and magnetic field 0.7 T at MRF tool tip on which stiffened ball end is formed. The surface roughness profiles are obtained by MITUTOYO surftest SJ400 for all the experiments and to understand the finished surface morphology and quality, the scanning electron microscope (SEM) is used.

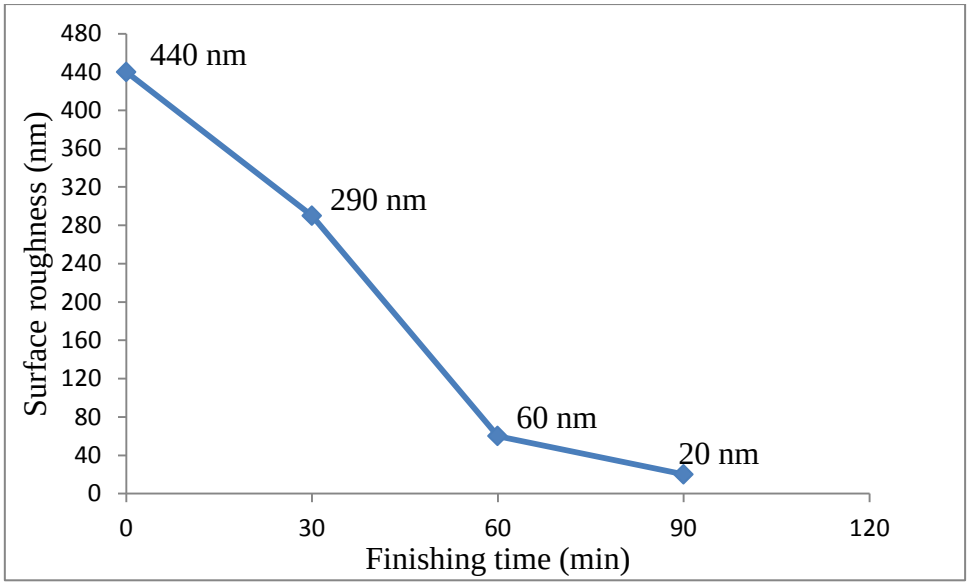

Figure 4.9: Effect of finishing time on surface roughness of magnetic workpiece

4.4.1 Effect of finishing on ferromagnetic workpiece

The outcome of finishing time on surface roughness of ferromagnetic workpiece is shown in Fig. 4.9. The initial average surface roughness value of ferromagnetic workpiece is 440 nm and it is checked with the help of MITUTOYO surftest SJ400. It is measured perpendicular to the direction of grinding. Fig. 4.8 shows the SEM analysis at 1000× and initial surface roughness profile. The surface roughness is checked after every 30 minutes. After 90 minutes surface roughness reduces to 20 nm. Therefore, it is confirmed that a newly developed low cost ball end MR finishing process is able of nanofinishing.

Initially, average surface roughness value of 440 nm is achieved with the help of surface grinder. After conducting experiment for first 30 minutes, the average surface roughness value reduces to 290 nm is shown in Fig. 4.9. The value of average surface roughness at random points on finished surface after first 30 minutes is shown in Fig. 4.10. The decrease in average surface roughness value describes the finishing capability of a new low cost ball end MR finishing method. The quantity of material which is sheared from the workpiece depends on the bonding strength of silicon carbide particle and carbonyl iron particles. The stiffened ball end MRF tool rotates relative to the workpiece in which cutting edge of abrasive particle is tightly held by carbonyl iron particles.

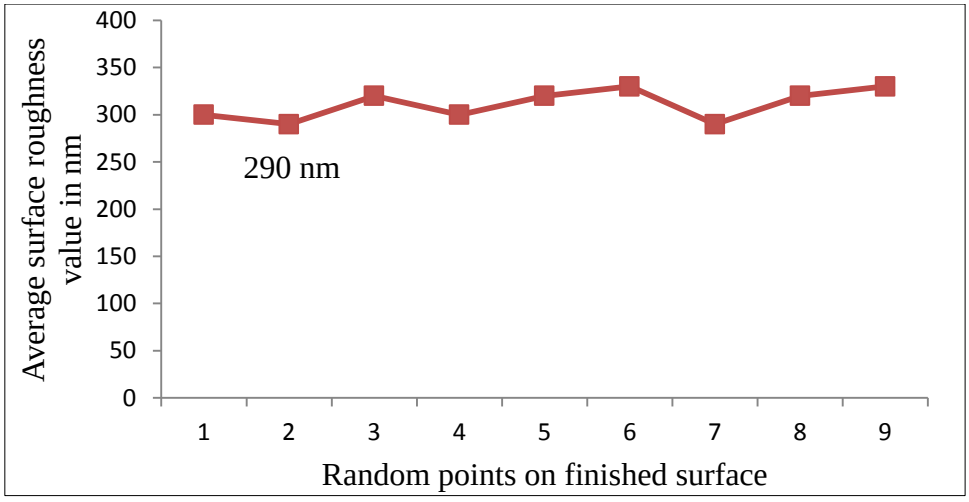

Figure 4.10: Average surface roughness values at random points on finished surface after first 30 mins

After first run, conditioning of MR polishing fluid can be done by adding new MR polishing fluid after removing the older one. For removing the MR polishing fluid on the tool tip, switch off the DC power supply. While supply of fresh MR polishing fluid turn on the DC power supply so that fluid attract towards the tool tip. After doing finishing for first 30 minutes, the cutting edge of abrasive particle may be blunt and unable to finish the surface gradually. So, in the second run this is for more 30 minutes average surface roughness value decreases to 60 nm from 290 nm is shown in Fig. 4.9 which is drastic change in surface finish. Hence nanofinishing is achieved after 60 minutes of experiment as average surface roughness values crosses to 100 nm. The value of average surface roughness at random points on finished surface after second 30 minutes is shown in Fig. 4.11.

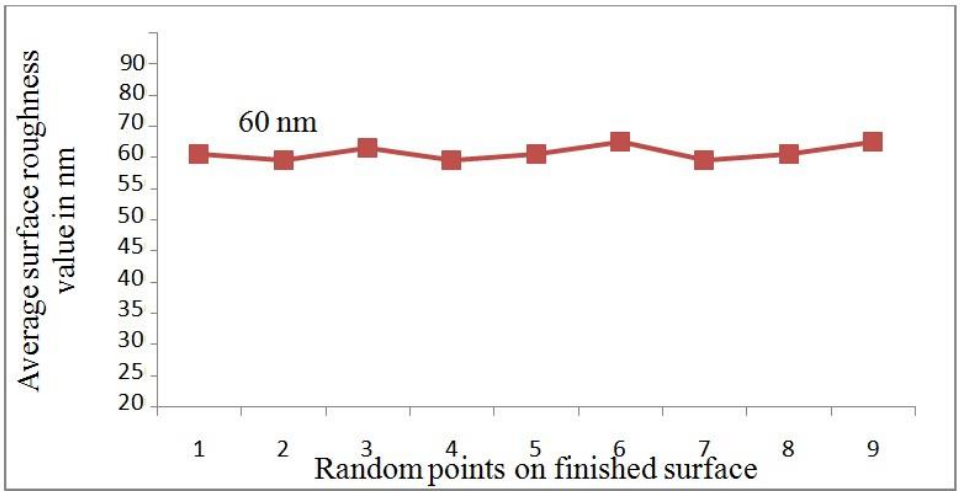

Figure 4.11: Average surface roughness values at random points on finished surface after second 30 mins

Then performing the experiment for next 30 minutes the values of average surface roughness decreases to 20 nm is shown in Fig. 4.9. But the more uniformity in the average surface roughness value is attainted in this run. The conditioning of MRP fluid is done before this experiment as well by following the same procedure as mentioned above. Due to the use of same mesh number abrasive particle, the change in average surface roughness is less. Now if same experiment is done for further 30 minutes on this experimental condition, deterioration will start. So, fine abrasive grain will use further for attaining super finishing. The value of average surface roughness at random points on finished surface after third 30 minutes is shown in Fig. 4.12.

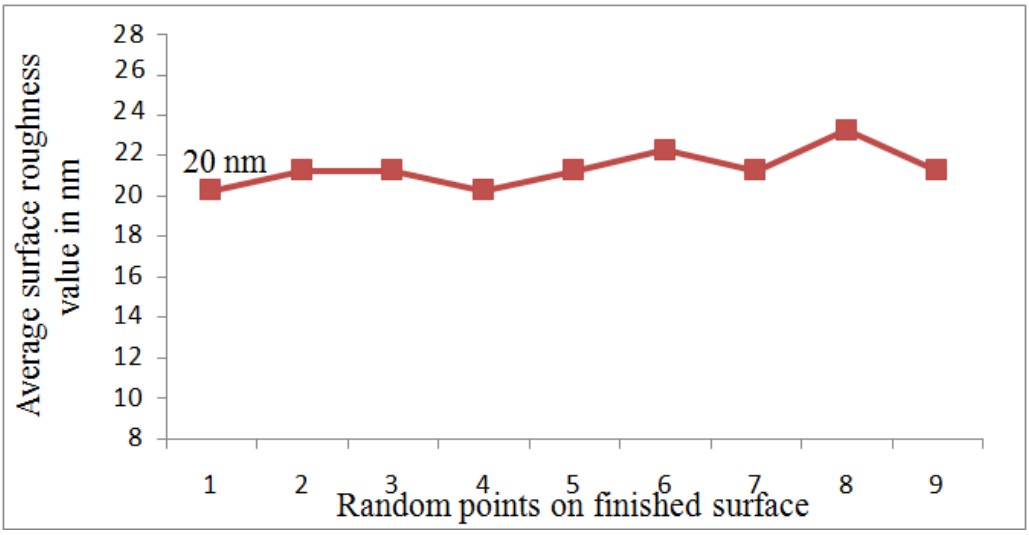

Figure 4.12: Average surface roughness values at random points on finished surface after third 30 mins

The SEM analysis at 1000× and surface roughness profile for finished ferromagnetic workpiece is shown in Fig. 4.13. It is cleared that a new low cost ball end MR finishing method is able of doing nanofinishing in less time and at favourable experimental conditions. But for reducing further surface roughness, more fine mesh number for abrasive particles should be used. Because in the last run abrasive particle start deteriorate the surface. This means at the starting for enhanced surface finish, coarse grain abrasive must used and for further surface finish, fine abrasive grain have to used.

(a)

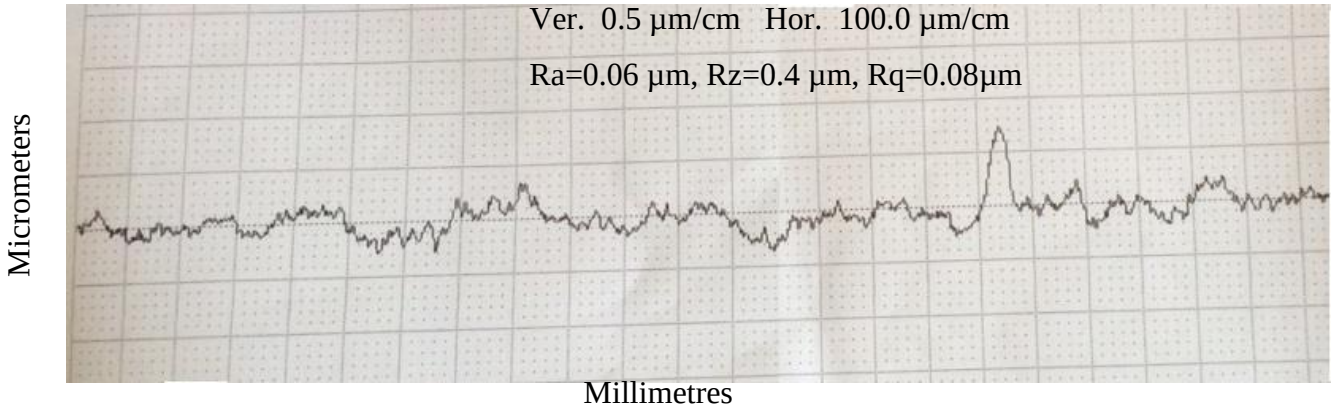

(b)

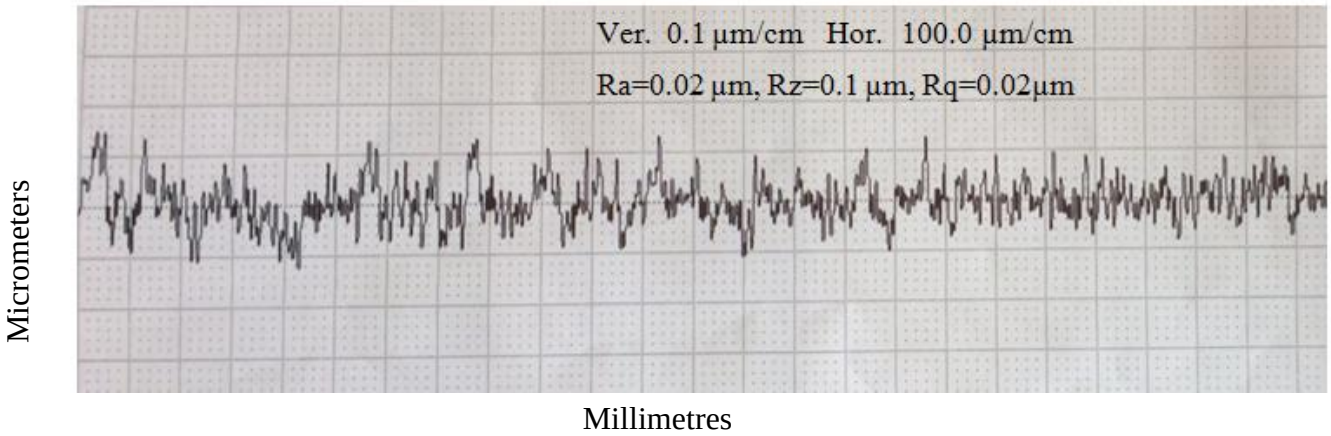

(c)

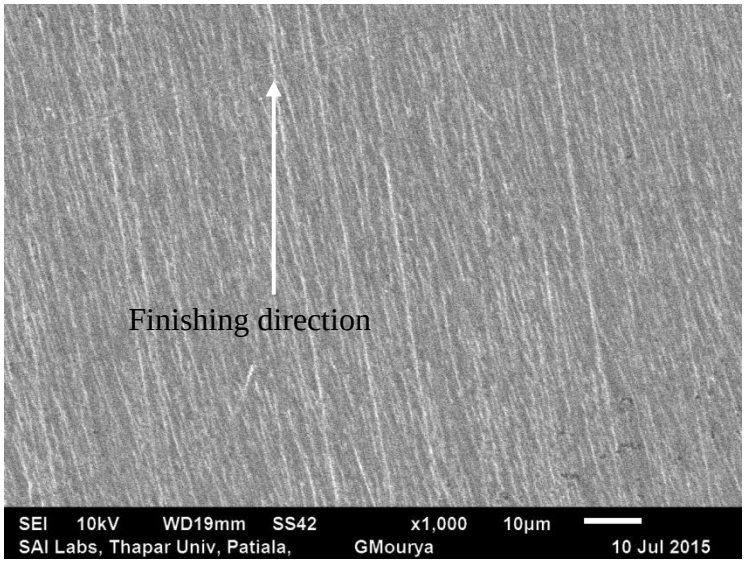

Figure 4.13: Finished surface of ferromagnetic workpiece surface roughness profiles for (a) 60 nm (b) 20 nm and (c) SEM analysis at 1000×

4.4.2 Comparison of experimental results of core with central hole and core without central hole

In the earlier ball end MRF process with central hole rotating core the reduction in surface roughness is achieved as 19.7 nm from 142.9 nm in 120 mins of finishing time at parameters (current = 4A, working gap = 0.66 mm, rotational speed of central core = 500 rpm) (Singh *et al*., 2012). In the present developed low cost ball end MRF process with central rotating core without hole the reduction in surface roughness value is achieved as 20 nm from 290 nm in 90 mins of finishing time at parameters (current = 1A, working gap = 0.6 mm, rotational speed of central core = 200 rpm) keeping all other design parameter constant like number of turns, rotating central core, MR polishing fluid composition etc. The considerable observations are explained below-

- The earlier process was capable to achieve 19.7 nm average surface roughness at 4A magnetizing current in 120 mins of finishing time but in the present developed low cost ball end MRF process approximate same level of average surface roughness value i.e. 20 nm is achieved at 1A magnetizing current in 90 mins of finishing time.
- The magnetic flux density distribution is almost uniform in the present developed low cost ball end MRF process which was not uniform in earlier ball end MRF process due to central hole in rotating core.

The different process parameters and their conditions for the core with central hole and core with central hole are shown in Table 4.7 below. The graph between surface roughness and finished time for both core with central hole and core without central hole is shown in Fig. 4.14 below.

Table 4.7: Experimental conditions for both core with central hole (Singh *et al*., 2012) and core without central hole

Process parameter	Conditions	
	For core with central hole	For core without central hole
Each finishing cycle (min)	30	30
Total rotation speed (rpm)	500	200
Working gap distance (mm)	0.66	0.66
SiC abrasive (20 vol %) (mesh)	800	800
DC power supply	4 A	1 A
Workpiece material	ferromagnetic	ferromagnetic

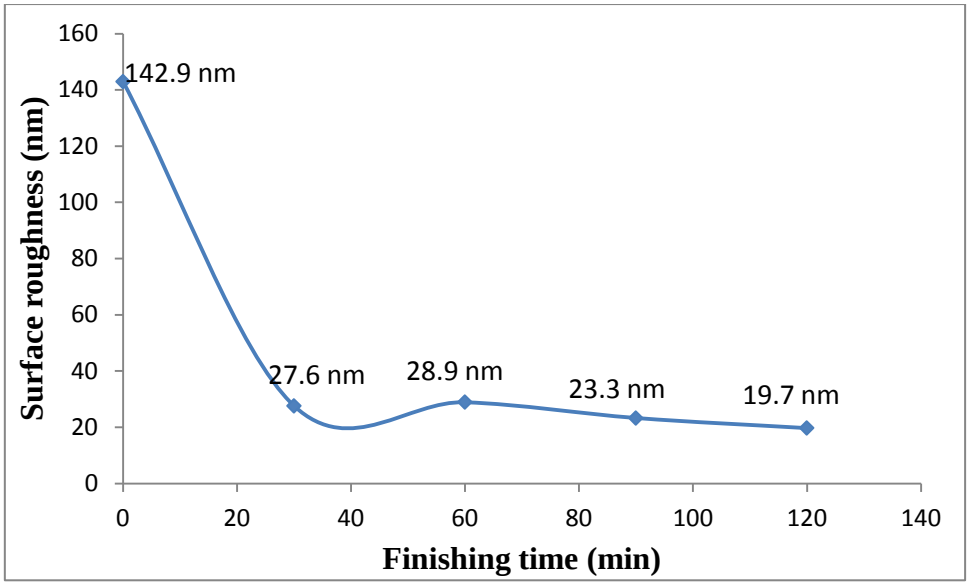

(a)

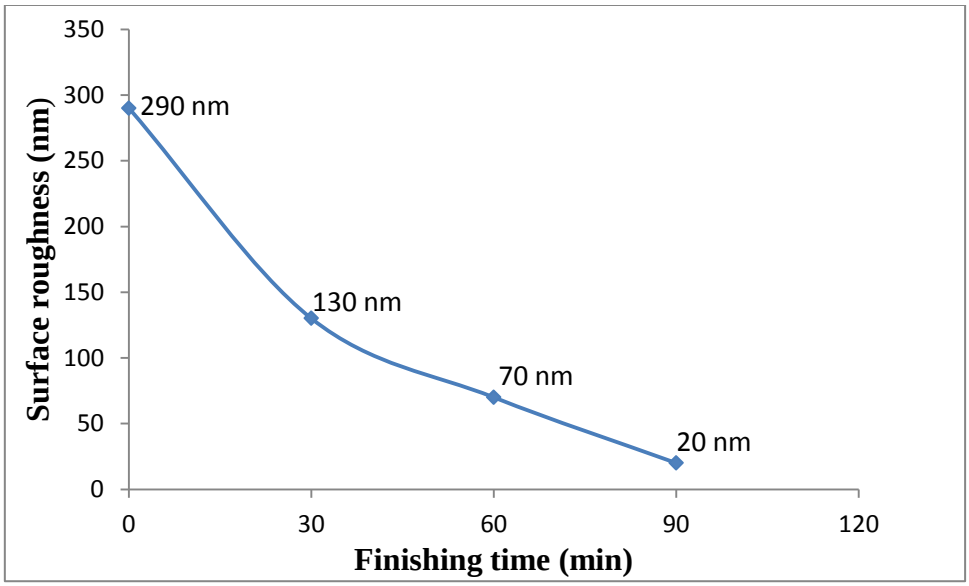

(b)

Figure 4.14: Effect of finishing time on (a) core with central hole (Singh *et al*., 2012) and (b) core without central hole

Chapter 5

Conclusions and Scope for Future Work

5.1 Conclusions

- A low cost ball end MR finishing tool without central hole in core has been developed for nanofinishing of workpiece surfaces.
- The magnetostatic simulation of the present developed MRF tool with ferromagnetic work material clearly shows that the almost uniform magnetic flux density in the working gap which results in nearly uniform finished surface even without any feed to the workpiece.
- Uniform finishing can be obtained on the surface of workpiece at low rpm of tool and at low magnetizing current using presently developed finishing process.
- The property of MR polishing fluid is utilized to accurately control the abrading forces for getting the precise surface finish.
- The overall results concluded that the value of average surface roughness of ferromagnetic material decreased from 440 nm to 20 nm almost uniformly over the surfaces with finishing time of 90 minutes in case of without giving feed.
- Comparatively the present developed finishing process was found likely more efficient to finish the surfaces with less time and more uniformity over the surfaces even without any feed to the workpiece.

5.2 Scope for future work

- The different 3D practical complex surfaces can be finished at nanometer level using the present developed finishing process.
- The effect of feed rate, different abrasive size and carbonyl iron particles size can be studied on the presently developed finishing process.
- A low temperature bath can be used for effective finishing of hard material such as chrome steel, EN 31 at higher magnetizing current to control and monitor the electromagnet coil temperature.

References

Cheng, H.; Yeung, Y.; Tong, H. (2008) Viscosity behaviour of magnetic suspensions in fluid-assisted finishing. *Progress in Natural Science*, 18: 91-96.

Jain, V.K. (2008) Abrasive-based nano-finishing techniques. *Machining Science and Technology*, 12: 257-294.

Jain, V.K. (2009) Magnetic field assisted abrasive based micro-/nano-finishing. *Journal of Materials Processing Technology*, 209: 6022-6038.

Jha, S.; Jain, V.K. (2006) Modeling and simulation of surface roughness in magnetorheological abrasive flow finishing process. *Wear*, 261: 856-866.

Niranjan, M.; Jha, S.; Kotnala, R.K. (2014) Ball End magnetorheological finishing using bidisperse magnetorheological polishing fluid. *Materials and Manufacturing Processes*, 29: 487-492.

Shankar, R.M.; Jain, V.K.; Ramkumar, *J. (2010)* Rotational abrasive flow finishing process and its effects on finished surface topography. *International Journal of Machine Tools and Manufacture, 50: 637-650.*

Sidpara, A.; Jain, V.K. (2011) Experimental investigations into forces during magnetorheological fluid based finishing process. *International Journal of Machine Tools and Manufacture, 51: 358-362.*

Sidpara, A.; Jain, V.K. (2013) Analysis of forces on the free form surface in magnetorheological fluid based finishing process. *International Journal of Machine Tools and Manufacture*, 69: 1-10.

Singh, D.K.; Jain, V.K.; Raghuram, V. (2004) Parametric study of magnetic abrasive finishing process. *Journal of Materials Processing Technology*, 149: 22-29.

Sidpara, A.; Jain, V.K. (2012) Theoretical analysis of forces in magnetorheological fluid based finishing process. *International Journal of Material Sciences*, 56; 50-59.

Wang, A.C.; Lee, S.J. (2009) Study the characteristics of magnetic finishing with gel abrasive. International Journal of Machine Tools and Manufactures, 49; 1063-1069.

Singh, A.K.; Jha, S.; Pandey, P.M. (2012) Nano finishing of a typical 3D ferromagnetic workpiece using a ball end magnetorheological finishing process. *International Journal of Machine tools and Manufacture*, 63: 21-31.

Wang, Y.; & Hu, D. (2005) Study on the inner surface finishing of tubing by magnetic abrasive finishing. *International Journal of Machine Tools and Manufacture*, 45; 43-49.

Singh, A.K.; Jha, S.; Pandey, P.M. (2013) Mechanism of material removal in ball end magnetorheological finishing process. *Wear*, 302: 1180-1191.

Yamaguchi, H.; Shinmura, T. (2004) Internal finishing process for alumina ceramic components by a magnetic field assisted finishing process. *Precision Engineering*, 28: 135-142.

Cheng, H.; Feng, Y.; Wang, T.; Dong, Z. (2010) Magnetorheological finishing of optical surface combined with symmetrical tool function. *Frontiers of Optoelectronics*, 3(4): 408-412.

Kang, J.; George, A.; Yamaguchi, H. (2012) High-speed internal finishing of capillary tubes by magnetic abrasive finishing. *Procedia CIRP*, 1: 414-418.

Das, M.; Jain, V.K.; Ghoshdastidar, P.S. (2008) Fluid flow analysis of magnetorheological abrasive flow finishing process. *International Journal of Machine Tools and Manufacture*, 48: 415-426.

Schmitt, C.; Moos, U.; Bahre, D. (2003) Comparison of different approaches to force controlled precision honing of bores. *Journal of Mechanics Engineering and Automation*, 3: 764-771.

Yin, S.; Shinmura, T. (2004) Vertical-assisted magnetic abrasive finishing and deburring for magnesium alloy. *International Journal of Machine Tools and Manufacture*, 44: 1297-1303.

Gheisari, R.; Ghasemi, A.A.; Jafarkarimi, M.; Mohtaram, S. (2014) Experimental studies on the ultraprecision finishing of cylindrical surfaces using magnetorheological finishing process. *Production & Manufacturing Research*, 2:1: 550-557.

Kordonski, W.I.; Shorey, A.B.; Tricard, M. Nov (2004) Magnetorheological (MR) jet finishing technology. Proceeding of ASME International Mechanical Engineering Congress, 13-19: 1-8.

Judal, K.B.; Yadava, V.; Pathak, D. (2013) Experimental investigation of vibration assisted cylindrical magnet abrasive finishing of Aluminium workpiece. *Materials and Manufacturing Processes*, 28: 1196-1202.

Das, M.; Jain, V.K.; Ghoshdastidar, P.S. (2010) Nano Finishing of stainless steel using rotational magnetorheological abrasive flow finishing process. *Machining Science and Technology*, 14: 365-389.

Jha, S.; Jain, V.K.; Komanduri, R. (2007) Effect of extrusion pressure and number finishing cycles on the surface roughness in Magnetorheological abrasive flow finishing process. *International Journal of Advanced Manufacturing Technology*, 33: 725-729.

Das, M.; Jain, V.K.; Ghoshdastidar, P.S. (2012) Nano finishing of flat workpiece using rotational magnetorheological abrasive flow finishing process. *International Journal of Advanced Manufacturing Technology*, 62: 405-420.

Hong, K.P.; Cho, Y.K.; Shin, B.C.; Cho, M.W.; Choi, S.B.; Cho, W.S.; Jae, J.J. (2012) MR fluid polishing of Alumina reinforced zirconia ceramics using diamond abrasive for dental application. *Materials and Manufacturing Processes*, 27: 1135-1138.

Kim, J.D. (1997) Development of a magnetic abrasive jet machining system for internal polishing of circular tubes. *Journal of Material Processing Technology*, 71: 384-393.

Seok, J., Lee, S.O., Jang, K.I., Min, B.K., Lee, S.J. (2009) Tribological properties of a magnetorheological (MR) fluid in a finishing process. *Tribology Transaction*, 52(4): 460-469.

Kordonski, W.I., Golini, D. (1999) Fundamentals of magnetorheological fluid utilization in high precision finishing, *Journal of Intelligent Material Systems and Structures*, 10(9): 683-689.

Mathur, R., Khare, Roopam, Chauhan, Vinesh,(2003) Magnetorheological Finishing of Optical Lenses, B.Tech. Project. Mechanical Eng. Dept., IIT Kanpur.

Jha, S., Jain, V.K. (2004) Design and development of the magnetorheological abrasive flow finishing (MRAFF) process, *International Journal of Machine Tools and Manufacture*, 44: 1019-1029.

Kordonski, W. I., Shorey, A.B., Tricard, M. (2006) Magnetorheological jet finishing technology. *Transactions of ASME,* 128: 20-26.

Sidpara, A., Das, M., Jain, V.K. (2009) Rheological characterization of magnetorheological finishing fluid. *Materials and Manufacturing Processes*, 24(2): 1467-1478.

Bica, I. (2002) Damper with magnetorheological suspension. *Journal of Magnetism and Magnetic Materials*, 241: 196-200.

Genc, S., Phule, P.P. (2002) Rheological properties of magnetorheological fluids. *Smart Materials and Structures*, 11: 140-146.

Ruben, H.J. (1987) In: A. Niku-Lari (Ed.), Advances in Surface Treatments, Pergamon Press, Oxford: United Kingdom.

Furst, E.M., Gast, A.P. (2000) Micromechanics of magnetorheological suspensions. *Physics Revolution, E* 61(6): 6732-6739.

Brecker, J.N., Brown, R., Matsuo, T., Saito, K., Sweeney, J.A., Vansaun, J.B., Shaw, M.C. (1969) Abrasive Grain Association on Investigation of Abrasive Grain Characteristics, 4th Annual Report, Carnegie Institute of Technology, USA.

Web References

http://www.azom.com/images/Article_Images/ImageForArticle_5657 (1).jpg

http://core.materials.ac.uk/repository/ou_manufacturing/t173_2_045i.jpg

http://blog.mechguru.com/wp-content/uploads/2011/09/honing.jpg

http://file.seekpart.com/productsimage/2013/7/19/201371914301215877.jpg

http://www.cross-morse.co.uk/images/tb1.jpg